Investigation of Si-Si Bond Formation by Rh(I) Catalysts

by

Catrin Elizabeth Hughes
B.Sc., Mount Allison University, 2002

A Thesis Submitted in Partial Fulfillment of the
Requirements for the Degree of

MASTER OF SCIENCE

in the Department of Chemistry

Supervisor: Dr. Lisa Rosenberg

ABSTRACT

Dehydrocoupling reactions of di-*n*-hexylsilane with Wilkinson's catalyst, $RhCl(PPh_3)_3$, **1**, Wilkinson's dimer, $[Rh(PPh_3)_2\mu\text{-}Cl]_2$, **2**, dppe dimer, $[Rh(dppe)\mu\text{-}Cl]_2$, **3**, and a cationic rhodium catalyst, $[Rh(COD)(PPh_3)_2]^+PF_6^-$, **4** are described herein. This class of catalysts was examined for their potential utility, on a synthetically useful scale, in the production of Si-H functionalized oligosilane reagents. All four of these Rh(I) phosphine complexes caused dehydrocoupling of di-*n*-hexylsilane to yield either disilane (1,1,2,2-tetra-*n*-hexyldisilane) or a mixture of disilane and trisilane (1,1,2,2,3,3-hexa-*n*-hexyltrisilane). Complexes **1** and **2** showed much higher activities, compared to complexes **3** and **4**. Hydrogen gas removal, reaction time and solubility factors were observed to affect the amount of monosilane consumption and the activity observed for each of the catalyst precursors (**1-4**) in the dehydrocoupling silane reactions.

Multiple stoichiometric reactions with complexes **1-4** were carried out to try and understand the importance of key catalyst structural features in a putative catalytic cycle and to identify species present in the catalytic mixture. Intermediates from Halpern's work on olefin hydrogenation by **1** and early silane addition chemistry by Osakada and Haszeldine were found to be useful guides. Complex **5**, $[(PPh_3)_2Rh(H)(Cl)(SiHR_2)]$, a product of oxidative addition of a Si-H bond to a Rh centre, was isolated from the reaction mixture of $[(PPh_3)_2Rh(\mu\text{-}Cl)]_2$, **2**, with one equivalent of di-*n*-hexylsilane per rhodium centre and found to be catalytically competent. The formation of this complex was proposed as the first step in the catalytic cycle for complexes **1** and **2**.

TABLE OF CONTENTS

LIST OF TABLES

LIST OF FIGURES

LIST OF ABBREVIATIONS

The following abbreviations, most of which are commonly found in the literature, are used in this thesis.

aq	aqueous medium
atm	atmosphere
br	broad
br d	broad doublet
br d m	broad doublets of multiplets
br m	broad multiplet
br s	broad singlet
C_6D_6	deuterated benzene
C_7D_8	deuterated toluene
° C	degrees Celsius
COD	cyclooctadiene
COE	cyclooctene
d	doublet
d m	doublet of multiplets
dd	doublet of doublets
dppb	bis(diphenylphosphino)butane
dppe	bis (diphenylphosphino)ethane
equiv	equivalent(s)
FT-IR	Fourier transformed – infrared spectroscopy
$^1H\{^{31}P\}$	observe proton while decoupling phosphorus

H_m	meta-hydrogen
H_o	ortho-hydrogen
H_p	para-hydrogen
hr	hour
Hz	Hertz, seconds^{-1}
$^nJ_{A-B}$	n-bond scalar coupling constant between A and B nuclei
K	Kelvin
kPa	kilopascals
M	central metal atom (or "molar", when referring to concentration)
mg	milligram(s)
MHz	megaHertz
mL	millilitre
mm	millimeter
mmol	millimole(s)
mol	mole
m	multiplet
NMR	nuclear magnetic resonance
ov	overlapping
$^{31}P\{^1H\}$	observe phosphorus while decoupling proton
pent	pentet
Ph	phenyl group, $-C_6H_5$
PPh_3	triphenylphosphine
ppm	parts per million

R	alkyl, aryl or alkoxy group
R.E.	reductive elimination
RI	relative intensity
RT	room temperature
s	singlet
$^{29}Si\{^{1}H\}$	observe silicon while decoupling proton
T	temperature
t	triplet
UV-vis	Ultraviolet – visible spectroscopy
VT	variable temperature
$\omega_{1/2}$	linewidth at half-height
X	anionic, unidentate donor ligand

ACKNOWLEDGEMENTS

I would like to extend thanks to the following people for their help and support in the completion of this thesis.

Dr. Lisa Rosenberg for all the advice and guidance with this project.

Sebastién Monfette for spending his summer making some much needed starting materials for me.

Chris Greenwood for running all my VT NMR spectra.

UVic Chemistry secretaries, stores, staff and fellow graduate students for smooth transitions and great conversations.

The Rosenberg lab group past and present: Dawn, Danielle, Dan, Eric, and Sarah. Thanks for all the great memories in and out of the lab (B.A.D.Hs forever!).

My family and friends for the constant encouragement, and lending of ears when I really needed to talk.

Rob for reminding me that laughter is the best medicine. You make me smile *grin*.

Dave Berry, and Kelli Fawkes for being great TA supervisors. You'll be the first to know if I go into teaching...I promise!

CHAPTER 1

Introduction

1.1 Polysilanes

In recent years, interest has developed in silicon polymers, also known as polysilanes. Depicted in Figure 1.1, these are long chains of organic silicon moieties linked by Si-Si bonds. Polysilanes (-[SiRR']$_n$-) demonstrate interesting electronic properties caused by delocalization of σ-electrons within the catenated chain. These properties may be correlated with *all-transoid*, or *anti*, conformations along the polymer backbone. Achieving exact conformational control in these essentially flexible polysilane chains presents considerable synthetic challenges.[1] Current applications of polysilanes are as ultraviolet acting photoresists for microelectronics, free radical photoinitiators and precursors for silicon carbide ceramics. They also have the potential to be used for photoconductors in electrophotography and their non-linear optical properties may make them useful in laser and other optical technologies.[2]

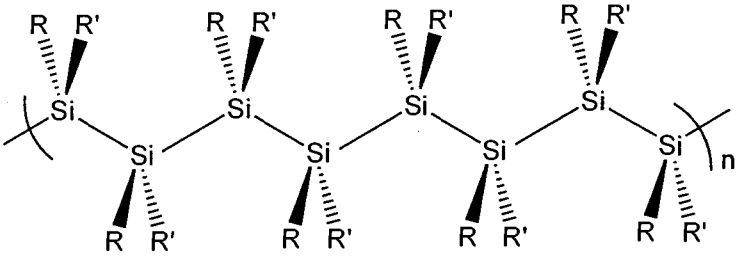

Figure 1.1: Polysilane chain

1.2 The methods of synthesis of Si-Si Bonds

Traditionally, the most common route to polysilanes and Si-Si bond formation in general is through Wurtz coupling reactions shown in Equation 1.1. This method involves highly reactive reagents, alkali metals and chlorosilanes (R_2SiCl_2), which are difficult to

References p13

handle and produce stoichiometric amounts of salts, which require removal. The major products formed with this type of coupling are cyclic oligomers or long chain polymers, typically in low yield (20-30%).[3] There are limited opportunities for functionalization and controlling the chain length is difficult.

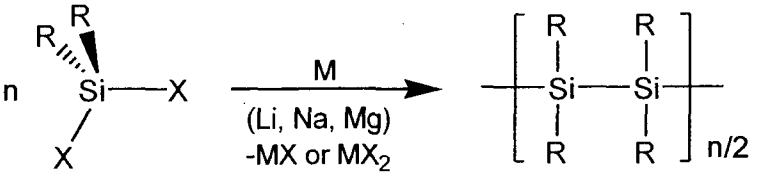

(1.1)

An alternative route to making these Si-Si bonds is through dehydrocoupling by transition metals.[4] This is essentially a condensation reaction involving the activation of Si-H bonds in silanes by a metal centre followed by the formation of Si-Si bonds and simultaneous elimination of H_2(g). First documented in 1970, the catalysis of dehydrogenative silicon-silicon coupling of disilanes (RMe_2Si-$SiMe_2R$, where R = H), by a transition-metal complex, was reported. In the presence of $(PEt_3)_2PtCl_2$, these disilanes were converted to a mixture of oligomers with chains observed up to six silicon atoms long.[5] Brown-Wensley, et al. also reported that a number of Rh, Ir, Pd and Pt complexes catalyze the formation of Si-Si bonds, to give oligomers. In this case, secondary silanes were found to be more reactive than tertiary silanes.[6]

Most intensively studied of dehydrocoupling catalysts have been early transition metals, such as the Group 4 metallocene catalyst systems, which can produce relatively high molecular weight (MW) polymers (degree of polymerization (DP) as high as 70-100 monomer units) from primary aryl silanes (See Equation 1.2).[7] In 1986 the oligomerization of primary silanes using Cp_2TiMe_2 was reported, the products having an average silicon chain length of ten.[8] The most active catalyst is $CpCp^*Zr[Si(SiMe_3)_3]Me$ which with phenylsilane, under certain conditions, will give linear poly(phenylsilane)

samples with average molecular weights of about 5300, corresponding to roughly 44 silylene units.[9]

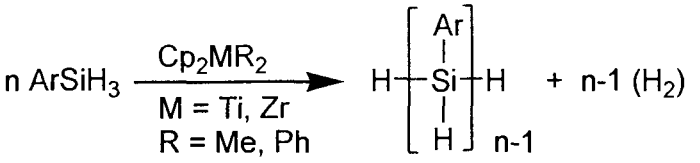

(1.2)

Late transition metal complexes have received less attention for the dehydrocoupling of silanes (Equation 1.3), as they show evidence of a competing reaction involving the redistribution of substituents at silicon (discussed further in Section 1.4).[10]

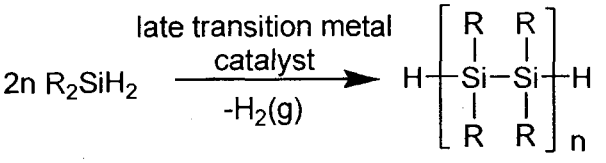

(1.3)

1.3 Oligosilane compounds

In order to study the interesting electronic properties of polysilanes it is desirable to work with smaller model compounds. Oligosilanes are attractive models for polysilanes. The presence of Si-H bonds can allow for further functionalization of these compounds (Figure 1.2).

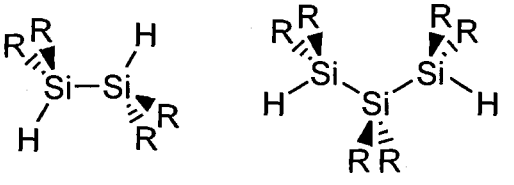

Figure 1.2: α,ω-Hydride substituted di- and trisilane compounds

Derivatization of these Si-H bonds can be accomplished via reactions such as halogenation, alcoholysis, and aminolysis to yield more substitutionally labile Si-X bonds (Figure 1.3). These functionalization methods can be optimized for post-polymerization

modification of polysilane chains, while other issues, such as conformational preferences of Si_2 or Si_3 units can be evaluated for a range of model compounds.

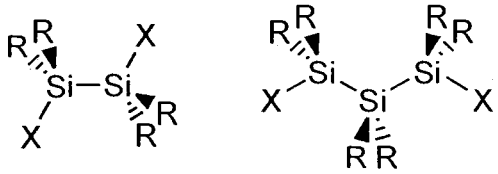

where X = H, Cl, Br, SR, OR', $NR"_2$

Figure 1.3: Di- and trisilane compounds with variable functional groups

Although 1,2-dichlorotetramethyldisilane, a byproduct of Rochow's direct synthesis route to dichlorodimethylsilane, is routinely commercially available[11], a limited number of other such functionalized di- or oligosilanes, with reactive Si-X bonds are available commercially or easily accessible by synthetic means.[12] As described above (Section 1.2), other groups have shown that hydride-substituted oligosilanes can be obtained from transition metal catalyzed dehydrocoupling reactions. Retention of terminal Si-H bonds in the oligosilane products is implicit in this method, since transition metal catalysts are active principally for the coupling of primary and secondary silanes.[1] These hydrosilane compounds are quite stable in air toward hydrolysis and oxidation, but are still reactive enough to allow for further functionalization. Under neutral conditions, the hydrolysis of hydrosilanes in solution occurs rather slowly to yield the silanol product and hydrogen gas as a by-product (Equation 1.4).[13] Unlike poly(hydrosilane)s, which can undergo autoxidation reactions to give peroxidative products (ROOH), the hydrosilane precursors are much more stable toward oxygen.[14]

$$R_3SiH + HOR' \longrightarrow R_3SiOR' + H_2(g) \qquad \textbf{(1.4)}$$

The traditional synthetic approach to preparing Si-Si bonds by Wurtz reductive coupling of dichloromonosilanes (R_2SiCl_2) is not a viable route to α,ω-functionalized oligosilanes, specifically α,ω-dihalo oligosilanes, since these reactive halide species are inevitably consumed to give longer chains or cyclic compounds. Although there is precedent for the synthesis of 1,2-dihydro-substituted disilanes through reductive coupling of $R_2Si(H)Cl$, these reactions are fickle and frequently give low yields.[15] Dehydrocoupling products (hydrosilane oligomers) resulting from late transition metal catalysis of silanes are almost invariably limited to short chains (2-5 silicons). In 1973, $RhCl(PPh_3)_3$, **1** was found to give low conversions of various secondary silanes to mixtures of di- and trisilanes.[16]

1.4 Redistribution reactions

As mentioned in Section 1.2, although many late transition metal complexes can affect the coupling of both aryl- and alkyl-substituted 1° and 2° silanes, they typically also exhibit competing catalytic activities for substituent redistribution reactions of the silane substrates.[10] An example of this competing side reaction has been observed and studied by previous students in the Rosenberg group through the coupling of a *diaryl*silane, Ph_2SiH_2, with Wilkinson's catalyst, $RhCl(PPh_3)_3$ (**1**) (Scheme 1.1).

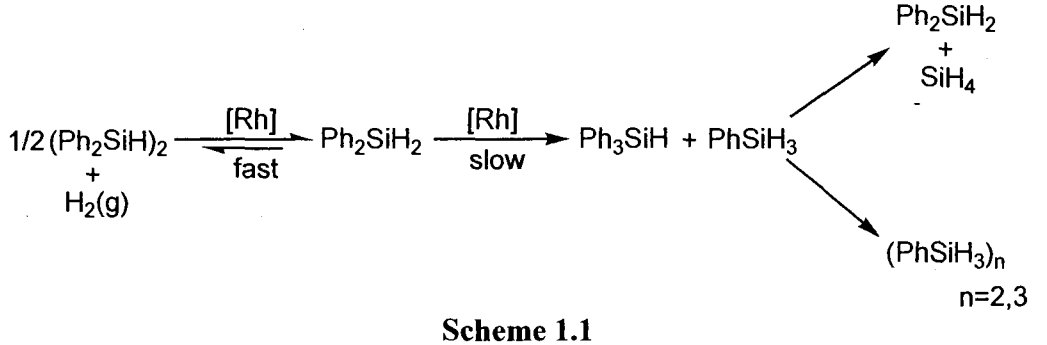

Scheme 1.1

Desired oligosilane product(s) are formed, accompanied by side-products, Ph_3SiH and $PhSiH_3$. This redistribution of products can pose challenges when the goal is to synthesize silane reagents on a useful scale. Optimal conditions, specifically concerning the rate of hydrogen gas removal, have been identified to preferentially obtain the oligosilane compounds. It was found that the redistribution of phenyl and hydrido groups in Ph_2SiH_2 proceed very slowly, relative to dimerization, at all catalyst concentrations, under these conditions. The same study showed that the coupling of dialkylsilanes by $RhCl(PPh_3)_3$, **1** gives no redistribution by-products.[17] This discovery led to my interest in studying these dehydrocoupling reactions further with a dialkylsilane substrate and a range of Rh-P complexes. The fact that no redistribution occurs for dialkylsilanes greatly simplifies my examination of these systems.

It should be noted that the established group 4 metallocene catalysts exhibit little or no activity for the coupling of dialkylsilanes. Slight activity of a titanocene-based catalyst for the coupling of $(n\text{-Pr})_2SiH_2$ has been reported, but requires the presence of cyclic olefins, which are hydrogenated in tandem with the coupling process and also lead to hydrosilylation by-products.[18]

1.5 Discussion of catalysis and mechanism in the context of Rh-catalyzed dehydrogenative coupling of silanes

Typically, catalysts interact with reactants (usually called substrates) in a cyclic series of associative (binding), bond-making and/or breaking, and dissociatative steps. During each cycle, the catalyst is regenerated so it may go through another cycle. Each cycle is called a turnover, and an effective catalyst may undergo hundreds, even thousands of turnovers before decomposing – each cycle producing a molecule of

product. Stoichiometric reactions undergo only one "turnover", with only one molecule of product produced and have only reagents involved, not catalysts.[19]

A major challenge associated with the study of catalytic processes is the determination of the nature of reactive intermediates or of the "active" catalyst. Often, when a catalyst is added to a reaction mixture, there is little knowledge as to whether the bulk of the added material is the catalyst, or whether only a trace amount of the added material is converted to a new material, which is the active catalyst (or something in between these extremes). This problem is particularly acute in homogeneous catalysis by transition-metal complexes, where the active catalytic intermediate is often extremely unstable and highly reactive.[20]

In the study of homogeneous catalytic systems, the inability to spectroscopically observe suspected intermediates in the reaction mixture does not preclude the activity of that species in the catalytic cycle. For example, kinetic studies on the use of Wilkinson's catalyst, $RhCl(PPh_3)_3$, **1**, in the hydrogenation of olefins showed that the catalysis was in fact being carried out by a series of complexes that, although related through equilibria to detected or isolated complexes, were not directly observed.[9b,21] This will be discussed further in Chapter 3.

Numerous transition-metal-catalyzed reactions of organosilanes are known. Some, like hydrosilylation (the addition of a Si-H bond to an unsaturated substrate) are industrially important. Typically these reactions involve metal-mediated Si-X bond-breaking and bond-forming processes (where X could be H, Cl, Br, OR', NRR', etc.). The key step for the hydrosilylation process is Si-H activation, where the catalyst metal centre involved 'activates' the Si-H bonds in silanes in order to facilitate the chemical reaction.

References p13

Factors that govern the reactivity of transition metal silyl complexes are still a subject of literature debate.[22]

1.5.1 Oxidative addition of Si-H bonds to late transition metals

The most common method for the synthesis of metal-silicon bonds is by activation and addition of a Si-H bond to a metal centre. Often the addition is accompanied by the elimination of a small molecule from the metal centre, such as H_2, CH_4 or HCl. In general, Si-H bonds are more reactive toward oxidative addition reactions than other Si-X bonds. Addition of Si-H bonds to transition metal centres is a general process occurring for both early and late transition-metal complexes. There are some other routes to metal silicon bonds that have been reported but few of these have general applicability.[23]

For late transition metals the silyl complexes generated are the result of oxidative addition to low-valent species that possess a vacant coordination site. In Equation 1.6 the addition is straightforward, with a change from Rh(I) to Rh(III) and the formation of a Rh-Si and a Rh-H bond.[24]

$$(PPr^{i}_{3})_2RhCl + HSiAr_3 \xrightarrow[Ar = Ph]{} (PPr^{i}_{3})_2Rh(H)Cl(SiAr_3) \qquad \textbf{(1.6)}$$

Most rhodium silyl complexes are formed from the oxidative addition of a Si-H bond to a Rh(I) centre, thus the silyl complexes generally contain rhodium in the +3 oxidation state. Exceptions include a few Rh(I) silyl complexes[25] and even more rare Rh(V) silyl complexes. An example of a silyl complex with rhodium in the +5 oxidation state is shown below in Figure 1.4.[26]

References p13

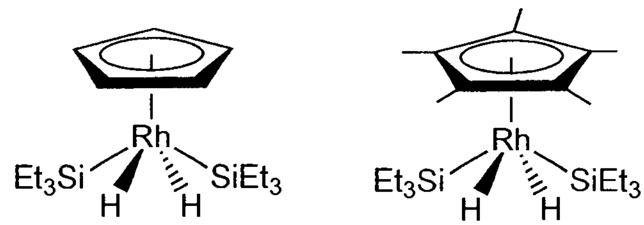

Figure 1.4: Rh(V) silyl complexes from reactions of silanes with some "half-sandwich" rhodium cyclopentadienyl complexes

In some cases the Si-H addition is accompanied by dissociation of an ancillary ligand to provide the necessary vacant coordination site, as shown in Equation 1.7.

$$(PPh_3)_3Ir(CO)H \underset{+\,PPh_3}{\overset{-\,PPh_3}{\rightleftharpoons}} (PPh_3)_2Ir(CO)H \underset{-\,R_3SiH}{\overset{+\,R_3SiH}{\rightleftharpoons}} (PPh_3)_2Ir(CO)H(SiR_3) \quad \textbf{(1.7)}$$

Wilkinson's catalyst, $RhCl(PPh_3)_3$, **1**, also follows the same type of ligand dissociation to obtain a vacant coordination site. Silyl complexes of the formula in Equation 1.8 are known for a wide variety of substituents on silicon and for many different phosphine ligands.[27] The work of Haszeldine and co-workers with $RhCl(PPh_3)_3$, **1**, and primary silanes to give chloro(hydrido)silylrhodium(III) complexes is attributed to an oxidative addition reaction of the Si-H bond.[28] X-ray diffraction and ^{31}P NMR results for some of these compounds confirm five-coordinate, monomeric species and suggest a trigonal bipyramidal configuration, with the phosphines in axial positions.

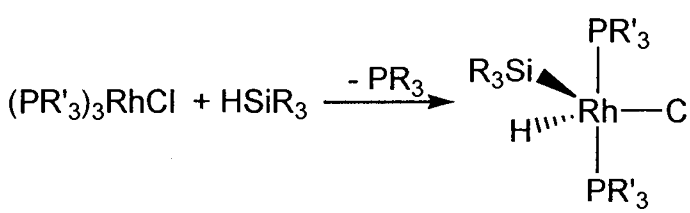

(1.8)

Based on literature examples by Osakada and other groups, it is suggested that the formation of dinuclear species, with silyl ligands, as intermediates in the hydrogenation

catalytic cycle is also a possibility.[29] It has not yet been proven whether these dinuclear systems are catalytically active and if so, their activity may vary from one metal system to another.

1.5.2 Formation of Si-Si bonds by late transition metals

Although Si-H activation has been intensively studied, the mechanisms by which metal-mediated silane dehydrogenative coupling reactions occur have been a subject of some debate. The currently accepted mechanism for Si-Si coupling catalyzed by group 4 metallocenes suggest that there is a stepwise growth of the silicon chains via four-centre transition states.[30] The mechanism is less well understood for late transition-metal catalysts that dehydrogenatively oligomerize silanes. Although the Si-Si coupling by late transition metals is thought to occur via a series of oxidative addition and reductive elimination steps, two different mechanisms have been postulated. One mechanism involves successive oxidative addition of Si-H bonds to a metal centre, with loss of hydrogen gas, and subsequent reductive elimination (R.E.) to facilitate the formation of Si-Si bonds. The second mechanism involves the same successive oxidative addition of Si-H bonds to a metal centre, with loss of $H_2(g)$, but then proposes a 1,2-hydrogen migration, followed by silylene insertion (1,3-silyl migration), and subsequent reductive elimination of a Si-H bond to give the Si-Si products. Most steps in these mechanisms have some precedent in stoichiometric chemistry.[31] This will be discussed further in Chapter 3.

Osakada, et al, has established literature evidence for the reversibility of Si-H addition to transition metal centres. They report that the oxidative addition of secondary

and tertiary silanes to chlororhodium(I) complexes with PMe_3 and with $P(i\text{-}Pr)_3$ ligands leads to the formation of chloro(hydrido)silylrhodium(III) complexes. The resulting Rh(III) complexes are often in equilibrium with Rh(I) complexes via a reversible reductive elimination of the organosilane and its re-oxidative addition in solution.[32]

1.5.3 Formation of Si-Cl bonds by late transition metals

Similar to the Si-Si and Si-H reductive eliminations, the R.E. of Si-Cl from silyl rhodium complexes has been studied; again most notably by Osakada. Work concerning chlororhodium(I) complexes with phosphine ligands has shown that it is possible to convert the Si-H group of an organosilane into the Si-Cl group under mild conditions. The formation of chlorosilanes from the rhodium complex is achieved by having the chloro and silyl ligands in the *cis* position.[32] Clear examples of the reduction of chloro-transition metals by triorganosilanes have been presented in the reactions of triorganosilanes with $PtCl_2(PR_3)_2$ (Equation 1.4) and with $IrCl(CO)(PR_3)_2$ (Equation 1.5) to give hydrido complexes of these transition metals accompanied by the formation of chlorotriorganosilanes.[33]

$$(R_3P)_2PtCl_2 + R'_3SiH \longrightarrow (R_3P)_2PtClH + R'_3SiCl \qquad \text{(1.4)}$$

R = alkyl, R' = alkyl, or aryl

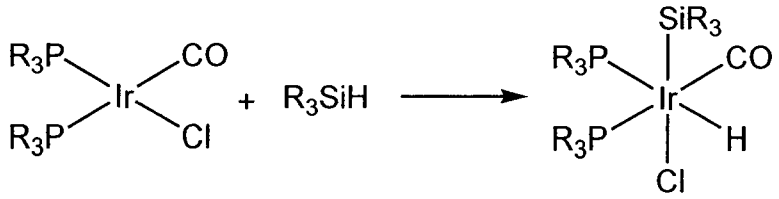

(1.5)

1.6 The scope of this thesis

This thesis describes the reactions of di-*n*-hexylsilane with Wilkinson's catalyst, $RhCl(PPh_3)_3$, (**1**), Wilkinson's dimer, $[(PPh_3)_2Rh(\mu\text{-}Cl)]_2$, (**2**), dppe dimer, $[Rh(dppe)\mu\text{-}Cl]_2$, (**3**), and a cationic rhodium catalyst, $[Rh(COD)(PPh_3)_2]^+PF_6^-$, (**4**). These catalysts were examined for their potential utility, on a synthetically useful scale, in the production of Si-H functionalized oligosilane reagents.

The original reason for studying these dehydrocoupling of silane reactions was based on a long-term goal of the Rosenberg research group concerning polysilanes, specifically, interest in conformational preferences and functionalization of these materials. In order to investigate these structure-related issues, smaller units of the polysilane chain with a variety of functional groups were needed to get to more elaborate, conformationally constrained oligosilane architectures. As discussed earlier, the lack of availability of these oligosilane compounds provided incentive for my project, i.e. the search for viable routes to these sought-after short-chain compounds.

Chapter 2 describes the attempts to identify the best catalyst precursor for the production of dialkyl-substituted di- and trisilanes. The dehydrocoupling reactions of a secondary dialkylsilane, di-*n*-hexylsilane, in the presence of four late transition metal Rh-P catalysts (**1-4**) are presented. Chapter 3 includes descriptions of complexes formed from the addition of 1, 2, and 2.5 or 5 equivalents of di-*n*-hexylsilane to Rh-P catalysts (**1-4**). The stoichiometric chemistry observed (along with results from Chapter 2) was used to try to understand the importance of key catalyst structural features in a putative catalytic cycle and to identify species present in the catalytic mixture. Possible future directions of this work are discussed in Chapter 4.

References p13

1.7 References

(1) Rosenberg, L. *Macromol. Symp.* **2003**, *196*, 347.

(2) a) Mark, J.E., Allcock, H.R., West, R. *Inorganic Polymers*; Prentice-Hall, Inc.: New York, 1992, p. 187; b) Miller, R.D., Michl, J. *Chem. Rev.* **1989**, *89*, 1359; c) For more information on NLO materials with polysilanes see: Hamada, T.J. *J. Chem. Soc., Faraday Trans.* **1998**, *94*, 509.

(3) Wiseman, A.J., Holder, S.J., Went, M.J., Jones, R.G. *Polym. Int.* **1999**, *48*, 157.

(4) A late transition metal is usually regarded as one occurring to the right of group 6 in the periodic table, with early transition metals belonging to groups 3, 4, or 5: Tilley, T.D. *The Chemistry of Organic Silicon Compounds: Chapter 24 Transition-metal silyl derivatives*; S. Patai and Z. Rappoport, Ed.; John Wiley and Sons Ltd: USA, 1989, p. 1417.

(5) Yamamoto, K, Okinoshima, H, Kumada, M. *J. Organomet. Chem.* **1970**, *23*, C7.

(6) Brown-Wensley, K.A. *Organometallics* **1987**, *6*, 1590.

(7) (a) Woo, H.-G., Tilley, T.D. *J. Am. Chem. Soc.* **1990**, *112*, 2843; (b) Corey, J.Y., Zhu, X-H., Bedard, T.C., Lange, L.D. *Organometallics* **1991**, *10*, 924; (c) Shu, R., Hao, L., Harrod, J. F., Woo, H.-G., Samuel, E. *J. Am. Chem. Soc.* **1998**, *120*, 12988.

(8) Aitken, C.T., Harrod, J.F. Samuel, E. *J. Am. Chem. Soc.* **1986**, *108*, 4059.

(9) (a) Tilley, T.D. *Acc. Chem. Res.* **1993**, *26*, 22; (b) Rosenberg, L. PhD. Thesis: University of British Columbia, **1993**, p. 14.

(10) Curtis, M.D., Epstein, P.S. *Adv. Organomet. Chem.* **1981**, *19*, 213.

(11) For example: Dichlorotetramethyldisilane: Sigma Aldrich Co. *Handbook of Fine Chemicals and Laboratory Equipment*; USA, 2000, p. 561.

(12) Examples of the preparation of functionalized oligosilanes include: (a) Pannell, K.H., Rozell, J.M., Hernandez, C., *J. Am. Chem. Soc.* **1989**, *111*, 4482; (b) Corey, J.Y., Kraichely, D.M., Huhmann, J.L. Braddock-Wilking, J., Lindeberg, A. *Organometallics* **1995**, *14*, 2704; (c) Sakurai, H., Eriyama, Y., Kamiyama, Y., Nakadaria, Y., *J. Organomet. Chem.* **1984**, *264*, 229; (d) Zech, J., Schmidbaur, H., *Chem. Ber.* **1990**, *123*, 2087; (e) Soldner, M., Schier, A., Schmidbaur, *J. Organomet. Chem.* **1996**, *521*, 295.

(13) Brook, M.A. *Silicon in Organic, Organometallic and Polymer Chemistry*; Wiley-Interscience: USA, 1999; p. 176.

(14) Chatgilialogu, C., Guerrini, A., Lucarini, M., Pedulli, G.F., Carrozza, P., Da Roit, G., Borzatta, V., Lucchini, V. *Organometallics* **1998**, *17*, 2169.

(15) Winkler, H.J.S., Gilman, H. *J. Org. Chem.* **1961**, *26*, 1265.

(16) Ojima, I. Inaba, S. Kogure, T. *J. Organomet. Chem.* **1973**, *55*, C7.

(17) Rosenberg, L., Davis, C.W., Junzhi, Y. *J. Am. Chem. Soc.* **2001**, *123*, 5120.

(18) Corey, J.Y., Zhu, X.-H., *Organometallics* **1992**, *11*, 672. Precedent for the lower migratory aptitude of Si-alkyls relative to Si-aryls in the presence of late transition metals see (a) Fryzuk, M.D., Rosenberg, L., Rettig, S.J., *Inorg. Chim. Acta.* **1994**, *222*, 345; (b) Chauhan, B.P.S., Shimizu, T., Tanaka, M., *Chem. Lett.* **1997**, 785.

(19) Spessard, G.O. and Meissler, G.L. *Organometallic Chemistry*; Prentice Hall: USA, 1996, p. 246.

(20) Gassman, P.G., Macomber, D.W., Willging, S.M. *J. Am. Chem. Soc.* **1985**, *107*, 2380.

(21) (a) Halpern, J., Okamoto, T., Zakhariev, A. *J. Mol. Cat.* **1976**, *2*, 65.

(22) Tilley, T.D. *The Chemistry of Organic Silicon Compounds: Chapter 24 Transition-metal silyl derivatives*; S. Patai and Z. Rappoport, Ed.; John Wiley & Sons Ltd: USA, 1989, p. 1459.

(23) (a) Tilley, T.D. *The Chemistry of Organic Silicon Compounds: Chapter 24 Transition-metal silyl derivatives*; S. Patai and Z. Rappoport, Ed.; John Wiley and Sons Ltd: USA, 1989, pp. 1415-1477; (b) Tilley, T.D. *The Silicon-Heteroatom Bond*; S. Patai and Z. Rappoport, Ed.; John Wiley and Sons Ltd: USA, 1991, pp. 309-364.

(24) Osakada, K., Koizumi, T., Yamamoto, T. *Organometallics* **1997**, *16*, 2063.

(25) (a) Joslin, F.L., Stobart, S.R. *J. Chem. Soc., Chem. Commun.* **1989**, 504; (b) Thorn, D.L., Harlow, R.L. *Inorg. Chem.* **1990**, *29*, 2017.

(26) (a) Fernandez, M., Bailey, P.M., Bentz, P.O., Ricci, J.S., Koetzle, T.F., Maitlis, P.M. *J. Am. Chem. Soc.* **1984**, *106*, 5458; (b) Duckett, S.B., Perutz, R.N. *J. Chem. Soc., Chem. Commun.* **1991**, 28.

(27) (a) Corey, J.Y. *The Chemistry of Organic Silicon Compounds*; S. Patai and Z. Rappoport, Ed.; John Wiley and Sons Ltd: USA, 1989, pp. 1-56; (b) Breliere, C., Carre, F., Corriu, R.J.P., Poirier, M., Royo, G. *Organometallics* **1986**, *5*, 388; (c) Rochow, E.G. *J. Am. Chem. Soc.* **1945**, *67*, 963; (d) Elschenbroich, C., Salzer, A. *Organometallics: A Concise Introduction, 2nd Ed.*; VCH Publishers Inc.: New York, 1992.

(28) (a) R.N. Haszeldine, R.V. Parish, D.J Parry. *J. Chem. Soc. (A)* **1969**, 683; (b) R.N. Haszeldine, R.V. Parish, R.J. Taylor. *J. Chem. Soc., Dalton Trans.* **1974**, 2311.

(29) (a) Osakada, K., Koizumi, T., Yamamoto, T. *Organometallics* **1997**, *16*, 2063; (b) Mann, B.E., Guzman, M.H. *Inorg. Chim. Acta.* **2002**, *330*, 143; (c) Fryzuk, M.D., Rosenberg, L., Rettig, S.J. *Organometallics* **1996**, *15*, 2871.

(30) (a) Woo, H.-G., Waltzer, J.F., Tilley, T.D. *J. Am. Chem. Soc.* **1992**, *114*, 7047; (b) Gauvin, F., Harrod, J.F., Woo, H.G. *Adv. Organomet. Chem.* **1998**, *42*, 363.

(31) Tilley, T.D. *Comments Inorg. Chem.* **1990**, *10*, 37.

(32) Osakada, K. *J. Organomet. Chem.* **2000**, *611*, 323.

(33) (a) Chalk, A.J., Harrod, J.F. *J. Am. Chem. Soc.* **1965**, *87*, 16; (b) Chalk, A.J. *J. Am. Chem. Soc. Chem. Commun.* **1969**, 1207.

CHAPTER 2

Catalysis

2.1 Introduction

As discussed in Chapter 1, Section 1.2, transition metal-catalyzed dehydrogenative coupling of hydrosilanes is a promising alternative to reductive coupling for the formation of Si-Si bonds. Since these catalysts are active for the coupling of secondary silanes, implicit in this method is the retention of reactive, terminal Si-H bonds in the catenated products.[1] The activity of Wilkinson's catalyst, $RhCl(PPh_3)_3$, **1** for the coupling of di-*n*-hexylsilane had already been established by the Rosenberg group.[2] I decided to pursue these discoveries further: to make di-and trisilanes on useful scale, to probe the optimum catalyst structure for these dehydrocoupling reactions, and to expand the understanding of the mechanism responsible for coupling.

The experiments and results described in this chapter address our research group's attempts to identify the best catalyst precursor for the production of dialkyl-substituted di- and trisilanes. The dehydrocoupling reactions of a secondary dialkylsilane, di-*n*-hexylsilane, in the presence of four late transition metal Rh-P catalysts are presented. Understanding the importance of key catalyst structural features in a putative catalytic cycle is also of interest.

2.2 Structural requirements for catalyst activity

My interest in late transition metal catalyzed dehydrocoupling reactions, specifically with Rh-P based complexes, lay in the possible catalyst structural criteria that may be important in successful silane dehydrocoupling. Through modification of the

References p44

catalyst structure it may be possible to answer such questions as the role of the phosphorus ligands, as well as the role and/or fate of the chlorine ligands in these dehydrocoupling reactions. Wilkinson's catalyst, $RhCl(PPh_3)_3$ (**1**) was the rhodium complex originally looked at by the Rosenberg group for the dehydrocoupling reactions of silanes. This is a square planar, 16-electron complex with rhodium in the +1 oxidation state [Rh(I)] and is comprised of three phosphorus ligands and one chloride ligand. This catalyst precursor is known, for catalytic olefin hydrogenation reactions, to lose one of its phosphorus ligands in order to give the coordinatively unsaturated, active catalyst, $[RhCl(PPh_3)_2]$, which is a 14 electron complex.[3] Through monitoring reactions of **1** with silanes by ^{31}P NMR there is evidence that confirms that complex **1** also loses PPh_3 in our systems. This will be discussed further in Chapter 3.

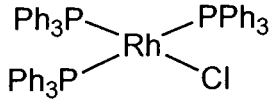

1

To help answer the question of how many phosphorus ligands at rhodium are required for dehydrocoupling catalysis to take place Wilkinson's dimer, $[(PPh_3)_2Rh(\mu\text{-}Cl)]_2$ (**2**), was chosen as a catalyst. Closely related to $RhCl(PPh_3)_3$, this is another square planar, Rh(I) complex, but contains now only two phosphorus ligands per rhodium center.

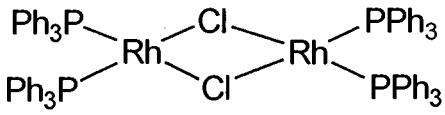

2

This dimer is known to cleave to give the same active catalyst fragment as complex **1**, a $[RhCl(PPh_3)_2]$ 14 electron complex, but without losing an extra phosphorus

References p44

ligand. It is observed by ^{31}P NMR that, in solution, **1** is inevitably in equilibrium with small amounts of **2** (Equation 2.1).[4]

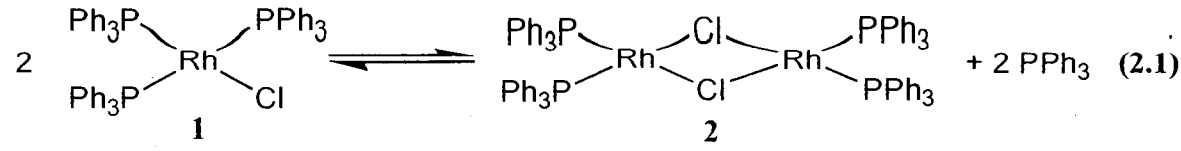

(2.1)

If a P_2Rh fragment is essential for catalytic Si-Si coupling, replacing P_2 with a chelating diphosphine should also give catalysis in these dehydrocoupling of silane reactions. Therefore, the dppe dimer, $[Rh(dppe)\mu\text{-}Cl]_2$ (**3**), a square planar Rh(I) complex with the chelating diphosphine ligand, 1,2- bis(diphenylphosphino)ethane, was also examined. The dppe system also allowed observation of the effect of having the phosphorus ligands in a mutually *cis* position in these dehydrocoupling reactions, since **3** has an ethane backbone linking the phosphines in the ligand that gives a bite angle of 90 degrees with the rhodium center, and does not allow the phosphorus ligands to be trans across a rhodium centre.

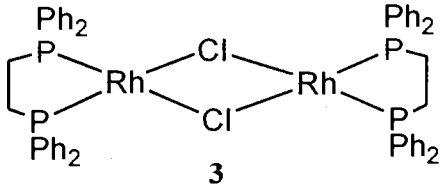

3

To probe whether the chloride ligands play a role in the catalysis of these dehydrocoupling of silane reactions and/or where it goes as the reaction proceeds, a cationic rhodium complex, $[Rh(COD)(PPh_3)_2]^+PF_6^-$ (**4**), with no chloride ligands, was examined. The olefin hydrogenation catalytic cycles for cationic rhodium catalysts (P_2Rh^+) show some differences, in terms of the intermediate species spectroscopically

observed, when compared to the mechanism described for the neutral Wilkinson catalyst (P_2RhCl).[5] Aspects of these catalytic cycles will be discussed further in Chapter 3.

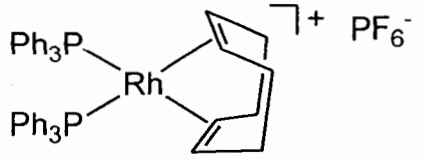

4

To address these basic questions concerning the catalyst structure and to screen for potentially more active and/or useful (e.g. work-up, vide infra) catalysts for synthetic scale production of di-and trisilanes, the performance of these four Rh(I) complexes in dehydrocoupling reactions was evaluated.

2.3 Coupling reactions of di-*n*-hexylsilane catalyzed by Rh-P complexes

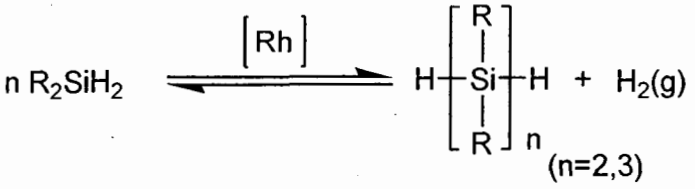

Figure 2.1: General dehydrocoupling reaction with a secondary silane and a rhodium catalyst. Monosilane reacts with Rh(I) complex to give desired di- and trisilane products

2.3.1 Research methods and techniques

The performance of each of the four catalyst precursors (**1-4**) in the dehydrocoupling of di-*n*-hexylsilane was judged by looking at their activity. The activity of a catalyst or turnover frequency (TOF) refers to the number of passes the catalyst makes through the catalytic cycle per unit time (in our case we are looking at one hour). For this thesis, the turnover frequency is calculated by taking the number of moles of monosilane consumed (as determined by ^{1}H NMR), dividing by the number of moles of

catalyst used in the reaction, multiplied by the time to produce the given amount of product. The units, therefore, are mol / mol · time (Equation 2.2).

$$\text{TOF} = \frac{\text{\# moles monosilane consumed}}{\text{\# moles catalyst used x time}} \qquad \textbf{(2.2)}$$

The catalyst precursor activity was also gauged qualitatively. For example, the extent of bubbling (hydrogen gas being released from the reaction as a by-product) was useful in determining how quickly the catalyst was 'turning-over'. A large amount of bubbles from a reaction mixture generally corresponded to a high activity for the catalyst involved. The catalysis was also monitored visually by the colour changes the dehydrocoupling reaction mixtures went through. These changes can correspond to a change in the type of catalyst species found in the reaction mixture, or simply a change in "catalyst resting state", as the catalysis progresses.

Two different experimental conditions were used for the catalytic dehydrocoupling reactions. One set of reactions was carried out under a nitrogen atmosphere in a glove box. The other set of reactions was under dynamic vacuum on a Schlenk (N_2/vac) line. If exposed to any moisture the starting Rh(I) complexes will catalyze a hydrolysis reaction with the silane substrate, di-*n*-hexylsilane, to form siloxanes (Si-O-Si) (Equation 2.3).[6] This reaction is analogous to the desired coupling as they both produce hydrogen gas as a by-product.

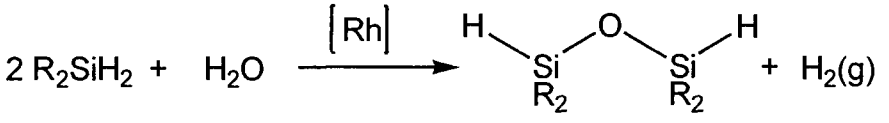

(2.3)

This sensitivity to moisture is so high that even moisture in the nitrogen gas from the Schlenk lines in the lab, if not dried further using molecular sieves in a purification column, will contribute to the formation of these undesirable siloxane compounds. Materials were handled under a purified nitrogen atmosphere at all times.

The catalytic trials were carried out in small glass vials or round bottom flasks, respectively, each containing approximately 2 mg of the Rh(I) complex with varying amounts of the di-*n*-hexylsilane substrate. All reactions were allowed to stir at room temperature and were worked up in the glove box. Work-up involved passing each reaction mixture through a small Florisil® column (a hard powdered magnesium-silica gel adsorbent) with hexanes as the eluent, in order to quench the reaction and remove the Rh(I) catalyst. Removal of the rhodium complexes from the reaction mixture, under a nitrogen atmosphere, is important to avoid hydrolytic decomposition in air, and to obtain only the desired oligosilane products. The hexanes were removed under vacuum and the residue analyzed by ^{1}H NMR (Appendix 1).

Di-*n*-hexylsilane, a high-boiling, non-volatile liquid was chosen as the substrate, to ensure that no loss of the silane occurred under vacuum conditions either during the reaction or during removal of hexanes after work-up (Figure 2.2). The cleanliness of the dehydrocoupling reactions carried out with di-*n*-hexylsilane is attributed to dialkylsilanes showing no redistribution, as described in Chapter 1, Section 1.4.

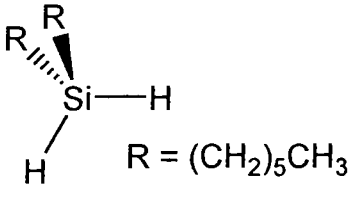

Figure 2.2: Di-*n*-hexylsilane

References p44

The conditions that were varied, other than the structures of the catalyst precursors, in order to gauge their effect on catalyst performance include the catalyst/substrate ratio (from 0.2 to 0.6 mol % catalyst/substrate ratio) and the reaction time (from 0.5 to 4 h) of the dehydrocoupling experiments. An effort was made to keep certain variables constant for these dehydrocoupling reactions, including the stir rate and silane volume. The temperature of the surrounding environment, for these dehydrocoupling reactions, was monitored to ensure that there was no large deviation between the experiments. No attempt was made to control the pressure (except by using vacuum conditions); the barometric pressure was assumed to be constant.

2.3.2 Sources of error

To estimate the reproducibility in the catalytic runs, data was acquired for five different trials (each trial consisting of four identical samples), run under identical conditions with $RhCl(PPh_3)_3$, **1**, under glove box conditions, at room temperature for one hour, and with neat di-*n*-hexylsilane. Results are shown in Figure 2.3. It should be noted that each set of trials was carried out on a different day, so they may have experienced slight changes in variables such as temperature, stir rate, and barometric pressure. Standard deviation calculations were done for each set of trials (range of ±3 to ±6% for each set of trials).[7] The standard deviation value was then divided by the average measured monosilane consumption to give a relative value of error for each trial (See Equation 2.4).

$$\frac{\text{standard deviation (absolute value of error)}}{\text{average measured monosilane consumption}} \times 100\ \% = \text{relative value of error} \qquad \textbf{(2.4)}$$

References p44

The average relative error for all five trials was 11%. This value is considered to be a more reliable estimate of typical error in the measured activities for the dehydrocoupling of silane reactions than just averaging the standard deviations of all twenty reactions, as it better quantifies the day-to-day changes in conditions.

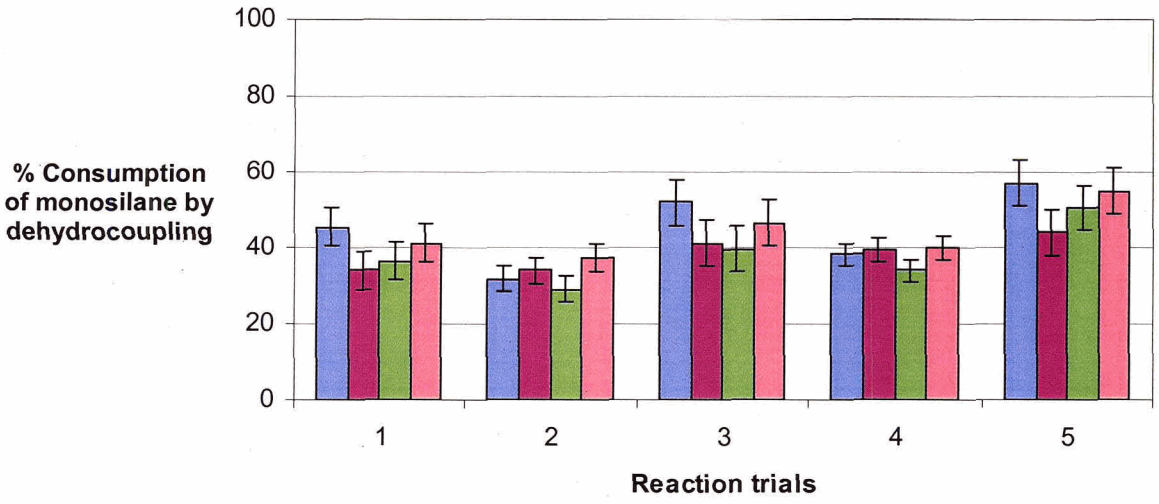

Figure 2.3: Standard deviation data for five different trials (each trial consisting of four vials), run under identical conditions with $RhCl(PPh_3)_3$, **1**, glove box, one hour, neat di-*n*-hexylsilane at 0.2mol% Rh

The consumption of monosilane in these dehydrocoupling reactions varied from trial to trial. The overall consumption varied from 29% to 57% and gave a range of 7.9% to 13.5% for the relative error. The dispersion of the solid rhodium complex on walls of the vessel could cause some problems with the reproducibility of these dehydrocoupling reactions. For example, if the rhodium complex was splashed up onto the side of the glass vials, leaving less complex to react with the silane, then the actual catalyst/substrate ratio would be lower than the assumed starting amount. The integration performed in the ^1H NMR spectra to quantify what amount of monosilane has been consumed may also

References p44

contribute some error towards the final measurements for the dehydrocoupling reactions (See Appendix 1).

The formation of siloxanes, described in Section 2.3.1, can impact the calculated activities for these dehydrocoupling reactions. Instead of the total consumption of monosilane going to form the di- and trisilane products, some monosilane will be used up to form these siloxanes, causing the overall activities/conversions to appear smaller than anticipated. Other groups studying these silane dehydrocoupling reactions have observed the same reproducibility and moisture sensitivity issues.[8] Within experimental error, the amount of siloxanes formed by these dehydrocoupling reactions did not significantly affect the overall activities/conversions. Precautions were taken with all of the dehydrocoupling reactions to try and maintain reproducibility and avoid the formation of siloxanes (See Section 2.3.1).

2.4 Results

2.4.1 Coupling of di-*n*-hexylsilane catalyzed by Rh(I) complexes

Rhodium complexes **2-4** were anticipated to show some activity toward the dehydrocoupling of silanes, based on literature precedent for the activity of these Rh complexes (**1-4**) and similar Rh(I) complexes in catalytic olefin hydrogenation and hydrosilylation processes, and based on their similarity to the highly active **1**.[9] Also, the amount of monosilane consumed by dehydrocoupling in one hour (i.e. the rate of monosilane consumption) was expected to increase with a corresponding increase in the catalyst/substrate ratio, within experimental error as described in Section 2.3.2.

References p44

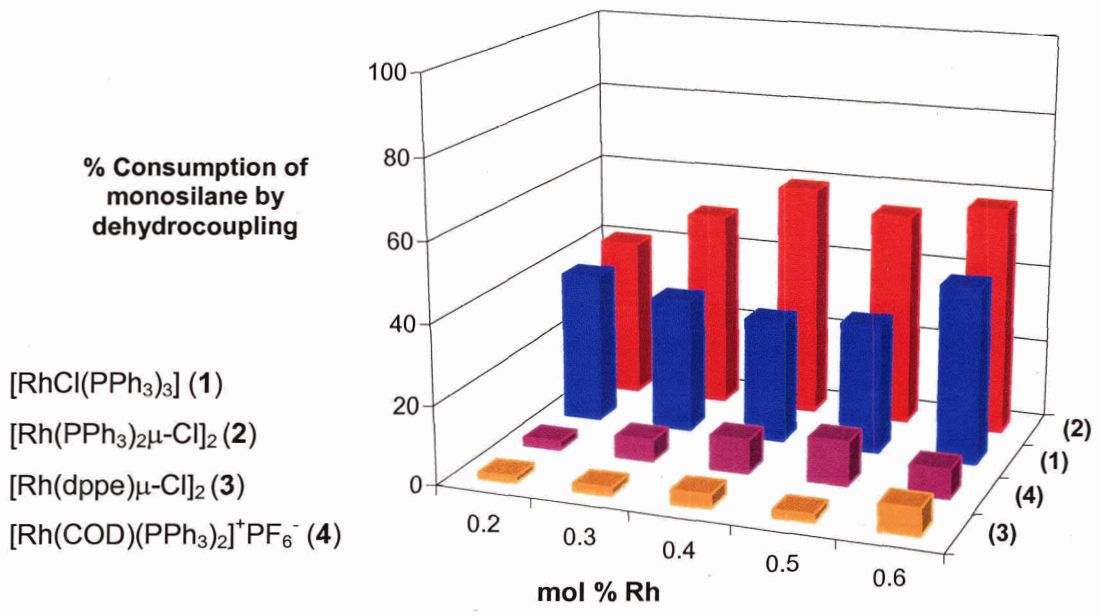

Figure 2.4: Consumption of monosilane by dehydrocoupling with neat di-*n*-hexylsilane and varying mol% Rh, glove box, one hour reaction time

The plot in Figure 2.4 indicates that for all four catalyst precursors, under identical conditions, the total consumption of monosilane increases slightly with the catalyst/substrate ratio used. There is a dramatic difference in the consumption of monosilane between complexes **1** and **2** versus **3** and **4**. Over the range of catalyst/substrate ratios studied, the conversions for $RhCl(PPh_3)_3$, **1**, and $[(PPh_3)_2Rh(\mu\text{-}Cl)]_2$, **2**, were approximately 30% higher than those for $[Rh(dppe)\mu\text{-}Cl]_2$, **3**, and $[Rh(COD)(PPh_3)_2]^+PF_6^-$, **4**.

The plot in Figure 2.4 also shows that for all four catalyst precursors, at a given catalyst/substrate ratio, the total consumption of monosilane increases in the order **3** < **4** << **1** ≤**2**. For example, with a 0.3 mol% catalyst/substrate ratio $[(PPh_3)_2Rh(\mu\text{-}Cl)]_2$, **2**, and $RhCl(PPh_3)_3$, **1**, show conversion percentages greater than 35%, while $[Rh(dppe)\mu$-

$Cl]_2$, **3**, and $[Rh(COD)(PPh_3)_2]^+PF_6^-$, **4**, show conversions below 15%. As discussed in Section 2.3.2, the relative value of error of these dehydrocoupling reactions is around 11%, so within experimental error complexes **3** and **4** show very little activity (i.e. ±1.7%).

Figure 2.5 shows the experimental results from Figure 2.4 in terms of catalyst activity (the number of passes the catalyst makes through the catalytic cycle per unit time), as opposed to monomer consumption.

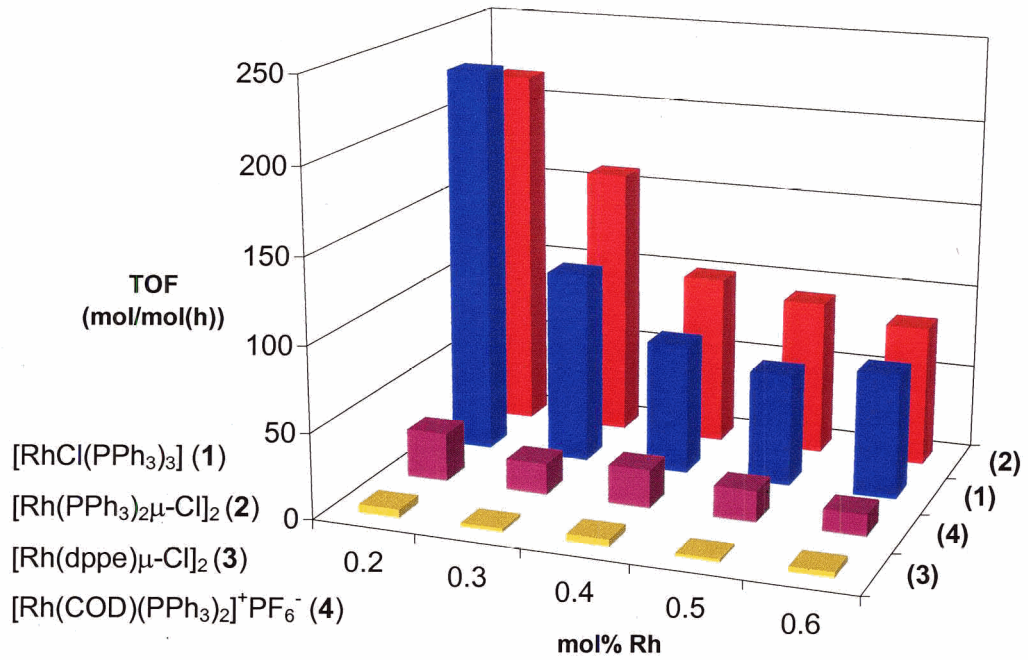

Figure 2.5: Catalytic activities of dehydrocoupling reactions with neat di-*n*-hexylsilane and varying mol% Rh, glove box, one hour reaction time

As in Figure 2.4, this plot also shows that for all four catalyst precursors, at a given catalyst/substrate ratio, the activity increases from lowest to highest corresponding to the complexes **3** < **4** << **1** ≤**2**. For example, with 0.2 mol% catalyst/substrate ratio $[(PPh_3)_2Rh(\mu\text{-}Cl)]_2$, **2**, and $RhCl(PPh_3)_3$, **1**, show activities/TOFs greater than 200

mol/mol(h), while $[Rh(dppe)\mu\text{-}Cl]_2$, **3**, and $[Rh(COD)(PPh_3)_2]^+PF_6^-$, **4**, show activities below 20 mol/mol(h).

Although I expected that the catalyst turnover frequency would increase with a corresponding increase in catalyst/substrate ratio, the plot in Figure 2.5 indicates that for all four catalyst precursors, under identical conditions, the catalyst turnover frequency apparently decreases with the catalyst/substrate ratio used. This phenomenon is related to the relative catalyst surface areas available for reaction with the silane substrate. The extent of dispersion of the catalyst in silane substrate may cause a lower activity to be observed for higher catalyst/substrate ratios. At large mol% catalyst/substrate ratios, there is observed non-homogeneity of the reaction mixtures due to the low volume of silane available relative to solid catalyst.

These initial screening experiments point to the exceptional activity of **1** and **2** toward the dehydrocoupling of di-*n*-hexylsilane. However, there are a number of other factors that affect the apparent activities of theses dehydrocoupling catalysts, apart from the catalyst/substrate ratio. These factors include rate and completeness of hydrogen gas removal, reaction time of the coupling reactions and solubility of the catalyst/substrate mixtures. Each of these variables affects the amount and rate of monosilane consumption in the dehydrocoupling reactions.

2.4.2 Effect of the method of hydrogen gas removal on conversion and activities

The by-product for these dehydrocoupling reactions is hydrogen gas ($H_2(g)$). Earlier work in our group, on the coupling reactions of a range of 2° silanes, showed that there appears to be an equilibrium occurring between the starting silane reagent and the

References p44

oligosilane products, which lies toward the monosilane (Equation 2.5). Removal of $H_2(g)$ helps to shift this rapid, monosilane-favoured equilibrium toward the preferred products.[2]

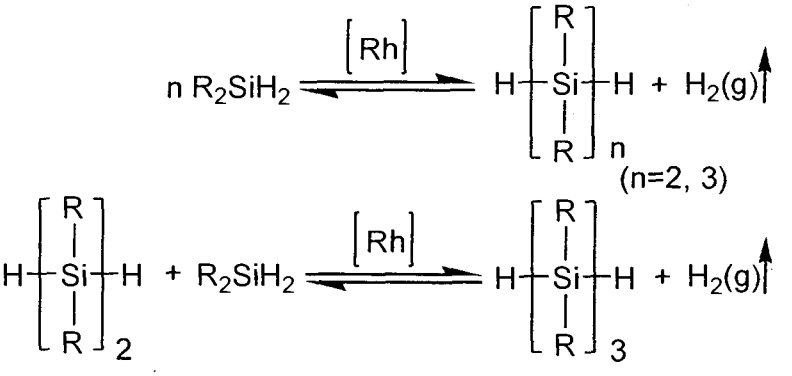

(2.5)

Two issues affect these dehydrocoupling reactions, one concerning the thermodynamics and another concerning kinetics. In terms of thermodynamics, the reactions are driven to completion by the removal of the hydrogen gas from the system. However, these dehydrocoupling reactions occur very quickly, as do the reverse hydrogenolysis reactions. Kinetically, the activities associated with these dehydrocoupling reactions are sensitive to how efficiently (i.e. the rate) hydrogen gas is removed. In the dehydrocoupling experiments carried out for this thesis, the oligosilane formation is very sensitive to the concentration of hydrogen gas and the production of di- and trisilane relies heavily on efficient removal of $H_2(g)$ from the reaction mixture.

In these dehydrocoupling reactions, the hydrogen gas is not completely removed by simply stirring in an open vessel. Incomplete removal leads to an observed rate dependence of the monosilane conversion to the speed of hydrogen gas abstraction. In order to study the importance of hydrogen gas removal to both rate and "completeness", reactions were carried out under both glove box conditions (an open vessel under ambient pressure) and dynamic vacuum conditions (an open vessel under low pressure of approximately 5 torr).

References p44

The amount of monosilane consumed by dehydrocoupling in one hour (i.e. the rate of monosilane consumption) was expected to increase if the reaction were carried out under low-pressure conditions (i.e. more efficient removal of hydrogen gas from the system).

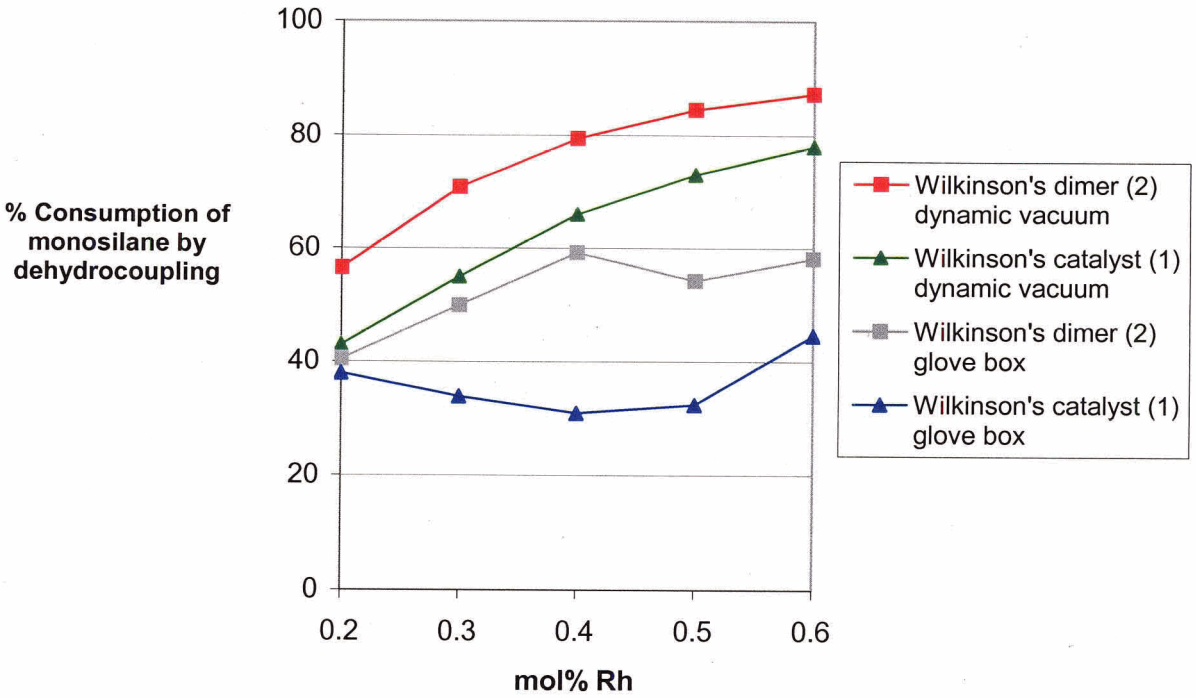

Figure 2.6: Consumption of monosilane by dehydrocoupling with complex **1** and **2** under ambient pressure and low-pressure conditions (one hour reaction time, neat di-*n*-hexylsilane)

The plot in Figure 2.6 indicates that for catalyst precursors, $RhCl(PPh_3)_3$, **1**, and $[(PPh_3)_2Rh(\mu\text{-}Cl)]_2$, **2**, under identical conditions, the amount of monosilane consumed by dehydrocoupling increases dramatically (approximately 40%) from ambient pressure to low pressure. The change in monosilane consumption is more pronounced for greater catalyst/substrate ratios. If there is a low volume of silane with a large amount of catalyst, the dehydrocoupling reactions can proceed giving a larger amount of monosilane

consumption in one hour compared to a smaller catalyst/substrate ratio over the same reaction time period. Therefore, inefficient removal of hydrogen gas under ambient pressure is more defined at higher catalyst/substrate ratios compared to more efficient removal of H_2(g) under low-pressure conditions.

Comparison of the turnover frequencies of the complexes at both ambient and low pressures showed the importance of hydrogen gas removal in these catalytic reactions. It was projected that the turnover frequency (or activity) from the dehydrocoupling reactions with complexes **1** and **2** would increase if carried out under low-pressure conditions and the plot in Figure 2.7 indicates that this was the case.

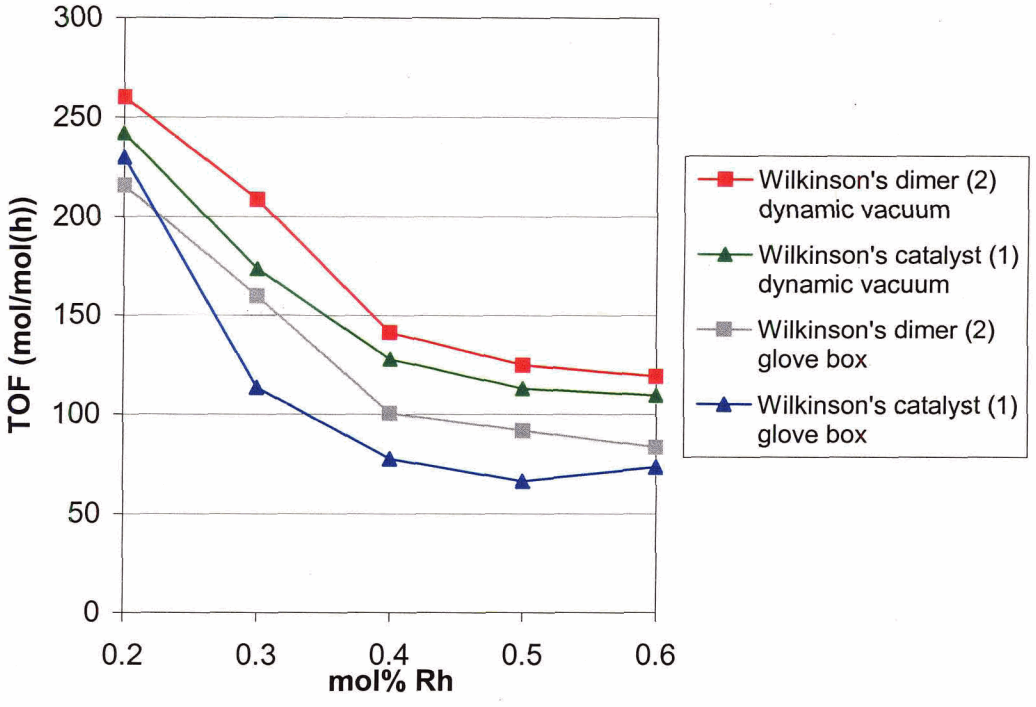

Figure 2.7: Catalytic activities of dehydrocoupling reactions with **1** and **2** under ambient and low pressure conditions (one hour reaction time, neat di-*n*-hexylsilane)

References p44

Figure 2.7 also shows that the catalyst turnover frequency decreases with an increase in the catalyst/substrate ratio used. A similar decrease in activity, observed in Figure 2.5, is explained as a function of the relative catalyst surface areas available for reaction and the extent of dispersion of the catalyst in silane substrate. If less hydrogen gas is produced overall at higher catalyst/substrate ratios, then less $H_2(g)$ is removed from the system regardless of efficiency, causing the activities to be lower. Similar to the trend from Figure 2.6, there is a dramatic difference in the activities of complexes **1** and **2** for dehydrocoupling on changing from ambient and low pressures. Overall, the turnover frequency of dehydrocoupling with **1** and **2** increased by approximately 1.5 times that of ambient pressure conditions.

2.4.3 Effect of reaction time on conversion and product distribution

An obvious factor affecting the conversion of monosilane to di- and trisilane from these dehydrocoupling reactions is their dependence on time. As expected, I observed that increased reaction time results in higher consumption of monosilane. Figure 2.8 (a) shows that the longer a reaction is left under ambient pressure conditions (0.5 to 4 hours), the higher the percent conversion to oligosilane product. After approximately two hours, the rate appears to level out at approximately 60% conversion indicating the presence of a thermodynamic equilibrium for the system under ambient pressure conditions. It should be noted that there is very little contribution from the trisilane product ($\leq 2\%$) under these ambient pressure conditions, so the data shown in Figure 2.8 (a) is only for the disilane product.

References p44

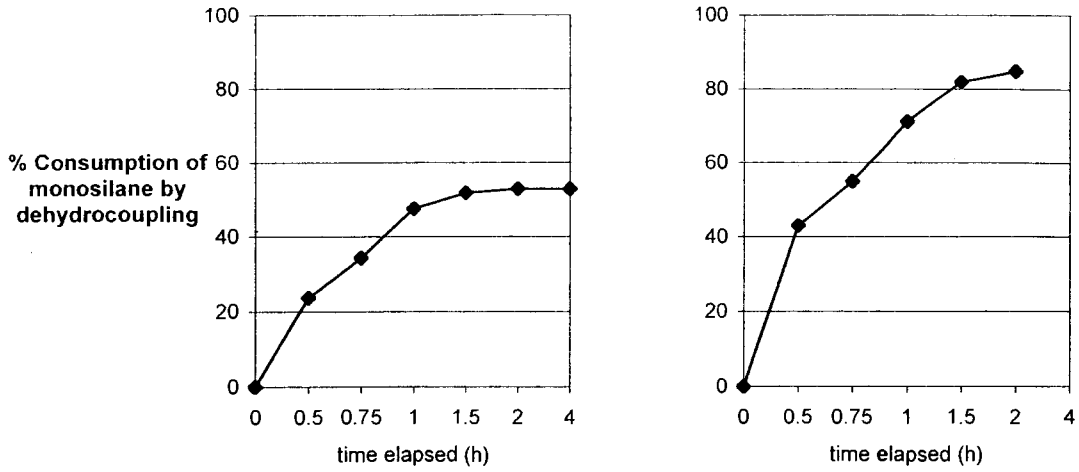

Figure 2.8: Dependence of monosilane consumption on the reaction time under **(a)** ambient pressure conditions; **(b)** low pressure conditions

Figure 2.8 (b) shows a much larger increase in the consumption of monosilane as time increases under low-pressure conditions. After approximately two hours, the conversion is approximately 90%. The line is steeper for low-pressure conditions compared to ambient pressure conditions indicating that a greater amount of conversion is taking place over a shorter period of reaction time. This may be explained due to the more efficient removal of hydrogen gas under low-pressure conditions, which in turn can facilitate a higher conversion to products over less time. Unlike the ambient pressure system, the rate of monosilane consumption under low-pressure conditions only begins to level out slightly after two hours, indicating the presence of an equilibrium, which appears to lie toward the oligosilane products. Under low-pressure conditions, as time increases, the amount of trisilane product becomes greater in relation to the disilane product (Figure 2.9).

References p44

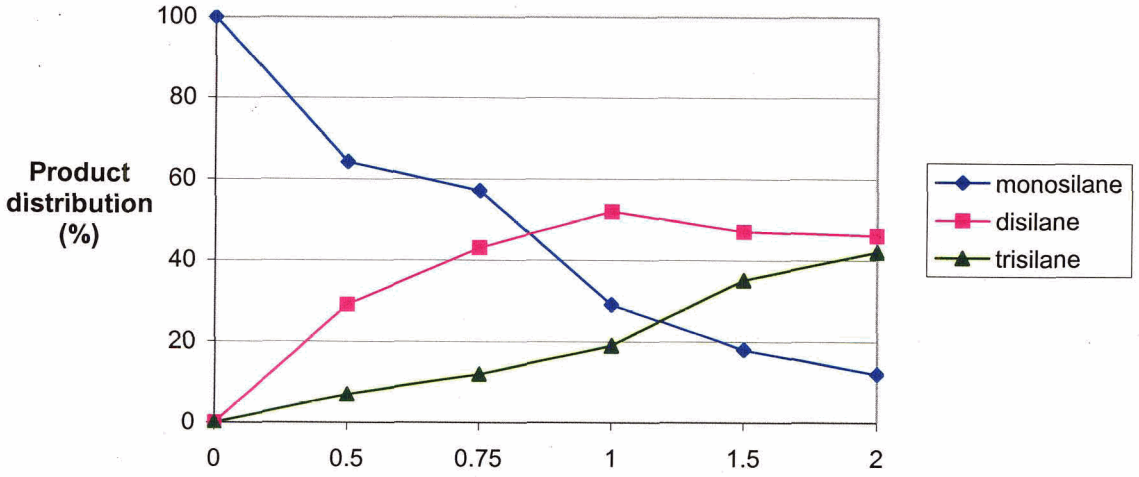

Figure 2.9: Dependence of consumption of monosilane on reaction time where hydrogen gas was removed efficiently under low pressure conditions ($RhCl(PPh_3)_3$, **1** with neat di-*n*-hexylsilane); Standard deviation ±3%

Ultimately, low-pressure conditions cause monosilane consumption and the ratio of trisilane/disilane to increase, which is a function of thermodynamics of the dehydrocoupling reaction. Kinetically, low-pressure conditions allow for the catalyst activities to increase due to more efficient removal of hydrogen gas from the system.

Dehydrocoupling reactions, under low pressure conditions, for $[Rh(dppe)\mu\text{-}Cl]_2$, **3**, and $[Rh(COD)(PPh_3)_2]^+PF_6^-$, **4**, were also studied. Although both of these systems showed an slight increase in monosilane consumption and activity, compared to ambient pressure conditions, they were still much lower compared to $RhCl(PPh_3)_3$, **1**, and $[(PPh_3)_2Rh(\mu\text{-}Cl)]_2$, **2**.

2.4.4 Effect of catalyst solubility on activities and reaction work-up conditions

All of the dehydrocoupling silane reactions discussed so far have involved neat silane substrate. $RhCl(PPh_3)_3$, **1**, and $[(PPh_3)_2Rh(\mu\text{-}Cl)]_2$, **2**, are both very soluble in neat

silane where the initial suspensions get "pulled" rapidly into solution. Factors that can determine how fast (and to what extent) these initial catalyst suspensions go into solution may depend on the rate of initial phosphine dissociation and/or Si-H oxidative addition step(s) that "pull" the catalyst into the silane. Conversely, $[Rh(dppe)\mu\text{-}Cl]_2$, **3**, and $[Rh(COD)(PPh_3)_2]^+PF_6^-$, **4**, are both sparingly soluble in neat silane. They form initial suspensions that persist and never get "pulled" completely into solution. Typically, solutions do not become as intensely coloured for complexes **3** and **4** compared to **1** and **2**, indicating lower solubility.

To see if incomplete dissolution of **3** and **4** in silane could be a cause of the low activities observed in Figure 2.5, trials were run with toluene and methylene chloride with a substrate concentration of approximately 0.5M. The di-*n*-hexylsilane was dissolved in the solvent and this solution was added to the Rh(I) complex. Data from these experiments (Figure 2.10) indicate that changing from neat to solvent conditions had very different effects on catalyst activity for **1** and **2** versus **3** and **4**.

References p44

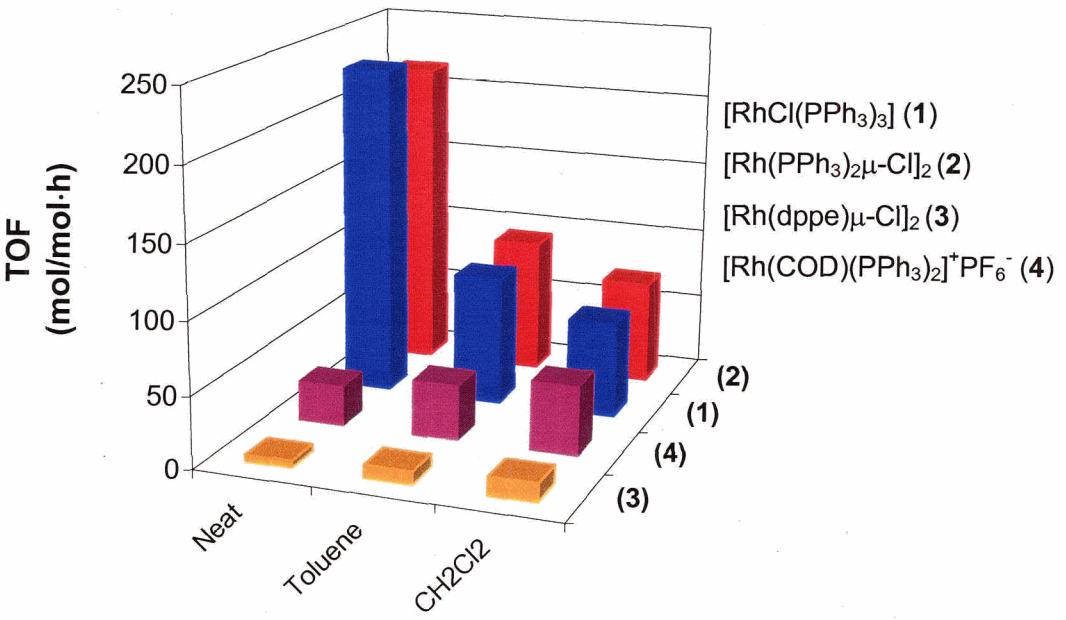

Figure 2.10: Catalytic activities of dehydrocoupling reactions with neat di-*n*-hexylsilane (4.0M) and 0.5M solutions of silane in toluene/or methylene chloride (0.2 mol% Rh, one hour reaction time)

The plot in Figure 2.10 shows that with the addition of solvent, the activity of $[Rh(dppe)\mu\text{-}Cl]_2$, **3**, and $[Rh(COD)(PPh_3)_2]^+PF_6^-$, **4**, increases relative to the low turnover frequency observed with neat silane. Thus, the lower activity observed in Figure 2.5 could be attributed to poor catalyst solubility. Complexes **3** and **4** are both partially soluble (basically a dispersion) in toluene and completely soluble in methylene chloride.

However, Figure 2.10 indicates that with the addition of solvent, the activity of $RhCl(PPh_3)_3$, **1**, and $[(PPh_3)_2Rh(\mu\text{-}Cl)]_2$, **2**, decreases compared to the high turnover frequency with neat silane. Complexes **1** and **2** are both completely soluble in toluene and methylene chloride. The opposite trend observed for these complexes (an decrease in activity when solvent is added) may be attributed to the hydrogen gas solubility in the reaction solutions. If there is an increased concentration of $H_2(g)$ trapped in the solvent, it could impede the conversion to products by allowing the monosilane-favoured

equilibrium to be established. It should be noted that kineticists generally agree that above a certain critical concentration, changes in concentration have no relevance to the rate (or activity) of a reaction.[10]

The relative solubility of $H_2(g)$ in toluene and chloroform (similar to methylene chloride) given by the Solubility Data Series are different for the amount of hydrogen gas that is dissolved in each solvent. At a partial pressure of hydrogen = 1 atm = 101.325 kPa the mole fraction of hydrogen, χ_{H2}, is given as 0.000382 at 298.15K for C_7H_8 (toluene), while for the mole fraction of hydrogen, χ_{H2}, is given as 0.000222 at 298.45K for $CHCl_3$ (chloroform).[11] These mole fraction amounts suggest that more hydrogen gas would be trapped in the toluene-containing dehydrocoupling reactions compared to the methylene chloride-containing dehydrocoupling reactions, thereby lowering the observed activities. However, within experimental error, $RhCl(PPh_3)_3$, **1**, and $[(PPh_3)_2Rh(\mu\text{-}Cl)]_2$, **2**, are seen to have very similar activities, whether the dehydrocoupling reactions were carried out in toluene or methylene chloride.

The activities of **3** and **4** are affected positively when the dehydrocoupling reactions are carried out in solvent. Differences in the rate of reaction for **3** and **4**, compared to **1** and **2**, may explain these results. For instance, if complexes **3** and **4** are slower to react with silane, producing less $H_2(g)$, their overall activities will not be significantly affected by the dissolution of hydrogen gas when placed in solvent. Complexes **1** and **2**, on the other hand, are quick to react with silane, producing large amounts of $H_2(g)$, causing their overall activities to be generally lower when placed in solvent.

References p44

Catalyst 'solubility' (or polarity) can also affect the ease in working up these reactions (see Section 2.3.1). It is observed that the remaining Rh-containing complexes from dehydrocoupling reactions with **3** and **4** are less soluble in the hexanes eluent and 'stick' better to the Florisil® column material, relative to the remaining Rh-complexes from dehydrocoupling reactions with **1** and **2**. This allows for an easier work-up of dehydrocoupling reactions with **3** and **4**, as they require only one Florisil® column to remove the catalyst. Complexes **1** and **2** require more than one Florisil® column to remove the catalyst (see Figure 2.11).

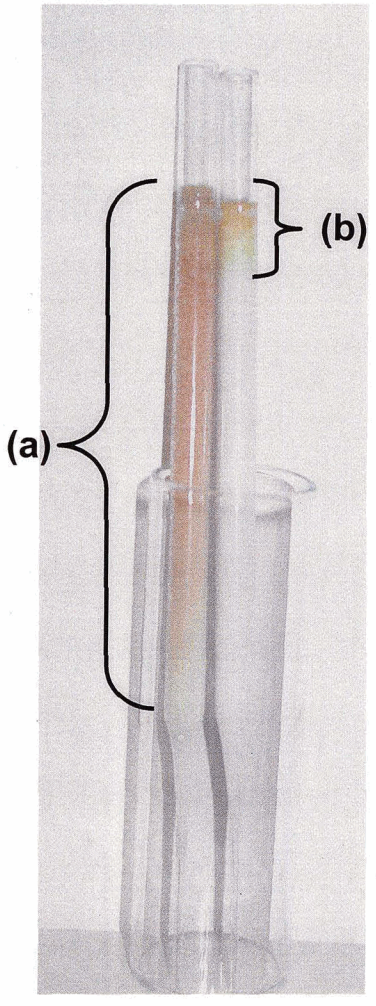

Figure 2.11: Florisil® columns used in work-up of silane dehydrocoupling reactions where: (a) represents an eluted mixture containing complex **2** (similar results observed for **1**) and (b) represents a mixture containing complex **4** (similar results observed for **3**)

References p44

If multiple Florisil® columns are needed in order to remove the catalyst from the reaction mixture it can lead to a prolonged work-up and a lack of confidence that the catalyst has been completely removed. Trace rhodium complexes, present in the reaction mixture, can lead to catalytic hydrolysis to give siloxanes. Another consequence of needing multiple Florisil® columns in the work-up of these dehydrocoupling reactions is that the use of large volumes of hexanes (the eluent solvent) is less environmentally friendly as we try and move toward practicing greener chemistry.

2.5 Conclusions

It was shown that all four complexes, $RhCl(PPh_3)_3$, **1**, $[(PPh_3)_2Rh(\mu\text{-}Cl)]_2$, **2**, $[Rh(dppe)\mu\text{-}Cl]_2$, **3**, and $[Rh(COD)(PPh_3)_2]^+PF_6^-$, **4**, do cause dehydrocoupling of di-*n*-hexylsilane to yield either disilane (1,1,2,2-tetra-*n*-hexyldisilane) or a mixture of disilane and trisilane (1,1,2,2,3,3-hexa-*n*-hexyltrisilane). Within experimental error there is an increase in conversions with an increase in catalyst/substrate ratio.

All four Rh(I) complexes show activity for the dehydrocoupling reactions. The turnover frequency is substantially greater with a small catalyst/substrate ratio relative to larger catalyst/substrate ratio. Overall consumption of monosilane is much greater for reactions under low-pressure conditions than for reactions under ambient pressure conditions. Turnover frequency (activity) is also much greater for reactions in low-pressure conditions than for reactions in ambient pressure conditions.

Other factors are involved with these dehydrocoupling reactions, including hydrogen gas removal, reaction time and solubility of the coupling reactions. The removal of $H_2(g)$ helps to shift a rapid, monosilane-favoured equilibrium toward the di-

References p44

and trisilane products and there is an observed rate dependence of the monosilane conversion to the speed of hydrogen gas abstraction. Catalyst turnover frequency decreases with an increase in catalyst/substrate ratio.

Increased reaction time results in higher consumption of monosilane for these dehydrocoupling reactions. As time increases, the amount of trisilane product becomes greater in relation to the disilane product under low-pressure conditions.

With addition of solvent, the activity of **3** and **4** increases compared to the low turnover frequency with neat silane, while the activity of **1** and **2** decreases compared to the high turnover frequency with neat silane. Lower activity for **3** and **4** is attributed to a function of catalyst solubility (or initial phosphine dissociation/ Si-H oxidative addition that "pulls" the catalyst into the silane), while the decrease in activity for **1** and **2** is explained by the hydrogen gas solubility in the dehydrocoupling reaction solutions (not a concentration effect). Catalyst 'solubility' (or polarity) also affects ease of dehydrocoupling reaction work-up.

2.6 Experimental

2.6.1 General conditions, reagents and instruments

All reactions and manipulations were done under an $N_2(g)$ atmosphere in an MBraun Unilab 1200/780 glove box or using conventional Schlenk line techniques. Hexanes, pentane, benzene and toluene were purified by distillation from Na/benzophenone under argon. Methylene chloride was purified by distillation from P_2O_5 under Ar. Cyclooctene and triphenylphosphine were purchased from Acros Organics while cyclo-octadiene, ammonium hexafluorophosphate (NH_4PF_6), and 1, 2-

References p44

bis(diphenylphosphino)-ethane (dppe) were purchased from Aldrich. Di-*n*-chlorodihexylsilane (*n*-hex_2SiCl_2) was purchased from Gelest and $LiAlH_4$ was purchased from ACP Chemicals Inc. Rhodium trichloride ($RhCl_3 \bullet 3H_2O$) was purchased from Engelhard Exceptional Technologies. No further purifications were performed. Literature methods were used to prepare $[Rh(COD)\mu\text{-}Cl]_2$ (**9**)[12], $[Rh(COE)_2\mu\text{-}Cl]_2$ (**10**)[13], $RhCl(PPh_3)_3$ (**1**)[14] and $[Rh(COD)(PPh_3)_2]^+PF_6^-$ (**4**).[15]

Florisil® was purchased from Aldrich and placed in small 9" Pasteur pipettes plugged with cotton wool. The packed columns were dried for at least 16h in an oven at 110-120°C, then cooled overnight under vacuum in the glove box antechamber. Deuterated benzene (C_6D_6, 99.6 atom % D) and deuterated toluene (C_7D_8, 99.6 % D) were purchased from Cambridge Isotopes or CIL and dried over sodium/benzophenone. The dried, deuterated solvents were then degassed using three "freeze-pump-thaw" cycles and were vacuum transferred before use.

NMR spectra were obtained on a Bruker AC300 instrument operating at 300.133 MHz (^1H), a Bruker AC360 instrument operating at 360.136 MHz (^1H) or 145.784 MHz ($^{31}P\{^1H\}$), or a Bruker AV500 instrument operating at 500.128 MHz (^1H) or 200.463 MHz ($^{31}P\{^1H\}$). With d_6-benzene as solvent ^1H chemical shifts were referenced to C_6D_5H at 7.15 ppm and with d_8-toluene as solvent the spectra were referenced to the CD_2H residual proton at 2.09 ppm), relative to external tetramethylsilane (TMS). ^{31}P chemical shifts were referenced relative to external 85% H_3PO_4(aq).

References p44

Synthesis of di-*n*-hexylsilane, $[(CH_3)(CH_2)_5]_2SiH_2$[16]

Di-*n*-hexylsilane (*n*-hex_2SiH_2) was prepared by $LiAlH_4$ reduction. Dichlorodihexylsilane, $(C_{12}H_{26})SiCl_2$ (25.0 mL, 21.9 g, 81.5 mmol) was added dropwise, with stirring, to an ice-cooled mixture of $LiAlH_4$ (3.85 g, 0.101 mmol) in 200 mL diethyl ether, in a three-necked 500 mL round-bottom flask equipped with a condenser, pressure-equalizing addition funnel and stir bar. After the addition was complete, the resulting mixture was allowed to warm to room temperature, and was stirred overnight. The resulting suspension was then allowed to settle, and the supernatant ether solution was decanted by cannula to a beaker containing a rapidly stirring HCl(aq) solution (3 M, 400 mL), cooled in an ice bath. The mixture was allowed to stir for 45 min, and then the organic layer was extracted. The aqueous layer was washed with diethyl ether (3 × 100 mL), and the combined organic fractions were dried over $MgSO_4$ and filtered. The solvent was removed by distillation, and the resulting residue was distilled under vacuum (47 °C, 0.005 mmHg) to yield a clear, colourless liquid (15.6 g, 95 % yield). ^{1}H NMR (500 MHz, C_6D_6, δ): 3.94 (quintet, 2H, Si-H, $^1J_{Si-H}$ = 183 Hz, $^3J_{H-H}$ = 3.7 Hz), 1.42-1.25 (m, 16H, -CH_2-), 0.91 (t, 6H, CH_3, $^3J_{H-H}$ = 7.1 Hz), 0.66-0.62 (m, 4H, Si-CH_2). $^{13}C\{^1H\}$ NMR (125.8 MHz, C_6D_6, δ): 33.4 (CH_2), 32.3 (CH_2), 26.3 (CH_2), 23.4 (CH_2), 14.7 (CH_3), 9.91 (Si-CH_2). ^{29}Si-INEPT NMR (99.4 MHz, C_6D_6, δ)): -28.4 (s, Si-H).

2.6.2 Syntheses of substrates and complexes

Synthesis of Wilkinson's dimer, $[(PPh_3)_2Rh(\mu\text{-}Cl)]_2$, 2. This catalyst was prepared by literature methods[17] with modifications (specifically the solvent used) as described: $[Rh(COE)_2(\mu\text{-}Cl)]_2$ (0.65 g, 0.91 mmol) was dissolved in dry, degassed CH_2Cl_2 (25 mL). Triphenylphosphine (0.95 g, 3.6 mmol) was added to give a dark

purple-red solution. After one hour of stirring the colour became cherry red and an orange precipitate was formed. The reaction mixture was allowed to stir overnight at room temperature. The solvent and cyclooctene were then removed under vacuum, and the remaining orange solid was filtered, washed with hexanes (3 × 10 mL) and stored in the glove box. ^{1}H-NMR (360 MHz, C_6D_6, δ): 7.82-7.76 (m, 18H, H_o), 6.89-6.83 (m, 36H, $H_{m/p}$). $^{31}P\{^1H\}$-NMR (145.8 MHz, C_6D_6, δ): 52.7 (d, $^1J_{Rh-P}$ = 196 Hz).

Synthesis of dppe dimer, [Rh(dppe)μ-Cl]$_2$, 3. This catalyst was prepared by literature methods[18] with modifications as described: $[Rh(COE)_2(\mu\text{-}Cl)]_2$ (0.43 g, 0.60 mmol) was dissolved in dry, degassed toluene (8 mL) at 60-75°C (with a condenser attached). To the stirred solution was added dppe (0.48 g, 1.2 mmol) in toluene (5 mL) dropwise via Pasteur pipette. During the second half of the addition a yellow crystalline precipitate formed in the orange solution. The mixture was heated for one hour at approximately 100°C, during which time, the orange colour intensified and the yellow precipitate was replaced by an orange crystalline solid. Hexanes (5 mL) was added and the solution was left to cool to room temperature. Crystals were collected by filtration in the glove box and washed with hexanes and pentane (3 × 10 mL); stored in the glove box freezer. ^{1}H-NMR (360 MHz, C_6D_6, δ): 1.71 (br d, 4H, $^3J_{H-H}$ = 45 Hz, PCH_2CH_2P); 7.00-6.95 (m, 24H, $H_{m/p}$); 7.99-7.94 (m, 16H, H_o). $^{31}P\{^1H\}$-NMR (145.8 MHz, C_6D_6, δ): 73.3 (d, $^1J_{Rh-P}$ = 199 Hz).

References p44

2.6.3 Catalytic control reactions

Reactions performed in open vials in the glove box (ambient pressure conditions). In a typical experiment, the catalyst (2 mg) was weighed into 1 dram, flat-bottomed vials. The n-hex_2SiH_2 substrate (50-200 mg, 0.25-1.0 mmol) and a flea stir bar were added to each vial, and the vials were placed on a stir plate, where vigorous stirring was established. After an allotted time period (0.5-4 h), hexane solutions (5 mL) of the reaction mixtures were filtered through Florisil® (described previously in Chapter 2, Section 2.3.1) to quench the reactions and remove the catalyst. An extra 5 mL of hexanes was used to remove the Si-containing products from the columns. The hexanes were removed under vacuum from aliquots (~2 mL) of these solutions, and the residues were dissolved in d_6-benzene for NMR analysis (See Appendix 1).

Reactions performed under dynamic vacuum (low pressure conditions). These reactions were carried out for catalyst on the same scale as described above. The catalyst was weighed into 5 mL round-bottom flasks and flea stir-bars were added. The flasks were attached to a Schlenk line via Teflon needle-valve adaptors (Kontes, 4 mm), evacuated and back-filled with nitrogen. Stir plates were placed underneath the flasks. The silane monomer was weighed in the glove box, and then transferred to 1.0 mL syringes equipped with short lengths of intramedic tubing. The syringes were removed from the glove box with knots tied at the end of the tubing. The knots were clipped off with scissors, immediately before adding the silane to the catalyst via the needle valve under a strong flow of nitrogen. The flasks were then evacuated, and were left under dynamic vacuum. Reaction start times were recorded as the time at which each flask was opened to full vacuum and vigorous stirring was established. To stop the reactions, the

References p44

flasks were sealed under vacuum, taken into the glove box, and quenched on Florisil® columns as described previously.

2.7 References

(1) Rosenberg, L. *Macromol. Symp.* **2003**, *196*, 347.

(2) Rosenberg, L., Davis, C.W., Yao, J. *J. Am. Chem. Soc.* **2001**, *123*, 5120.

(3) Spessard, G.O., Miessler, G.L. *Organometallic Chemistry*; Prentice-Hall: New Jersey, 1997, p. 278.

(4) Cotton, F.A., Wilkinson, G., Murillo, C. A., Bochmann, M. *Advanced Inorganic Chemistry, 6th Edition*; John Wiley & Sons, 1999, p. 1245.

(5) Collman, J. P., Hegedus, L. S., Norton, J. R., Finke, R. G. *Principles and Applications of Organotransition Metal Chemistry*; University Science Books: USA, 1987, p. 535.

(6) (a) Corey, J.Y., John, C.S., Omsted, M.C., Chang, L.S. J. *Organomet. Chem.* **1986**, 304, 93; (b) Corey, J.Y., Chang, L.S., Corey, E.L. *Organometallics* **1987**, *6*, 1595.

(7) For small samples (*N* from 2 to about 10) the range, R = x(largest) – x(smallest), can be used to obtain a reasonably accurate estimate of standard deviation. The range when multiplied by the appropriate value of K_2 (0.43 for five samples) gives an approximate but useful estimate of the standard deviation. See Shoemaker, D.P., Garland, C.W., Steinfeld, J.I., and Nibler, J.W. *Experiments in Physical Chemistry, 4th Edition*; McGraw Hill: New York, 1981, p. 34.

(8) (a) Corey, J.Y., Zhu, X-H., Bedard, T.C., Lange, L.D. *Organometallics* **1991**, *10*, 924; (b) Brown-Wensley, K.A. *Organometallics* **1987**, *6*, 1590; (c) Bessmertnykh, A.G., Blinov, K.A., Grishin, Y.K., Donskaya, N.A., Tveritinova, E.V., Yur'eva, N.M., Beletskaya, I.P. *J. Org. Chem.* **1997**, *62*, 6069; (d) Chang, L.S., Corey, J.Y. *Organometallics* **1989**, *8*, 1885.

(9) Hydrosilylation: (a) Brook, M.A. *Silicon in Organic, Organometallic and Polymer Chemistry*; Wiley-Interscience: USA, 1999, p 413 and references therein; Hydrogenation: (b) Elschenbroich, C., Salzer, A. *Organometallics: A Concise Introduction*; VCH Publishers, Inc.: New York, 1992, p. 427.

(10) The rhodium coordination sphere will only allow so many units of silane to approach. Critical concentration value generally accepted to be around 0.4 to 0.5M. Bohne, C. Private communication. University of Victoria, June 24th, 2005.

(11) Young, C.L. *Solubility Data Series: Volume 5/6: Hydrogen and Deuterium* (1981), pp. 247 (chloroform) and 170 (toluene).

(12) van der Ent, A., Onderdelinden, A.L. *Inorg. Synth.* **1990**, *28*, 90.

(13) Giordano, G., Crabtree, R.H. *Inorg. Synth.* **1990**, *28*, 89.

(14) Young, J.F., Osborn, J.A., Jardine, F.H., Wilkinson, G. *Chem. Commun.* **1965**, 131.

(15) Schrock, R.R., Osborn, J.A. *J. Am. Chem. Soc.* **1971**, *93*, 2403.

(16) Kunai, A., Sakurai, T., Toyoda, E., Ishikawa, M. *Organometallics* **1996**, *15*, 2478.

(17) (a) Osborn, J.A, Jardine, F.H., Young, J.F., Wilkinson, G. *J. Chem. Soc. A.* **1966**, 1711; (b) Haines, L.M. *Inorg. Chem.* **1970**, *9*, 1517; (c) Phillipot, K. PhD. Thesis. L'Universite Paul Sabatier de Toulouse, **1993**, p.152.

(18) (a) Fairlie, D.P., Bosnich, B. *Organometallics* **1988**, *7*, 936; (b) Ball, G.E., Cullen, W.R., Fryzuk, M.D., James, B.R. *Organometallics* **1991**, *10*, 3767.

CHAPTER 3

Mechanistic Considerations

3.1 Introduction

The mechanisms of Si-Si bond formation at late transition-metal centers remain a subject of some debate. The debate centers around whether a metal silylene ("M=Si") intermediate is involved in (or required for) Si-Si bond formation, or whether oxidative addition and reductive elimination steps involving only M-Si single bonds are responsible for Si-Si coupling.[1] The right-hand side of Figure 3.1 shows successive oxidative addition of Si-H bonds to a metal centre and subsequent reductive elimination to facilitate the formation of Si-Si bonds. The left-hand side of Figure 3.1 shows a different route involving the oxidative addition of Si-H bonds, a 1,2-hydrogen migration, insertion of a silyl ligand into a metal-silylene, and subsequent reductive elimination of a metal-silicon bond to give the Si-Si products.

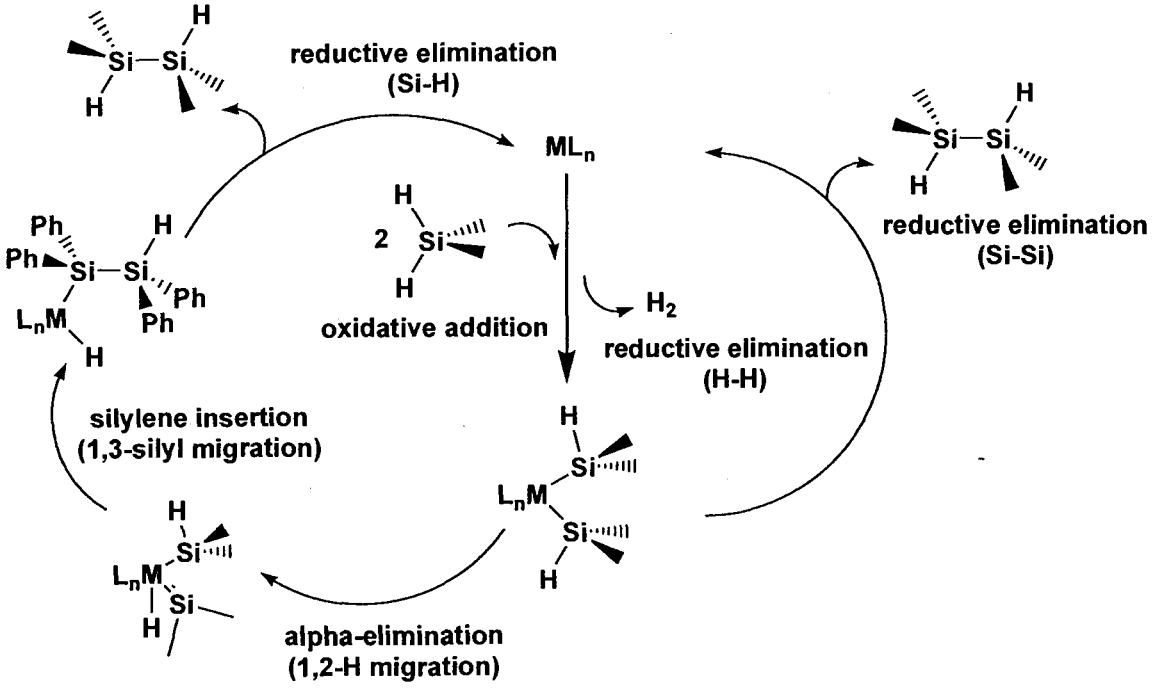

Figure 3.1: Proposed mechanisms for the formation of Si-Si bonds [1]

The discovery by Wilkinson (and independently and nearly simultaneously by Coffey) in 1965 that $RhCl(PPh_3)_3$, **1**, could catalyze the hydrogenation of alkenes was a momentous event in the history of organometallic chemistry.[2] This breakthrough stimulated a great deal of research on the elucidation of catalytic mechanisms in general, and in particular on the determination of the mechanism of homogeneous hydrogenation using Rh(I) complexes. These studies provide insight and a starting point of reference into mechanistic issues to do with Rh-catalyzed dehydrocoupling of silanes.

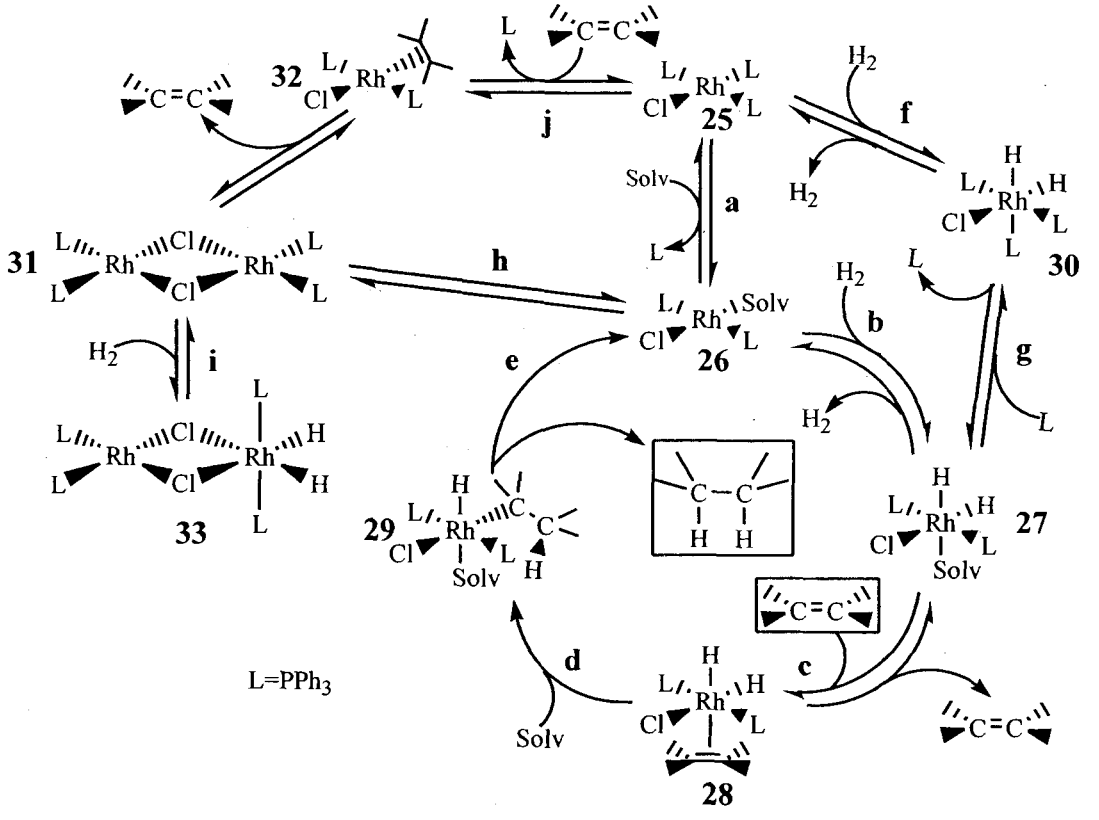

Figure 3.2: Mechanism of hydrogenation by Wilkinson's catalyst (Spessard, Gary O.; Meissler, Gary L., Organometallic Chemistry, 1st Edition, © 1997. Reprinted by permission of Pearson Education, Inc., Upper Saddle River, NJ.)[2]

An accepted mechanism for the catalytic hydrogenation of alkenes by Wilkinson's catalyst, **1** is shown in Figure 3.2.[3] It is useful as a guide to possible intermediates for our Rh(I) dehydrocoupling of silane systems. The active rhodium

complex [RhCl(L_2)(Solv)], **26**, is similar to the rhodium-based complexes described in this thesis. According to work done by Halpern et al., dissociation of a phosphorus ligand from **25** occurs to give **26**. The same dissociation step is observed in reactions of complex **1** with di-*n*-hexylsilane by $^{31}P\{^1H\}$ NMR in this thesis (See Section 3.3.2.2). Although the mechanism in Figure 3.2 involves olefin hydrogenation, the reverse of this catalytic cycle, alkane dehydrogenation, may help in identifying intermediate Rh complexes, be they mononuclear or dinuclear in nature, which could be present in our silane dehydrocoupling reaction mixtures. Essentially, H-H bonds can be considered analogous with HR_2Si-H type bonds studied in this thesis. The types of products that might be observed could consist of Rh-Si, Rh-H and/or Rh-P containing complexes along with some organosilanes. For example, oxidative addition of dihydrogen as seen in pathway **b** to give complex **27** in Figure 3.2 could be replaced by the addition of a Si-H bond, to give [RhCl(L_2)(Solv)(H)($SiHR_2$)], as a possible first step in the silane dehydrocoupling reactions. Halpern and colleges identified eight intermediate species (**25-33**) in Rh-catalyzed olefin hydrogenation mixtures. It should be noted that not all intermediates contribute to productive catalysis. Some of these species/intermediates can still access the catalytic cycle, but not directly. In Figure 3.2 the hydrogenated dimer, complex **33**, does not have a direct role in catalytic olefin hydrogenation. The equilibria involving **31** and **33** are insignificant in the presence of H_2, which intercepts complex **26**, preventing its dimerization.[4] If one of the hydrogen ligands, in complex **33**, were replaced by a silyl ligand, [(Rh(L_2)(μ-Cl))$_2$(H)($SiHR_2$)], this could be another possible intermediate in the Rh-catalyzed silane dehydrocoupling reactions that are the focus of this thesis.

References p111

To investigate the mechanism of our dehydrocoupling reactions we wanted to find spectroscopic evidence for specific intermediates. To see whether a metal silylene ("M=Si") intermediate is involved or whether oxidative addition and reductive elimination steps are solely responsible for Si-Si coupling, possible intermediates containing silylene and/or silyl-type ligands were searched for in these reactions. Stoichiometric studies were carried out and the hydrogenation intermediates from Halpern's work (Figure 3.2) and early silane addition chemistry, described in Chapter 1, Section 1.5.1, were used to guide the analysis of the resulting spectra.

3.2 Guide to NMR spectroscopic analysis of rhodium-phosphine complexes
Monitoring by NMR spectroscopy

The NMR-active nuclei observed and discussed in this thesis include ^{1}H, ^{31}P, ^{103}Rh and ^{29}Si. All of these nuclei have a quantum spin number (I) of ½ and natural abundances of 100% with the exception of ^{29}Si, which is 4.70%. The most commonly used experiments are ^{1}H and ^{31}P NMR as we can 'see' the ^{103}Rh, ^{31}P, and ^{29}Si nuclei via the ^{1}H NMR spectra and the ^{103}Rh nuclei and ^{1}H (if necessary) via the ^{31}P NMR spectra.

3.2.1 First and second-order spin coupling patterns

Nuclei that are physically close to one another, through bonding, exert an influence on each other's effective magnetic field. This effect shows up in the NMR spectrum when the nuclei are nonequivalent and is called spin-spin coupling or J coupling. The systems that generate these kinds of spectra are usually first-order, and give easily predicted splitting patterns. Second-order spectra arise when the frequency separation between multiplets due to different equivalent sets of nuclei is similar in

magnitude to the coupling constant between them; under these circumstances the effects due to spin coupling and chemical shift have similar energy and become intermingled, leading to less straightforward relative line intensities and line positions.

A nomenclature has been adopted for cases in which the chemically non-equivalent sets of spins are labelled with letters from the alphabet, choosing letters that are well separated in the alphabetic sequence to signify large chemical shift separation. When the chemical shifts between the coupled nuclei are relatively small, the spins are labelled with letters close together in the alphabet. For example, two coupled phosphorus nuclei with similar chemical shifts are given the letters AB. Mixed systems are also possible and a commonly encountered one is the three spin ABX grouping where two nuclei resonate close together and a third has a very different chemical shift or is of a different element.[5] For example, the $^{31}P\{^{1}H\}$ NMR spectrum of the mononuclear rhodium complex $RhCl(PPh_3)_3$, **1**, shows a pair of doublets assignable to the two equivalent ^{31}P nuclei and a pair of triplets due to the unique P nucleus trans to chloride (Figure 3.3). The smaller splitting is due to P-P coupling, the larger to Rh-P coupling. The spin system for complex **1** follows an A_2BX pattern where A, B = P and X = Rh as shown in Figure 3.4. Meanwhile, the $^{31}P\{^{1}H\}$ NMR spectrum of $[(PPh_3)_2Rh(\mu\text{-}Cl)]_2$, **2**, shows only a doublet, assignable to four equivalent ^{31}P nuclei (Figure 3.5). The spin system for complex **2** follows an A_2X pattern where A = P and X = Rh (Figure 3.6). This arrangement is effectively due to the presence of a centre of inversion for the dinuclear $[(PPh_3)_2Rh(\mu\text{-}Cl)]_2$, **2**.

References p111

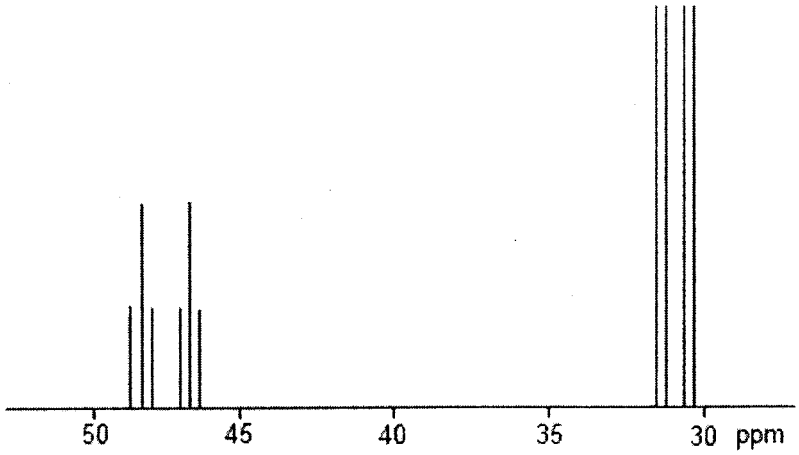

Figure 3.3: Line representation of the $^{31}P\{^{1}H\}$ NMR spectrum of $RhCl(PPh_3)_3$, **1**

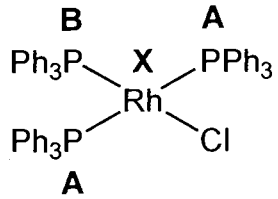

Figure 3.4: A_2BX spin system of $RhCl(PPh_3)_3$, **1**

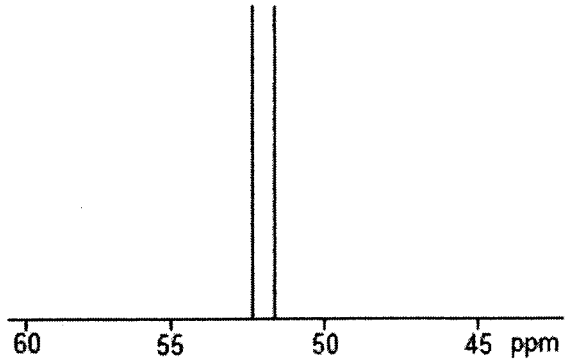

Figure 3.5: Line representation of the $^{31}P\{^{1}H\}$ NMR spectrum of $[(PPh_3)_2Rh(\mu\text{-}Cl)]_2$, **2**

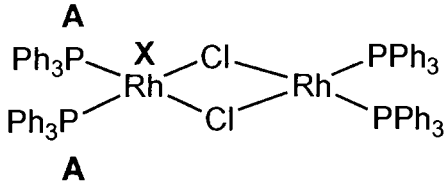

Figure 3.6: A_2X spin system of $[(PPh_3)_2Rh(\mu\text{-}Cl)]_2$, **2**

3.2.2 Diagnostic features of ^{31}P NMR spectra relevant to structures discussed in this thesis

In this thesis, the most evident observed spin-spin couplings are between ^{1}H, ^{31}P and ^{103}Rh as the natural abundance for ^{1}H, ^{31}P, and ^{103}Rh nuclei is 100% while ^{29}Si is only 4.70%. This coupling can make the resulting NMR spectra more complicated. The ^{31}P NMR experiment typically is run proton decoupled. This ^{1}H decoupling means that spin-spin couplings between ^{31}P and ^{1}H are seldom observed, greatly simplifying the ^{31}P spectrum and making it less crowded. All of the ^{31}P NMR experiments in this thesis are of this form and are denoted as $^{31}P\{^{1}H\}$.

Typically, a signal in the $^{31}P\{^{1}H\}$ NMR spectrum for one phosphorus nucleus will show up as a singlet. Uncomplexed and complexed PR_3 can be distinguished by $^{31}P\{^{1}H\}$, since the uncomplexed ligands (PR_3, or $O{=}PR_3$ impurities) give single lines in the $^{31}P\{^{1}H\}$ NMR spectrum and the Rh-complexed phosphine ligands show a doublet, due to coupling to the (100% abundant ^{103}Rh with I = ½) rhodium nuclei. The complexity of these NMR spectra depends on how many types of ^{31}P environments there are in the Rh-P complex. Although some dinuclear complexes such as $[Rh(PPh_3)_2(\mu\text{-}Cl)]_2$, **2**, have a very simple NMR spectrum other, less symmetric or simple dinuclear complexes can have quite complex NMR spectra. An example of a slightly more complex system with a much more complicated $^{31}P\{^{1}H\}$ spectrum is the dinuclear compound $[\{Rh(dppe)\}_2(\mu\text{-}H)(\mu\text{-}Cl)]$ from the work of Ball et al.[6] Due to the bridging hydride, chloride and the ethylene linkers in the chelate ligand, the four phosphorus ligands are not equivalent and exhibit the following $^{31}P\{^{1}H\}$ NMR spectrum in Figure 3.7.

References p111

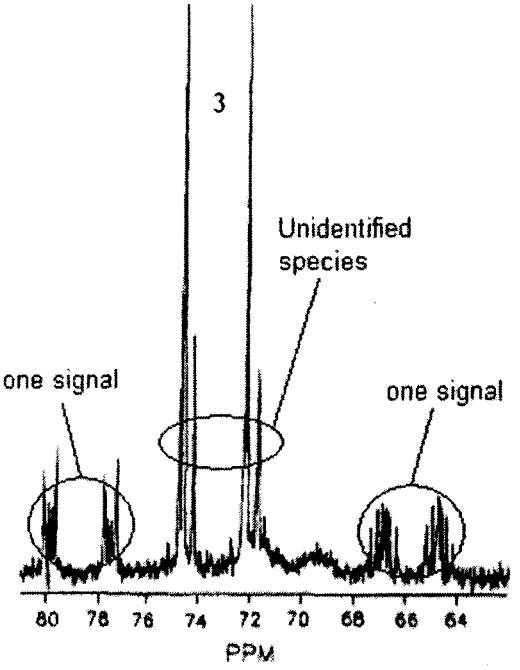

Figure 3.7: 121.2 MHz $^{31}P\{^{1}H\}$ NMR spectrum (3:1 C_6D_6/CD_3OD) of an Rh-catalyzed hydrogenation reaction at 1 atm of H_2. Peaks due to $[\{Rh(dppe)\}_2(\mu\text{-}H)(\mu\text{-}Cl)]$ are centered at about 78.7 ppm ($^{1}J_{P\text{-}Rh}$ = 196 Hz) and 65.8 ppm ($^{1}J_{P\text{-}Rh}$ = 167 Hz); major doublet is due to $[Rh(dppe)\mu\text{-}Cl]_2$, **3** [6]

The spin system for this complex follows an AA'BB'XX' pattern where A, B = P and X = Rh (Figure 3.8). As mentioned above, the four phosphorus ligands are not equivalent. More specifically, the phosphorus nuclei labelled A and A' (or B, B') are chemically equivalent, but magnetically inequivalent. To differentiate between the two very similar phosphorus nuclei, the prime symbol (') is used. This nomenclature is also applied to the rhodium nuclei in these complexes (X and X'). Similarly complex spectra were observed for the systems presented in this thesis.

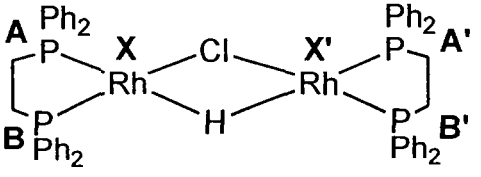

Figure 3.8: AA'BB'XX' spin system of $[\{Rh(dppe)\}_2(\mu\text{-}H)(\mu\text{-}Cl)]$

3.2.2.1 Diagnostic chemical shift features of ^{31}P NMR spectra relevant to structures discussed in this thesis

The chemical shift values that are typically observed for the Rh-P systems in this thesis range from –20 to approximately 100 ppm. More specifically, the signals that are observed in the 35-90 ppm range correspond to phosphorus-containing Rh complexes, whether mono- or dinuclear in nature. Signals in the 20-30 ppm region correspond to the oxide derivatives of the phosphine ligands (for example $O=PPh_3$), which can arise due to the air-sensitivity of these compounds. The solution mixtures were also monitored to –20 ppm to encompass the region of the $^{31}P\{^1H\}$ NMR spectrum that includes the signals for free $PPh_2CH_2CH_2PPh_2$ (dppe) at –12 ppm and –5 ppm for free PPh_3 (triphenylphosphine). The J coupling values that are typically observed for four-to-six coordinate Rh-phosphine complexes are around $^1J_{P\text{-}Rh}$ = 120-210 Hz and $^2J_{P\text{-}P}$ = 15-35 Hz (cis J values < trans J values). The $^1J_{P\text{-}Rh}$ values for Rh(I) phosphine complexes are usually in the range of 140 to 210 Hz, while Rh(III) phosphine complexes are usually found at lower J values.[7]

3.2.3 Diagnostic chemical shift features of ^1H NMR spectra relevant to structures discussed in this thesis

The ^1H chemical shift range that was monitored for the systems in this thesis was from -20 to 8.5 ppm. This covers four regions, each specific to a particular type of proton environment: [-20-0ppm (Rh-H), 0-2.5 (alkyl C-H), 2.5-6.5ppm (Si-H), 6.5-8.5ppm (aromatic C-H)]. For each of these regions in the ^1H NMR there were certain changes that I was looking for, which are discussed further below.

Signals observed in the rhodium hydride region from –20 to 0 ppm would indicate oxidative addition of Si-H to the Rh center of the complex had occurred. Agostic Si-H bonds, as well as bridging hydrides from dinuclear complexes, may also show up in this region of the ^{1}H NMR spectrum.[8]

The hexyl groups, $CH_3(CH_2)_5$, of di-*n*-hexylsilane are observed from 0 to 2.5 ppm in the alkyl region of the ^{1}H NMR spectrum. Signals for hexyl groups attached to the mono-, di- and trisilane products tend to shift downfield in the order monosilane > disilane > trisilane. Although signals in this region of the spectrum can give information about the hexyl groups, it is comprised of mostly overlapping multiplets that are difficult to resolve and/or assign. ^{1}H NMR chemical shift values for the R groups of a metal-silylene (=SiR_2), are typically observed at much higher field than those of metal-silyl (-$SiHR_2$) complexes.

A signal due to the starting silane reagent in this thesis, di-*n*-hexylsilane, is observed in the Si-H region at 3.9 ppm (see Figure 3.9). The Si-H signals for any new silicon-containing products will be observed in the silicon-hydride region from approximately 2.5-6.5 ppm in the ^{1}H NMR spectrum, as will those for Rh complexes that contain a silyl (-$SiHR_2$) ligand. Any new organosilane products containing Si-Cl as well as Si-H can also be found in this region such as SiR_2HCl and any of the oligomeric derivatives (Equation 3.1).

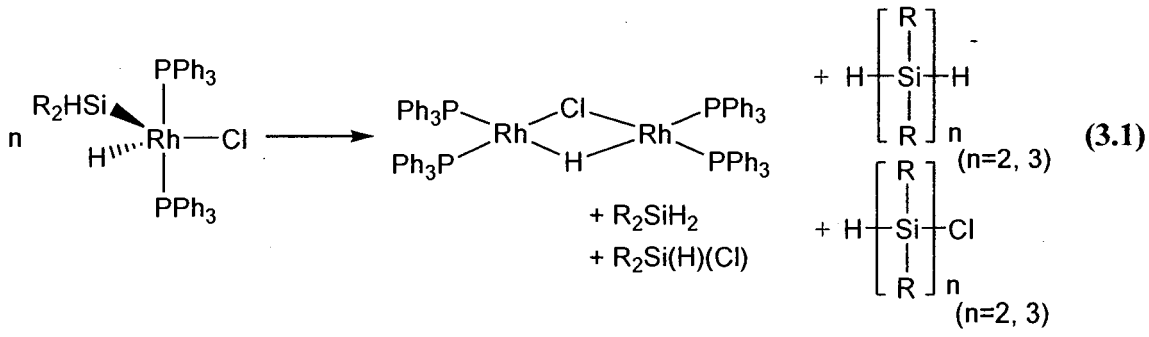

(3.1)

Although definitive assignments have not yet been made, Si-H signals for organosilanes containing chlorine ligands (e.g. SiR_2HCl) are expected to be around 4.5 to 5.5 ppm in the ^1H NMR spectrum.[9] Signals corresponding to these organosilanes are observed in many of the ^1H NMR spectra for the stoichiometric dehydrocoupling reactions described in this thesis. The Si-H signals of siloxanes (-Si-O-Si-) that are formed from exposure of these sensitive reactions to water can also show up in this region. There are also additional, smaller spin satellite lines observed in this Si-H region of the ^1H NMR spectrum due to coupling to the 4.70% of ^{29}Si. These are usually found in the base line centered around the intense signal due to the main Si-H resonance and, while weak, they can often be used to obtain extra information about the molecules.

References p111

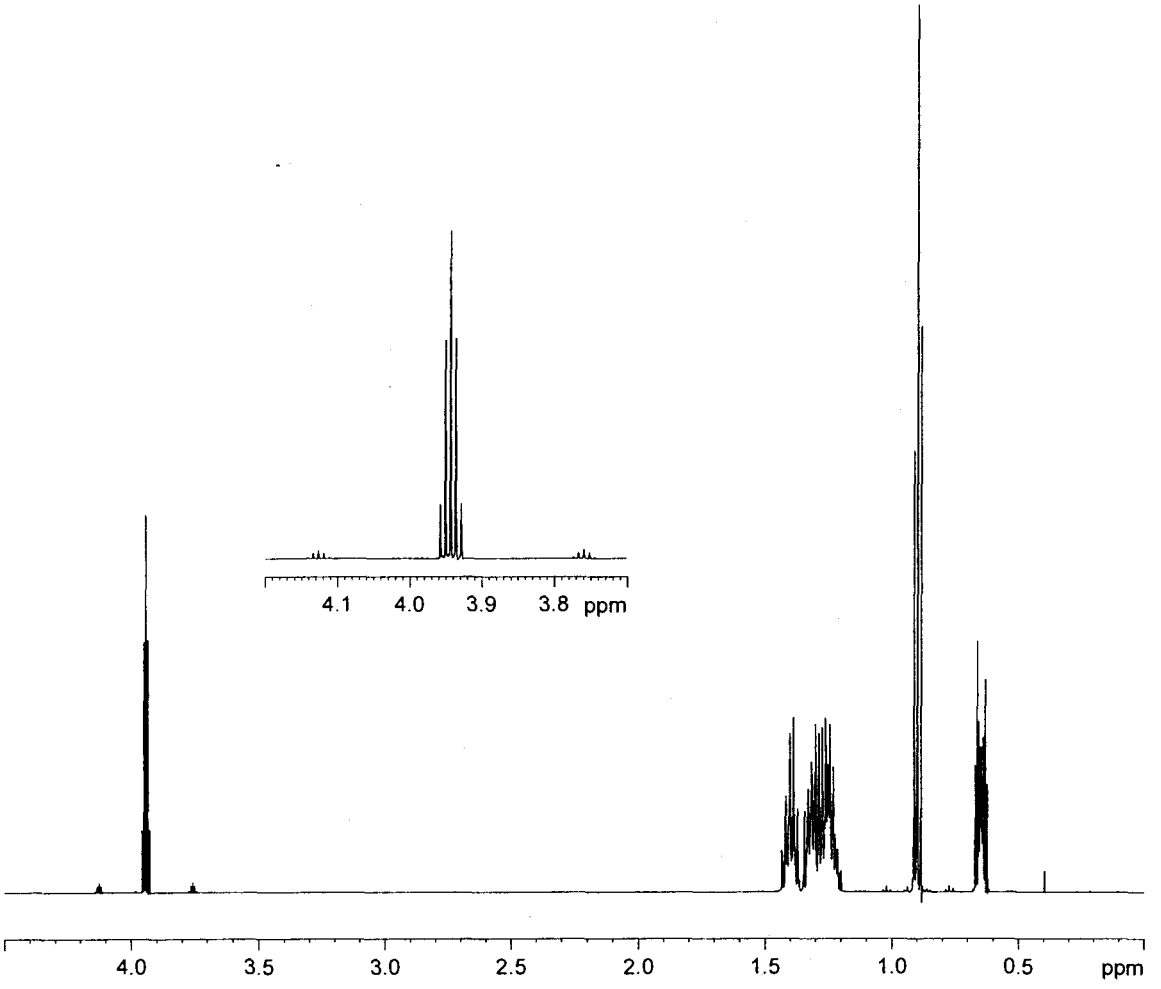

Figure 3.9: 500 MHz ^{1}H NMR spectrum of di-*n*-hexylsilane in C_6D_6

Any changes in the phenyl groups on the phosphorus ligands may be observed in the aromatic region (6.5-8.5 ppm) of the ^{1}H NMR spectrum. Unfortunately, due to the overlapping multiplets that are usually seen in this aromatic region, it can be difficult to identify each species' signal. Addition of further signals corresponding to the oxides for PPh_3 and bis(diphenylphosphino)ethane (dppe) ligands can also make this aromatic region quite complex. ^{31}P decoupled proton experiments (^{1}H{^{31}P}) can also be useful in some cases as the Rh-H coupling can be observed without the interference of phosphorus

ligands and their subsequent coupling. Some of the ^{1}H NMR experiments in this thesis will follow this form and are denoted as $^{1}H\{^{31}P\}$.

3.3 Stoichiometric Reactions of di-*n*-hexylsilane with rhodium catalyst precursors

Stoichiometric reactions were carried out in deuterated benzene or toluene for each of the four Rh(I) complexes of interest using 1, 2, and 2.5 or 5 equivalents of neat di-*n*-hexylsilane per rhodium center. Colour changes were noted throughout these reactions and the samples were monitored by ^{1}H and $^{31}P\{^{1}H\}$ NMR spectroscopy to follow the evolution of these mixtures over a period of several days. When the stoichiometric reaction mixtures appeared to reach a steady state, they were also analyzed by variable temperature NMR and 2D NMR experiments.

I focused mainly on reactions of the rhodium complex $[(PPh_3)_2Rh(\mu\text{-}Cl)]_2$, **2**, which is a clean source of the P_2RhCl fragment we suspect may be active in the silane dehydrocoupling reactions. Stoichiometric reactions were carried out with **2** and di-*n*-hexylsilane in deuterated benzene or toluene, in which both starting materials were completely soluble. This extent of total solubility was not observed for complexes $[Rh(dppe)\mu\text{-}Cl]_2$, **3**, or $[Rh(COD)(PPh_3)_2]^{+}PF_6^{-}$,**4**. Although the solubility of $RhCl(PPh_3)_3$, **1**, was comparable to that of **2**, under the conditions of these reactions, there are other factors that become an issue with this complex (see below).

As described in the Introduction: Section 3.1, one of the possible by-products/ or steps of the hydrogenation catalyzed by these rhodium complexes is the loss of a phosphine ligand.[4] We presume that in order to gain the active catalyst species needed for catalysis the starting complex $RhCl(PPh_3)_3$, **1**, loses one PPh_3 to give $[RhCl(PPh_3)_2]$. From monitoring reactions of complex **1** with di-*n*-hexylsilane by $^{31}P\{^{1}H\}$ NMR there is

evidence of free PPh_3 ligand signal growing in. If the starting complex includes free PPh_3 ligand, as an impurity, it may be difficult to distinguish between it and any additional PPh_3 given off during catalysis from the reaction as part of the catalytic cycle. $[(PPh_3)_2Rh(\mu\text{-}Cl)]_2$, **2**, does not contain any free triphenylphosphine (PPh_3) ligand in the starting material, unlike $RhCl(PPh_3)_3$, **1**. The absence of free PPh_3, in the reaction mixture, could be important when studying the stoichiometric reactions and their subsequent products.

3.3.1 Stoichiometric reactions of Wilkinson's dimer (2) with di-*n*-hexylsilane

3.3.1.1 Isolation of complex 5, $[(PPh_3)_2Rh(H)(Cl)(SiHR_2)]$, from addition of two equivalents of di-n-hexylsilane to $[(PPh_3)_2Rh(\mu\text{-}Cl)]_2$, 2

Numerous reactions were performed aimed at isolating pure Rh-containing compounds resulting from silane additions. Addition of two equivalents (one equivalent per Rh centre) of di-*n*-hexylsilane in toluene to $[(PPh_3)_2Rh(\mu\text{-}Cl)]_2$, **2**, caused an orange solution to form. Addition of a non-polar solvent (e.g. pentane or hexanes) to this mixture at -5°C caused precipitation of a yellow powder, **5**, $[(PPh_3)_2Rh(H)(Cl)(SiHR_2)]$, which was isolated and characterized by NMR ($^{31}P\{^1H\}$, ^1H, 2D experiments, and variable high and low temperature).

At room temperature a single rhodium hydride resonance, a sharp multiplet (dt) with a relative intensity of one, was observed in the ^1H NMR spectrum (Figure 3.10) of complex **5**. The ^1H NMR spectrum of complex **5** showed a broad signal in the Si-H region at around 3.6 ppm (baseline) and only one set of hexyl group signals in the alkyl region.

References p111

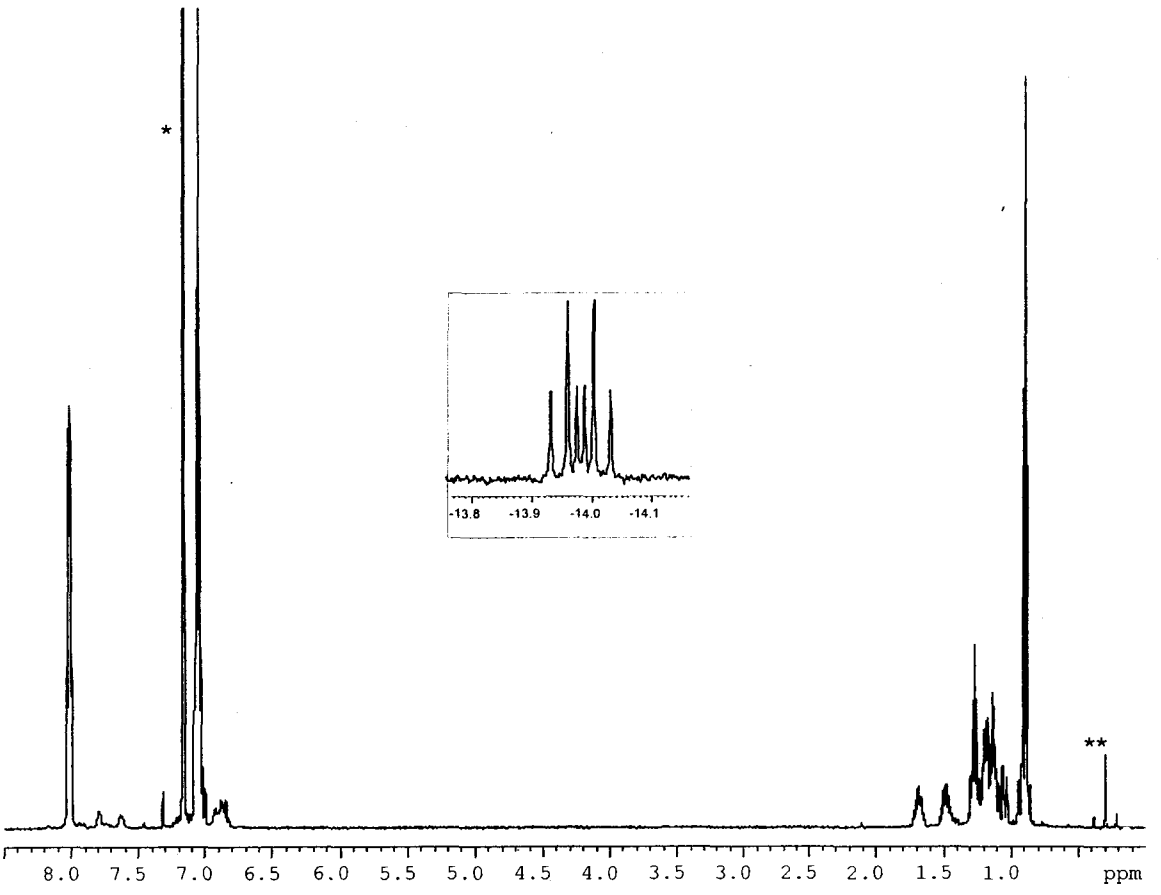

Figure 3.10: 500 MHz ^{1}H NMR spectrum of complex **5** in C_6D_5H (*). The "**" marks an impurity, silicone grease

A simple doublet is observed at δ 39.5 in the $^{31}P\{^{1}H\}$ NMR spectrum of **5** (not shown here). These results are consistent with the product structure shown in Equation 3.2, with one rhodium hydride and one rhodium silyl ligand. Haszeldine and co-workers have characterized compounds similar to Equation 3.2 with a range of 3° silane substrates.[10]

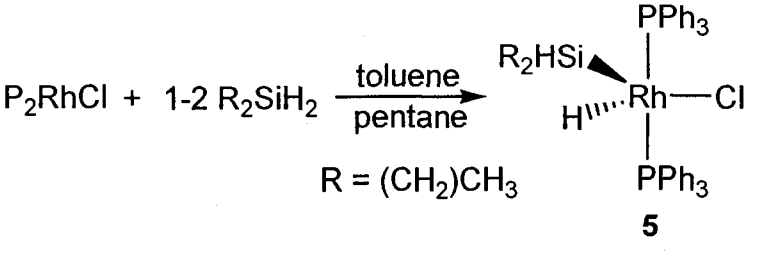

(3.2)

The rhodium centre in Equation 3.2 goes through an oxidative addition of the Si-H bond to go from a +1 oxidation state to a +3 oxidation state, giving a five-coordinate complex. The spin-spin coupling values measured for **5** included $^{1}J_{P\text{-}Rh}$ = 123 Hz, $^{1}J_{H\text{-}Rh}$ = 22 Hz, and $^{2}J_{H\text{-}P}$ = 14 Hz which are consistent with coupling values for other known five-coordinate Rh(III) silyl complexes.[7a]

Five-coordinate systems are quite notorious for fluxional behavior (e.g. via Berry pseudo rotation[11]) as the energy barrier between trigonal bipyramid and square pyramidal geometries is often quite low. A fluxional molecule is one that undergoes a dynamic molecular process that interchanges two or more chemically and/or magnetically different groups in a molecule. If the rate of this exchange is faster than the time scale of spectroscopic observation, these two different groups can appear to be identical. When the two peaks merge, to give a broad signal, such that there is no distinguishable valley between them we say that the peaks have coalesced.[12] A general example of this exchange is shown in Figure 3.11.

References p111

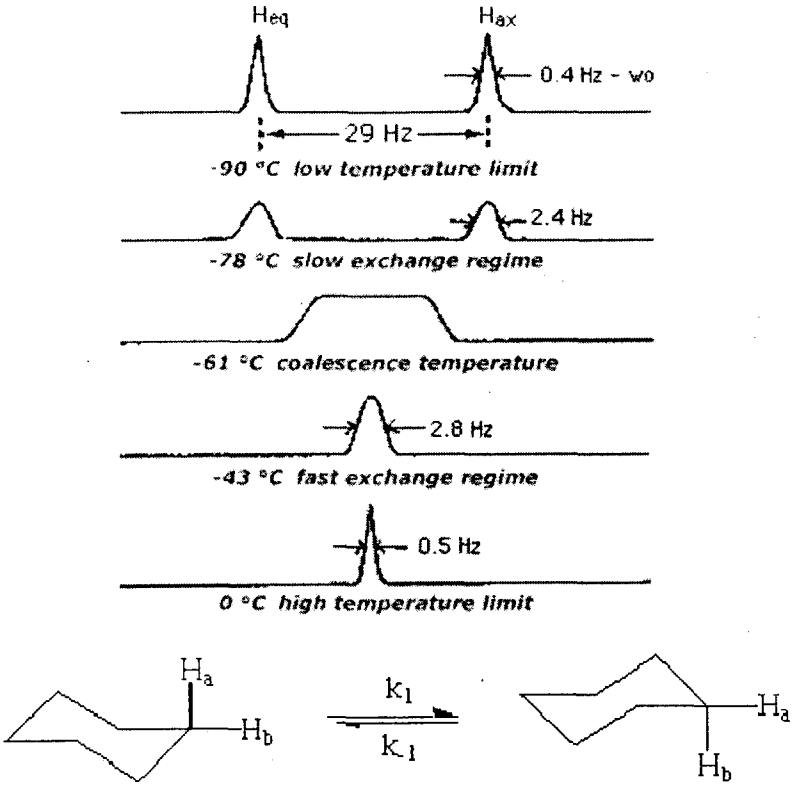

Figure 3.11: VT-NMR spectrum of fluxional cyclohexane-d_{11}.[13] Note: All signals are singlets instead of doublets because $J_{H\text{-}D}$ is small and 11 of the 12 protons are deuterated. In a non-deuterated sample, each signal would be a doublet

In order to investigate whether this five-coordinate Rh-Si species, **5**, undergoes any structural changes in solution both low and high temperature NMR experiments were carried out. The variable temperature $^{31}P\{^{1}H\}$ and ^{1}H (hydride region) NMR spectra of complex **5** are shown in Figure 3.12 and Figure 3.13.

The $^{31}P\{^{1}H\}$ NMR spectrum of complex **5** showed no change, except for a gradual broadening of the doublet signal, when the solution mixture was run at low temperatures (190 K). At high temperatures two new sets of signals were observed in the $^{31}P\{^{1}H\}$ NMR spectrum (Figure 3.12 (c)). When the solution was brought back down to ambient room temperature the colour had changed from a pale yellow to a dark red-orange. The $^{31}P\{^{1}H\}$ NMR spectrum showed one major Rh-containing species with

signals at 45.0 and 34.6 ppm and a sharp singlet at –5 ppm indicating the presence of free triphenylphosphine ligand. Similar to $[(PPh_3)_2Rh(\mu\text{-}Cl)]_2$, **2**, described in Section 3.3, complex **5** does not contain any free PPh_3 in the starting material, indicating that the signal at –5 ppm may correlate with the broad baseline signal observed at 40.0 ppm (Figure 3.12 (d)).

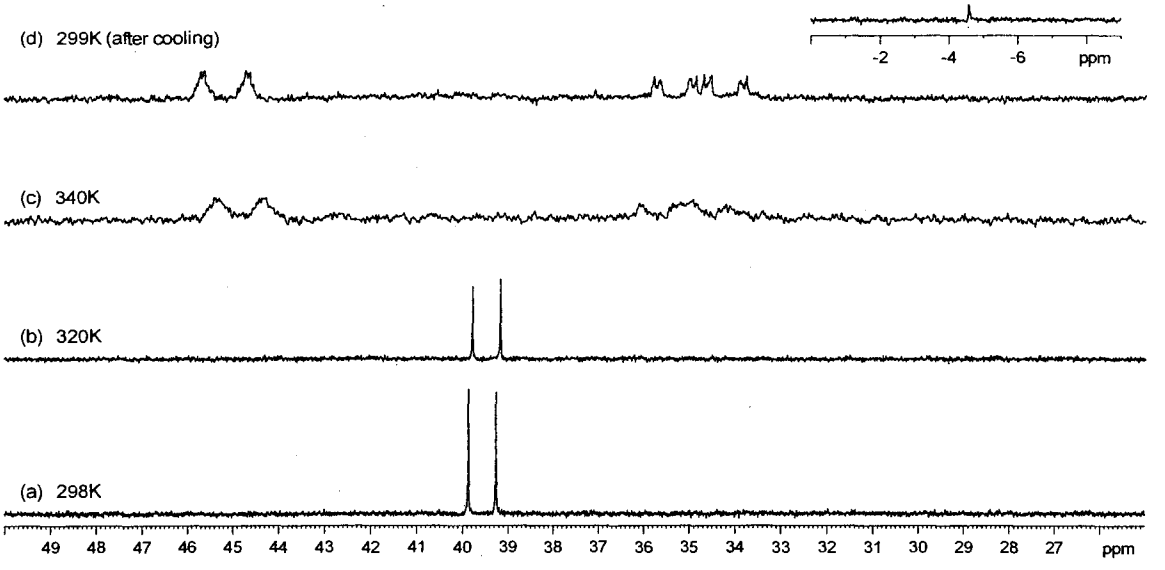

Figure 3.12: High temperature 202 MHz $^{31}P\{^1H\}$ NMR spectra of complex **5** isolated from the reaction of one equivalent of di-*n*-hexylsilane per rhodium centre with $[(PPh_3)_2Rh(\mu\text{-}Cl)]_2$, **2** in C_7D_8

The two centre-symmetric doublets of multiplets that are shown in Figure 3.12 (c) and (d), at 45.0 and 34.6 ppm are consistent with the dimeric structure **6**, shown in Figure 3.13.

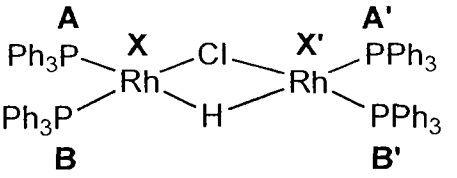

Figure 3.13: Possible structure in solution of complex **6**

The geometry at rhodium is square planar with one bridging rhodium hydride and one bridging chloride ligand, giving an AA'BB'XX' spin system where A, B = P and X = Rh. The signals for complex **6** are also observed in experiments monitoring the progression of this reaction at room temperature by $^{31}P\{^{1}H\}$ NMR spectroscopy ('C' in Figure 3.16 (b); time = 48 h). It should be noted that the signals for 'C' at 45.0 ppm ($^{1}J_{P\text{-}Rh}$ = 194 Hz) and 34.6 ppm ($^{1}J_{P\text{-}Rh}$ = 161 Hz) in all spectra where these signals are observed, are always in the same ratio, which suggests they are attributable to one compound. These signals are similar to those assigned to a known bridged hydride species of formulation [{Rh(dppe)}$_2$(μ-H)(μ-Cl)], which was shown in Section 3.2.2, Figure 3.7.[6] The $^{31}P\{^{1}H\}$ NMR spectrum of this complex has signals centered at 78.7 ppm ($^{1}J_{P\text{-}Rh}$ = 196 Hz) and 65.8 ppm ($^{1}J_{P\text{-}Rh}$ = 167 Hz).

The ^{1}H NMR spectrum of complex **5** showed no change in the hydride region when the solution mixture was run at low temperatures. At high temperatures three new signals at –8.4, –12.1, and -14.8 ppm were observed in the hydride region of the ^{1}H NMR spectrum (Figure 3.14 (c)). When the solution was brought back down to ambient room temperature two signals were observed in the ^{1}H (hydride region) NMR spectrum. The major signal is a single rhodium hydride resonance, a sharp multiplet at –8.4 ppm with a relative intensity of one and a spin system of AA'MM'XX' where A = H, M = P and X = Rh corresponding to complex **6** (Figure 3.14 (d)).

References p111

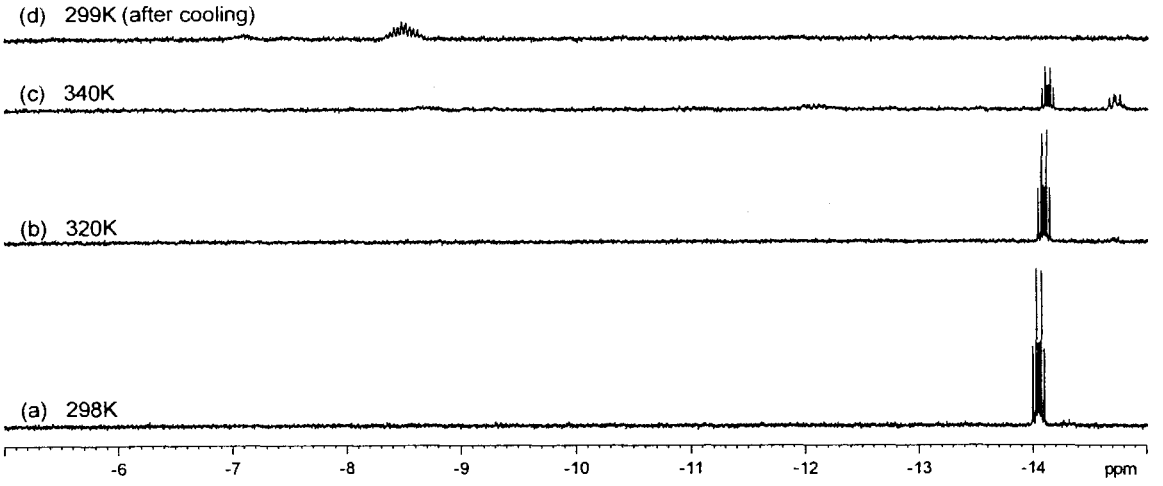

Figure 3.14: High temperature 500 MHz ^{1}H NMR (hydride region) spectra of complex **5** isolated from one equivalent of di-*n*-hexylsilane per rhodium centre with $[(PPh_3)_2Rh(\mu\text{-}Cl)]_2$, **2** in C_7D_8

The ^{1}H NMR spectrum (not shown) of the thermal decomposition products shows one broad singlet at around 3.7 ppm (Si-H region) and more than one set of hexyl groups in the alkyl region indicating the presence of silicon-containing by-products (See Section 3.2.3).

These VT-NMR studies show that complex **5** is not stable in solution. After 24 h $^{31}P\{^{1}H\}$ NMR showed the formation of the starting catalyst $[(PPh_3)_2Rh(\mu\text{-}Cl)]_2$, **2**, and other Rh-P containing species. The formation of **5** probably corresponds to the first step in catalytic Si-Si bond formation following generation of an active P_2Rh fragment. To confirm that this complex is a viable intermediate in the reaction cycle, neat di-*n*-hexylsilane was added to **5** in excess. Complex **5** was found to be successful in causing dehydrocoupling of the silane to yield a mixture of disilane and trisilane products as identified by ^{1}H NMR. The colour progression and amount of bubbling for this

dehydrocoupling reaction were essentially the same as observed previously for $RhCl(PPh_3)_3$, **1**, and $[(PPh_3)_2Rh(\mu\text{-}Cl)]_2$, **2** with addition of excess neat di-*n*-hexylsilane under the same reaction conditions, as discussed in Chapter 2, Section 2.3.1. The total consumption of monosilane appears to be similar for complex **5** compared to **1** and **2** (Figure 3.15). Thus, we conclude that the rhodium silyl hydride complex, **5**, is catalytically competent, and that its formation may represent the first step in the catalytic cycle for coupling of di-*n*-hexylsilane by both **1** and **2**.

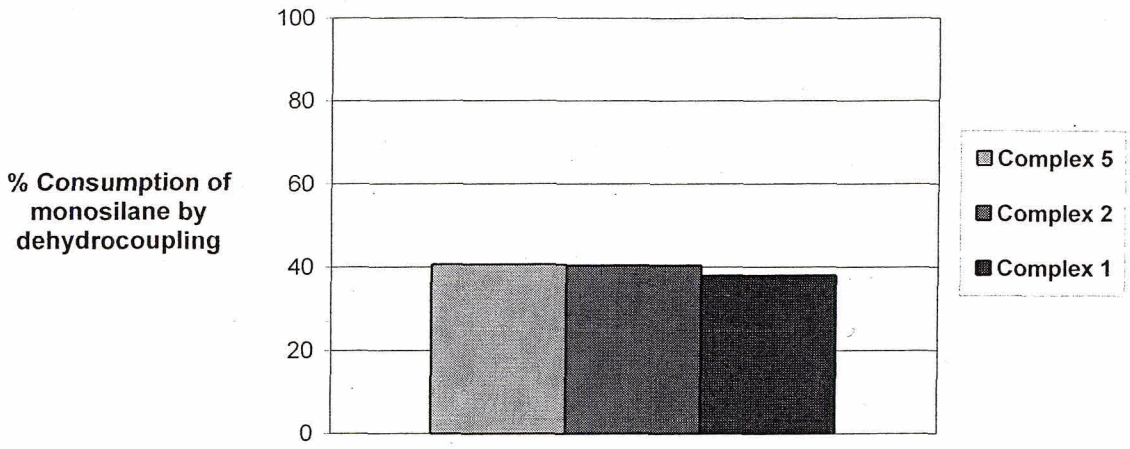

Figure 3.15: Consumption of monosilane by dehydrocoupling for complex **5**, $[(PPh_3)_2Rh(\mu\text{-}Cl)]_2$, **2**, and $RhCl(PPh_3)_3$, **1** (0.2 mol % Rh, neat di-*n*-hexylsilane, ambient pressure, one hour reaction time)

^{29}Si INEPT NMR experiments were attempted for complex **5** and the reaction mixtures resulting from $[(PPh_3)_2Rh(\mu\text{-}Cl)]_2$, **2**, plus one equivalent of di-*n*-hexylsilane per Rh centre. Unfortunately, no signals could be observed for any of the solution mixtures at room temperature. If there were dissociation and recoordination of a silane ligand, caused by the oxidative addition and reductive elimination of $H\text{-}SiR_2H$ to/from the Rh centre, it would cause fluxionality between the complexed and uncomplexed silane ligand in the system (Equation 3.3).

References p111

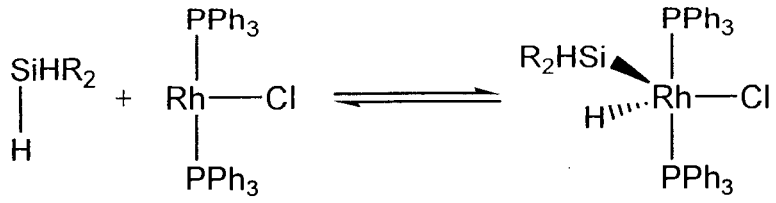

(3.3)

If the coalescence point of ^{29}Si NMR signals due to complexed and uncomplexed silane ligand is at/or near room temperature this could cause a very broad signal in the baseline of the ^{29}Si NMR spectrum that may be hard to observe. Low temperature ^{29}Si NMR experiments were carried out in the event that a dissociation/recoordination was occurring and the coalescence point was at room temperature, but still no signals were found. Based on the few references for ^{29}Si NMR chemical shift values for rhodium-silyl complexes, we would expect to find them in the range anywhere from -120 to 90 ppm.[14] ^{29}Si NMR experiments carried out for this thesis used a wide chemical shift window (-180 to 250 ppm), encompassing the δ values given above.

3.3.1.2 Monitoring the reaction of $[(PPh_3)_2Rh(\mu\text{-}Cl)]_2$, 2, with two equivalents of n-hex_2SiH_2

Upon addition of two equivalents (one equivalent per Rh centre) of di-*n*-hexylsilane to a pale orange suspension of $[(PPh_3)_2Rh(\mu\text{-}Cl)]_2$, **2**, in d_6-benzene, the mixture immediately became yellow and then light orange and bubbled vigorously. This evolution of H_2(g) slowed after 5-10 minutes. Approximately one hour after the silane was added to the Rh complex **2** a darker orange colour was observed. The solution turned red-orange after 24 hours. When the solution was left at room temperature for several days or more it eventually changed to a deep red-purple colour.

References p111

The above reaction of $[(PPh_3)_2Rh(\mu\text{-}Cl)]_2$, **2**, with two equivalents of di-*n*-hexylsilane afforded initially two major products, labelled A and B in Figure 3.16 (a). The signals for compound 'A' are the same as those for complex **5**, discussed in Section 3.3.1.1. After 48 h in solution a total of four products were observed by room temperature $^{31}P\{^1H\}$ and ^1H NMR (hydride region) spectroscopy.

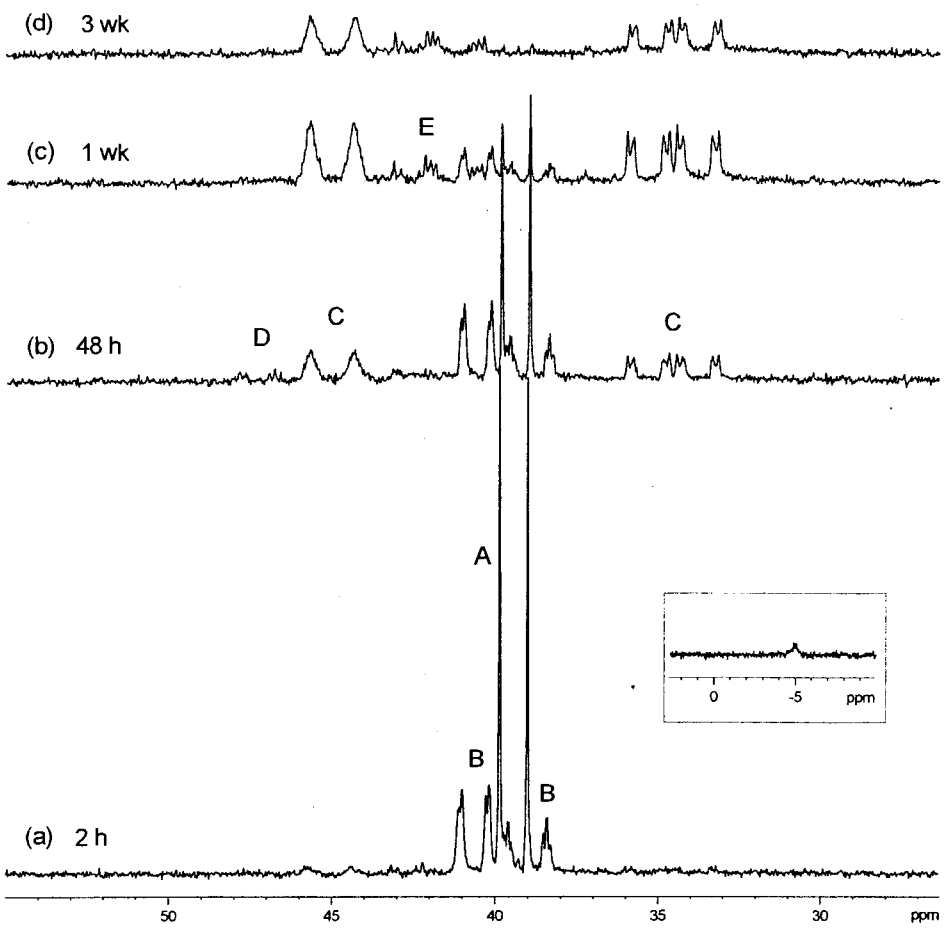

Figure 3.16: Room temperature 145.8 MHz $^{31}P\{^1H\}$ NMR spectra of $[(PPh_3)_2Rh(\mu\text{-}Cl)]_2$, **2** with one equivalent of di-*n*-hexylsilane per rhodium centre in C_6D_6

The signals labelled A and B start to diminish as the signals labelled C, D and E grow in after 48 h (Figure 3.16 (b)). After one week, signals A and B are almost gone,

while C and E become larger in Figure 3.16 (c). By week three the major species observed in Figure 3.16 (d) is compound C, while A and B have completely disappeared. Although ^{31}P-^{31}P COSY NMR experiments were attempted to see whether the signals for 'B' (39.0 and 40.6 ppm) or 'C' (45.0 and 34.6 ppm) were correlated, the NMR sample concentration was too low and no new information was gained. A similar pattern of signals, as seen in the $^{31}P\{^1H\}$ NMR spectra of $[(PPh_3)_2Rh(\mu\text{-}Cl)]_2$, **2** with one equivalent of di-*n*-hexylsilane per rhodium centre (growth and disappearance), is observed in the hydride region of the ^1H NMR spectra shown in Figure 3.17.

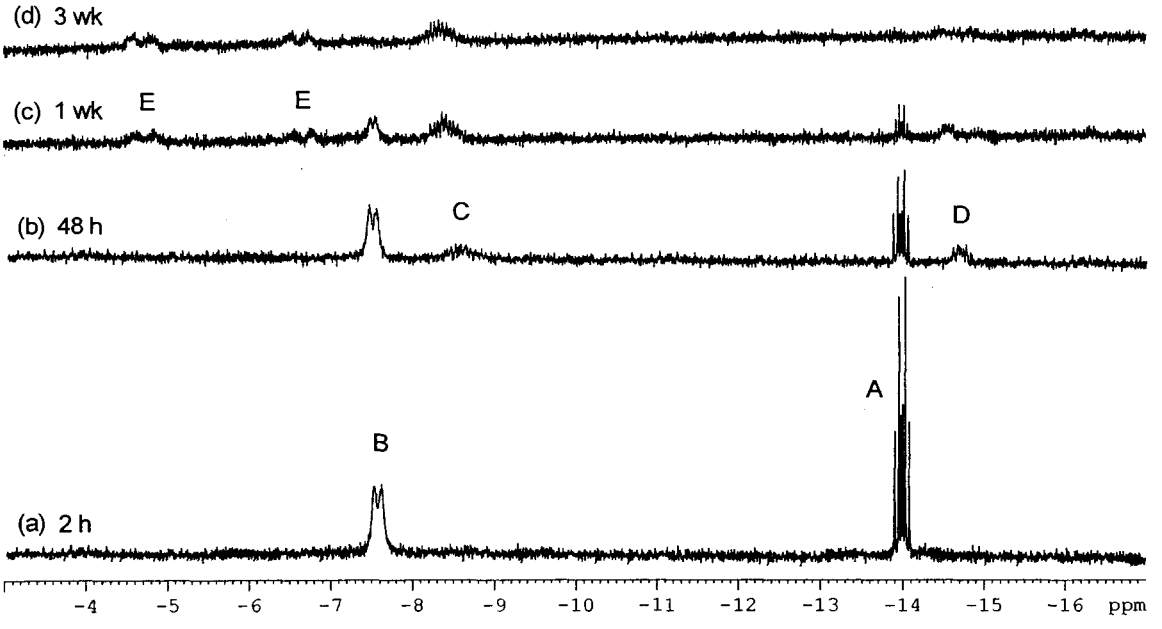

Figure 3.17: Room temperature 360 MHz ^1H NMR (hydride region) spectra of $[(PPh_3)_2Rh(\mu\text{-}Cl)]_2$, **2** with one equivalent of di-*n*-hexylsilane per rhodium centre in C_6D_6

The signal at –5ppm in the $^{31}P\{^1H\}$ NMR spectra, after 2 h in Figure 3.16 (a), corresponds to free triphenylphosphine. This signal at –5ppm is not observed in any of the other $^{31}P\{^1H\}$ NMR spectra in Figure 3.16 (b) to (d). Since $[(PPh_3)_2Rh(\mu\text{-}Cl)]_2$, **2**,

does not contain this PPh_3 ligand in excess from the starting material, we can assume that it must be Rh-dissociated PPh_3. The ^1H NMR spectrum (not shown here) has multiple signals in the hexyl region and three signals around 5.2-4.8 ppm These signals are attributed to Si-H containing by-products, possibly some chloroorganosilanes and/or the Si-H bond of Rh-Si complexes (i.e. Rh-$SiHR_2$). No unreacted di-*n*-hexylsilane or di-, trisilane compounds were observed. Some of these signals are the same as the thermal decomposition products observed for complex **5** (Equation 3.2; Section 3.3.1.1).

3.3.1.3 Monitoring the reaction of $[(PPh_3)_2Rh(\mu\text{-}Cl)]_2$, 2, with five equivalents of n-hex_2SiH_2

Upon addition of five equivalents (2.5 equivalents per Rh centre) of di-*n*-hexylsilane to a pale orange suspension of $[(PPh_3)_2Rh(\mu\text{-}Cl)]_2$, **2**, in d_6-benzene, the mixture immediately became yellow and then light orange and gave even more bubbles than complex **2** with one equivalent of silane per Rh centre. This evolution of $H_2(g)$ slowed after 10-15 minutes. Approximately 24 hours after the silane was added to the Rh complex **2** a darker orange colour was observed. Unlike the colour progression for complex **2** with one equivalent of silane per Rh centre, the sample of **2** with 2.5 equivalents of silane per Rh centre took longer to turn a dark orange colour and did not become a red-purple colour even after several days at room temperature.

References p111

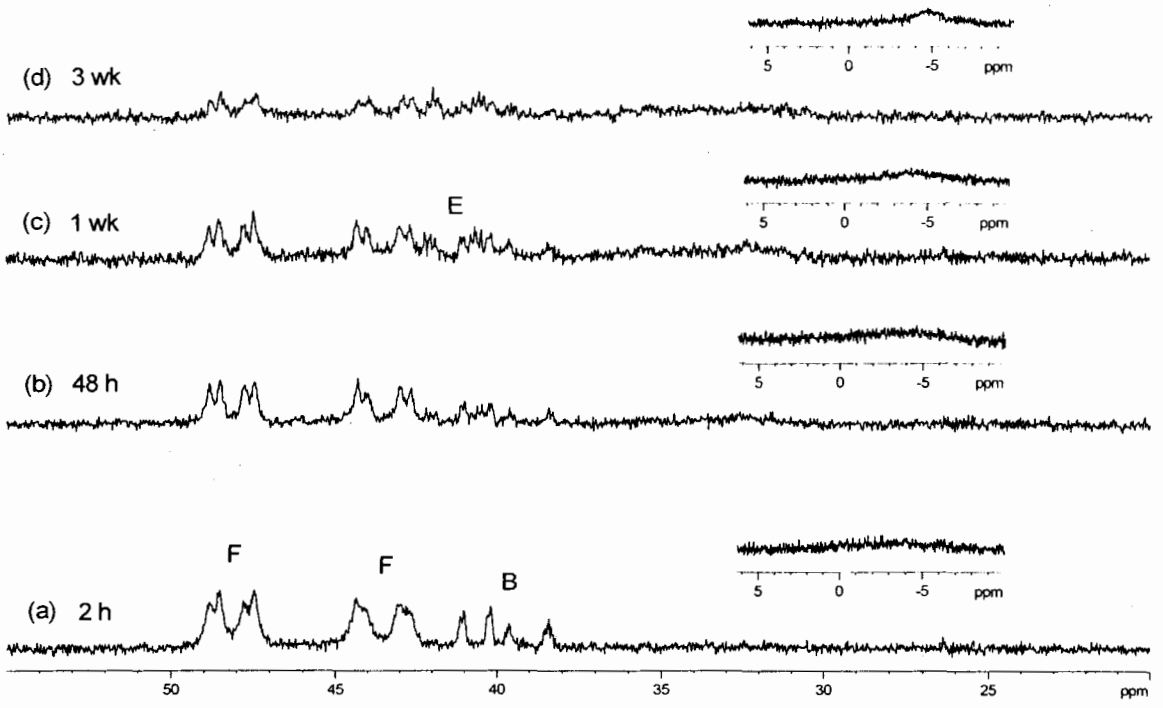

Figure 3.18: Room temperature 145.8 MHz $^{31}P\{^{1}H\}$ NMR spectra of $[(PPh_3)_2Rh(\mu\text{-}Cl)]_2$, **2** with 2.5 equivalents of di-*n*-hexylsilane per rhodium centre in C_6D_6

Initially two major products were observed, labelled F and B in Figure 3.18 (a). After 48 h in solution a total of three products were observed in the $^{31}P\{^{1}H\}$ NMR spectrum. The signals labelled F and B start to diminish as the signal labelled E grows in after 48 h in Figure 3.18 (b). After one week, signals F and B were slightly smaller, while E became slightly larger in Figure 3.18 (c). After three weeks, the previously identified species, F, B and E were still observed in Figure 3.18 (d) in relatively the same ratios to each other. A similar pattern of signals (growth and disappearance) is observed in the hydride region of the ^{1}H NMR spectra shown in Figure 3.19 (a) to (d).

References p111

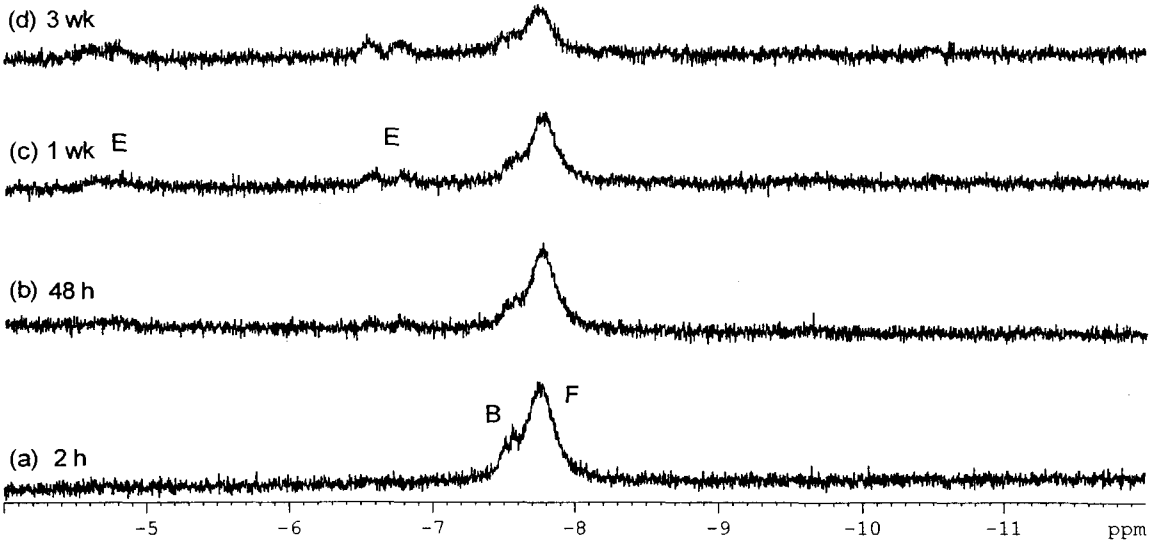

Figure 3.19: Room temperature 360 MHz ^{1}H NMR spectra of $[(PPh_3)_2Rh(\mu\text{-}Cl)]_2$, **2** with 2.5 equivalents of di-*n*-hexylsilane per rhodium centre in C_6D_6

The ^{1}H NMR spectrum after 2 h, in Figure 3.20, shows multiple signals in the hexyl region, three signals around 5.3-4.8 ppm, and a broad singlet at around 3.8 ppm. These signals are attributed to Si-H containing by-products, possibly some chloroorganosilanes and/or the Si-H bond of Rh-Si complexes (i.e. Rh-$SiHR_2$). No unreacted di-*n*-hexylsilane or di-, trisilane compounds were observed.

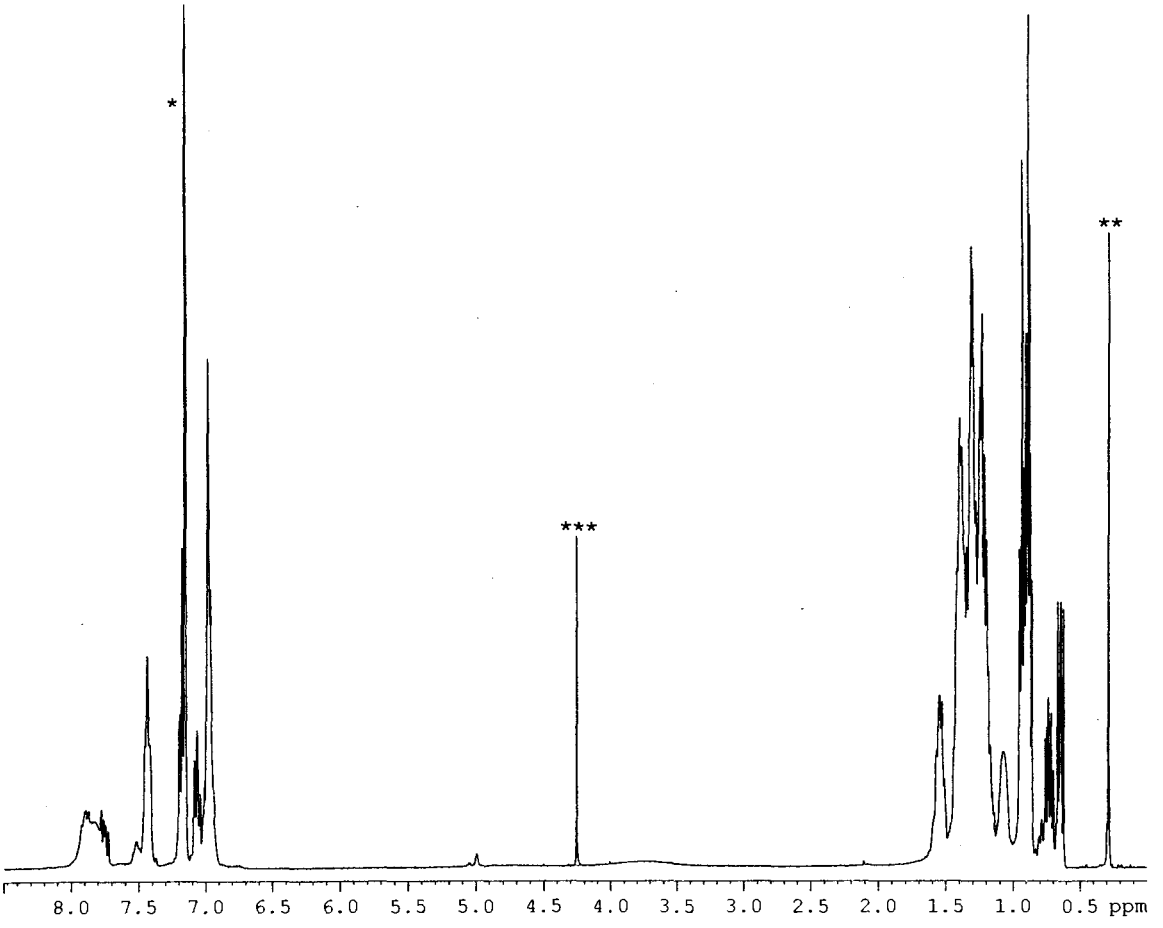

Figure 3.20: Room temperature 360 MHz ^{1}H NMR spectrum of $[(PPh_3)_2Rh(\mu\text{-}Cl)]_2$, **2** with 2.5 equivalents of di-*n*-hexylsilane per rhodium centre in C_6D_5H(*), recorded 2 h after mixing. The "**" and "***" marks impurities of silicone grease and methylene chloride, respectively.

Broad doublet of multiplet patterns are observed in the $^{31}P\{^{1}H\}$ NMR spectra in Figure 3.18 (a) to (d) for the signals labelled F. It should be noted that the signals for 'F' at 48.2 and 43.5 ppm, in all spectra where these signals are observed, are always in the same ratio suggesting they correspond to a single compound. The broadness of the signals suggests that this complex may be fluxional in solution. Variable temperature $^{31}P\{^{1}H\}$ and ^{1}H NMR spectroscopic studies were carried out after the mixture had become a dark orange colour and had reached a steady state. The low temperature

$^{31}P\{^{1}H\}$ and ^{1}H (hydride region) NMR spectra of $[(PPh_3)_2Rh(\mu\text{-}Cl)]_2$, **2**, with five equivalents (2.5 equivalents per Rh centre) of di-*n*-hexylsilane are shown in Figure 3.21 and Figure 3.22, respectively.

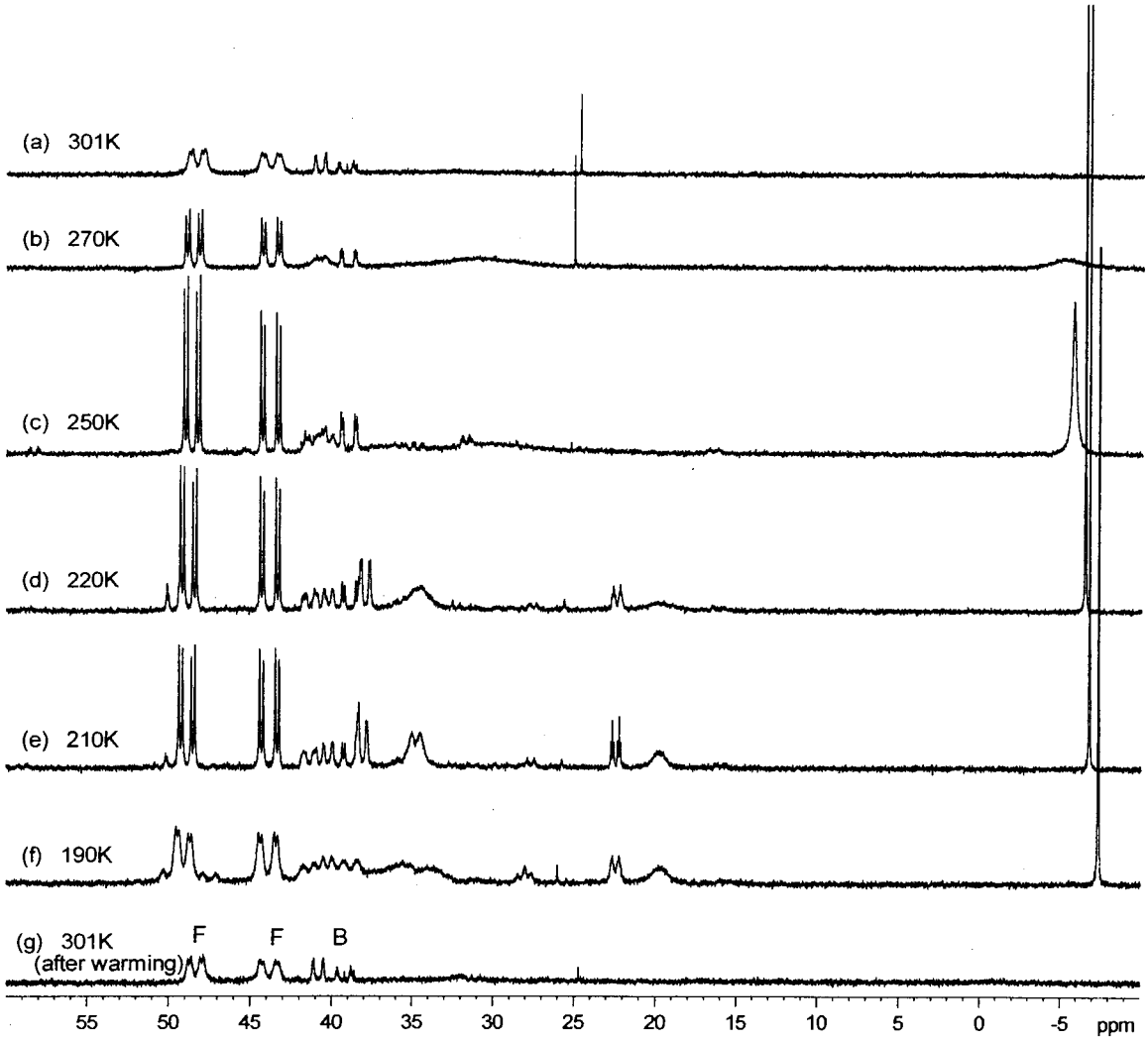

Figure 3.21: Low temperature 202 MHz $^{31}P\{^{1}H\}$ NMR spectra of $[(PPh_3)_2Rh(\mu\text{-}Cl)]_2$, **2** with 2.5 equivalents of di-*n*-hexylsilane per rhodium centre in C_7D_8, run after reaction had reached equilibrium at RT (three weeks)

Using these variable temperature NMR experiments, the signals corresponding to F have been better resolved at low temperature. The $^{31}P\{^{1}H\}$ NMR spectrum shows two doublet of doublet patterns at 48.2 and 43.5 ppm that are further resolved in Figure 3.21

(d) to give spin-spin coupling values of $^{1}J_{Rh\text{-}P}$ = 154 Hz, $^{2}J_{P\text{-}P}$ = 47 Hz and $^{1}J_{Rh\text{-}P}$ = 195.4 Hz, $^{2}J_{P\text{-}P}$ = 46 Hz, respectively. These signals seem to indicate the presence of a Rh(I) mononuclear complex with two non-equivalent phosphorus ligands. The corresponding hydride signal for compound F at –7.8 ppm in the ^{1}H NMR spectrum appears to decoalesce, becoming more resolved, in Figure 3.22 (d) indicating that F contains one or more hydride ligands.

The two signals labelled B in the $^{31}P\{^{1}H\}$ NMR spectrum behave differently as the temperature is lowered, as shown in Figure 3.21 (a) to (e). Half of the signals for compound B stay sharp and half of the signals decoalesce to give a more complex pattern with evidence of fine splitting. The corresponding hydride signal for compound B at –7.5 ppm in the ^{1}H NMR spectrum appears to decoalesce, becoming more resolved, in Figure 3.22 (d) indicating that B also contains one or more hydride ligands.

In addition to the above changes in signals B and F, new signals appear in the low temperature $^{31}P\{^{1}H\}$ NMR spectra of $[(PPh_3)_2Rh(\mu\text{-}Cl)]_2$, **2**, with five equivalents (2.5 equivalents per Rh centre) of di-*n*-hexylsilane. These signals are broad lumps, which show two or more decoalescences in Figure 3.21 (a) to (g). One of these signals corresponds to a compound apparently involved in a process with free PPh_3 versus coordinated PPh_3. Although no signal for free PPh_3 at –5ppm was observed at room temperature in the $^{31}P\{^{1}H\}$ NMR (could have been broad and in the baseline of the spectrum), it was seen to sharpen up (become better resolved) as the temperature was lowered. Since the original sample of $[(PPh_3)_2Rh(\mu\text{-}Cl)]_2$, **2**, did not contain free PPh_3 as an impurity, any free PPh_3 detected by $^{31}P\{^{1}H\}$ NMR must have dissociated from **2** or one of its derivatives. At least one, more complex, decoalescence appears to be occurring

References p111

for these peaks with broad signals emerging at 35.0, 23.0 and 19.0 ppm in Figure 3.21 (c) to (e). When the sample was returned to ambient room temperature in Figure 3.21 (g), the signals observed in the $^{31}P\{^{1}H\}$ spectrum appear to be the same as the initial starting sample.

As mentioned above, two rhodium hydride resonances, overlapping broad singlets labelled F and B, are observed in the ^{1}H NMR spectrum recorded after 2 h at room temperature (Figure 3.22 (a)). The hydride region of the ^{1}H NMR in Figure 3.22 (a) to (f) shows a number of signals that remain relatively broad, even for spectra run at very low temperatures, similar to the broad signals observed in the low temperature $^{31}P\{^{1}H\}$ NMR spectra in Figure 3.21 (a) to (f). When the sample is returned to ambient room temperature in Figure 3.22 (g), the signals observed in the ^{1}H NMR spectrum appear to be the same as the initial starting sample.

References p111

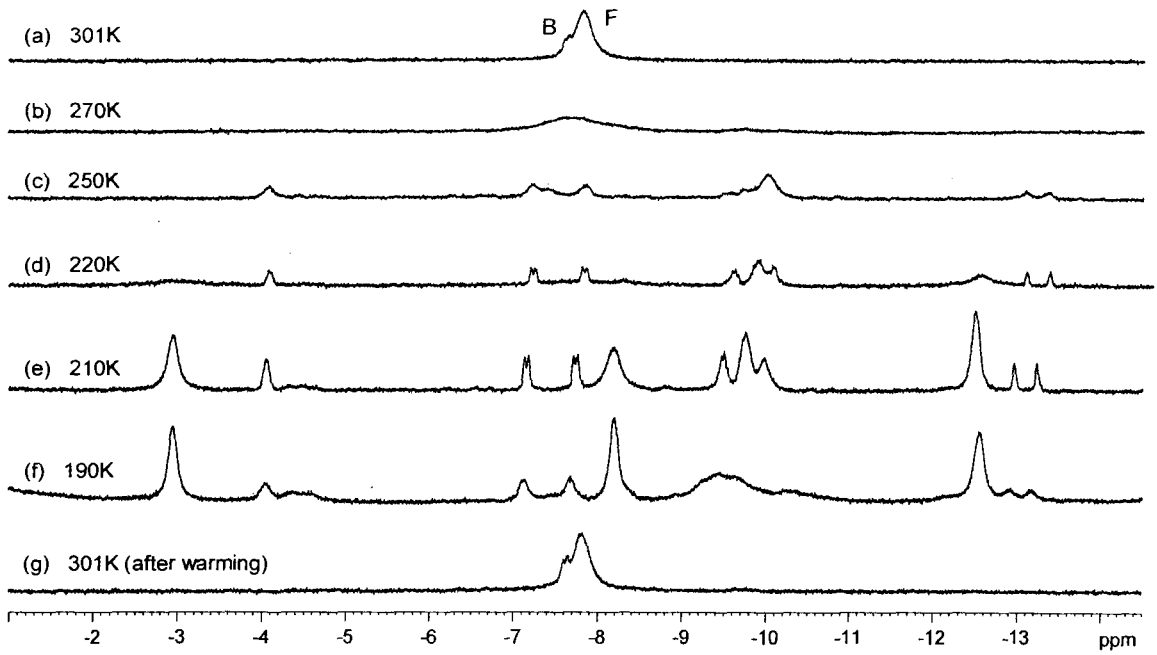

Figure 3.22: Low temperature 500 MHz ^{1}H NMR (hydride region) spectra of $[(PPh_3)_2Rh(\mu\text{-}Cl)]_2$, **2** with 2.5 equivalents of di-*n*-hexylsilane per rhodium centre in C_7D_8, run after reaction had reached equilibrium at RT (three weeks)

The high temperature $^{31}P\{^{1}H\}$ and ^{1}H (hydride region) NMR spectra of **2** with five equivalents (2.5 equivalents per Rh centre) of di-*n*-hexylsilane are shown in Figure 3.23 and Figure 3.24, respectively. The $^{31}P\{^{1}H\}$ NMR spectra show compounds F and B reaching a semi-coalescence point in Figure 3.23 (c) at 340 K. When the sample was returned to ambient room temperature in Figure 3.23 (d), the signals observed in the $^{31}P\{^{1}H\}$ NMR spectrum do not appear to be the same as the initial starting sample. It was observed that compounds F and B still remained, but new signals at 57.1, 41.5, 35.8, 33.0 and 31.0 ppm were also evident. A broad signal at –5 ppm indicates that formation of one or more of these new compounds involve phosphine dissociation from the rhodium centre.

References p111

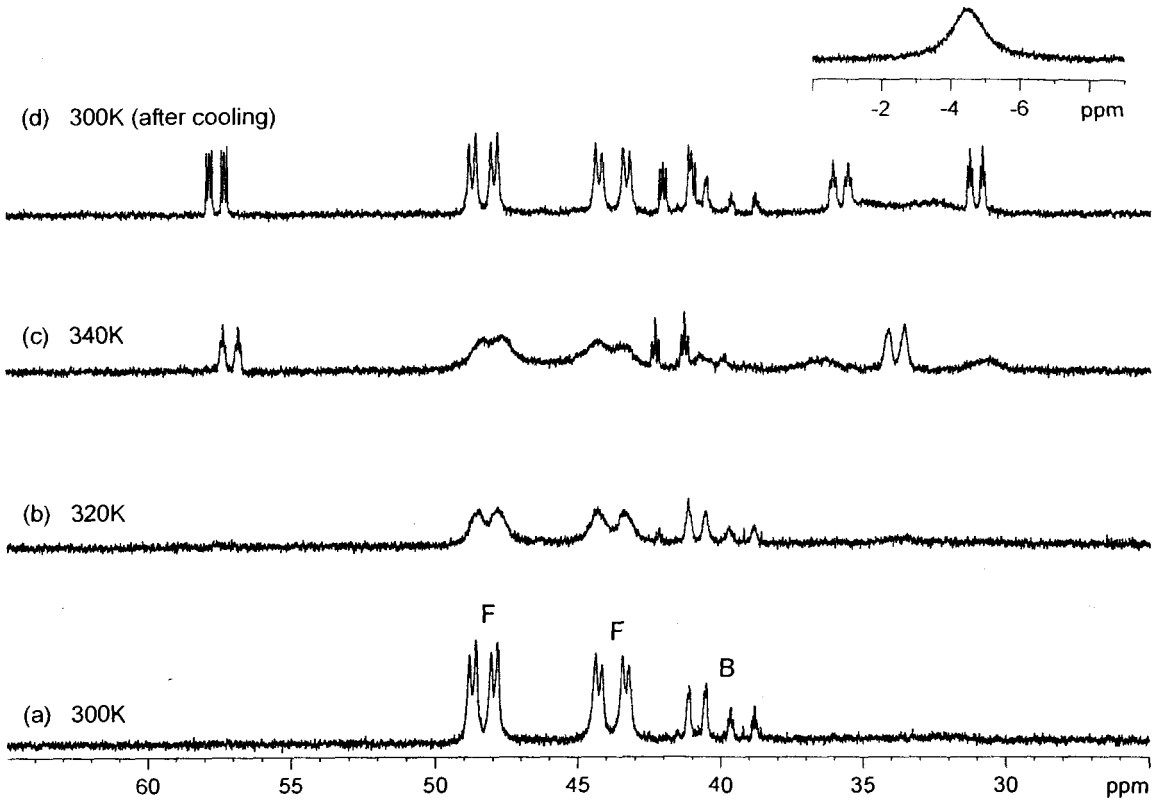

Figure 3.23: High temperature 202 MHz $^{31}P\{^{1}H\}$ NMR spectra of $[(PPh_3)_2Rh(\mu\text{-}Cl)]_2$, **2** with 2.5 equivalents of di-*n*-hexylsilane per rhodium centre in C_7D_8, run after reaction had reached equilibrium at RT (three weeks)

The corresponding high temperature ^{1}H (hydride region) NMR spectrum of **2** with five equivalents (2.5 equivalents per Rh centre) of di-*n*-hexylsilane show the broad signals for F and B also each reaching a semi-coalescence point in Figure 3.24 (c). When the sample was returned to ambient room temperature in Figure 3.24 (d), the signals observed in the hydride region of the ^{1}H NMR spectrum did not appear to be the same as the initial starting sample, similar to the high temperature $^{31}P\{^{1}H\}$ NMR spectrum in Figure 3.23 (d). It was observed that compounds F and B still remained, but new signals at –4.8, –6.9, –8.6, –10.8 and –14.7 ppm were also evident.

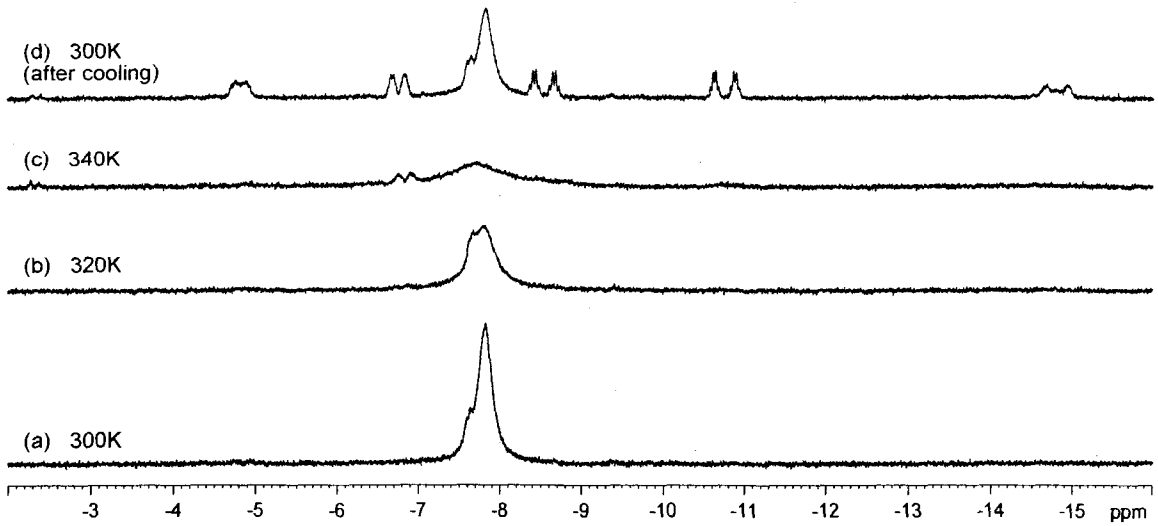

Figure 3.24: High temperature 500 MHz ^{1}H NMR spectra of $[(PPh_3)_2Rh(\mu\text{-}Cl)]_2$, **2** with 2.5 equivalents of di-*n*-hexylsilane per rhodium centre in C_7D_8, run after reaction had reached equilibrium at RT (three weeks)

The complete room temperature ^{1}H NMR spectrum (not shown here) has a number of signals in the Si-H region, including multiple signals in the hexyl region (-SiR_2- containing by-products), a broad peak around 3.8 ppm and at least four more signals around 5.7-4.1 ppm. These signals are attributed to Si-H containing by-products, possibly some chloroorganosilanes and/or the Si-H bond of Rh-Si complexes (i.e. Rh-$SiHR_2$). A small signal at 4.2 ppm indicates the presence of the disilane product, while some unreacted di-*n*-hexylsilane was observed at 3.9 ppm.

Stoichiometric studies of $[(PPh_3)_2Rh(\mu\text{-}Cl)]_2$, **2** with one and/or 2.5 equivalents of di-*n*-hexylsilane per rhodium centre have helped to show that the possible first step in the catalytic cycle involves oxidation addition of an Si-H bond to a Rh centre. The resulting rhodium silyl hydride complex, **5**, is also catalytically competent, giving similar activities and conversions to **1** and **2**. The major thermal decomposition product of complex **5** was assigned to a dinuclear species, $[\{Rh(dppe)\}_2(\mu\text{-}H)(\mu\text{-}Cl)]$, **6**, based on comparison of its

^{31}P NMR spectrum to a previously reported, similar complex. Complex **6** was also observed at room temperature as the major species in solution after one week.

There are still a number of signals observed in the $^{31}P\{^{1}H\}$ and ^{1}H NMR spectra for the reactions of $[(PPh_3)_2Rh(\mu\text{-}Cl)]_2$, **2** with one and/or 2.5 equivalents of di-*n*-hexylsilane per rhodium centre that have not yet been assigned to specific structures. Patterns in the $^{31}P\{^{1}H\}$ NMR spectra suggest the presence of both mono- and dinuclear Rh-P containing complexes. Some potential structures are presented in Figure 3.25, which may correspond to some of the unknown signals found in the NMR spectra for these stoichiometric reactions. Sigma complexes of both H-H and Si-H bonds are also included in the possible structures of intermediates for $[(PPh_3)_2Rh(\mu\text{-}Cl)]_2$, **2** with one and/or 2.5 equivalents of di-*n*-hexylsilane per rhodium centre.

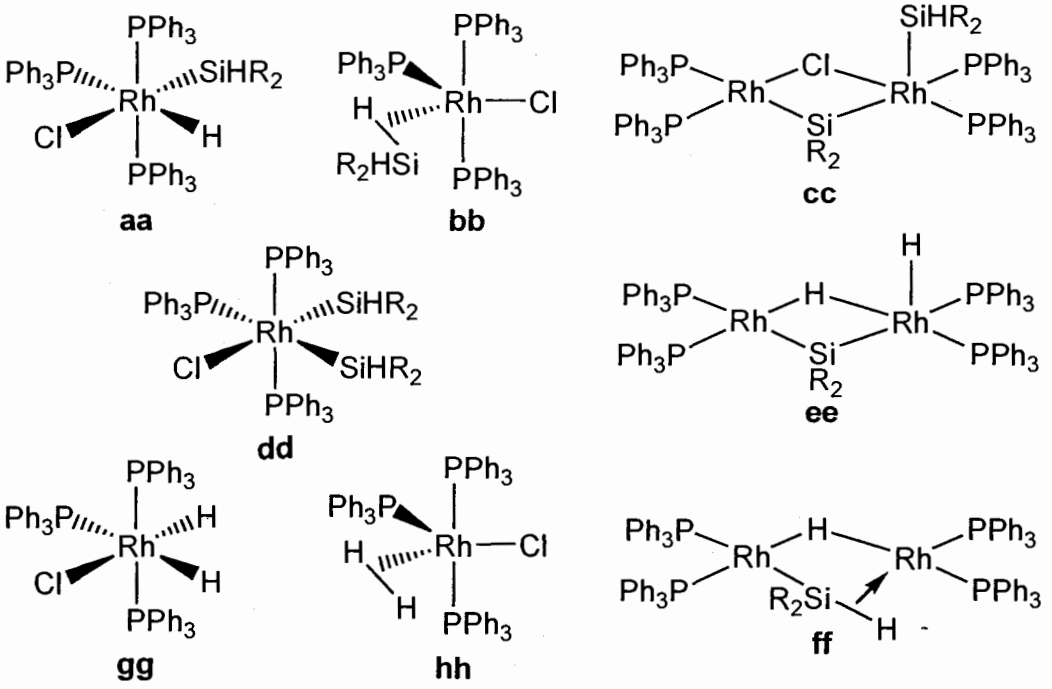

Figure 3.25: Possible mono- and dinuclear Rh-P structures present in solution for $[(PPh_3)_2Rh(\mu\text{-}Cl)]_2$, **2** with one and/or 2.5 equivalents of di-*n*-hexylsilane per rhodium centre

3.3.2 Stoichiometric reactions of Wilkinson's catalyst (1) with di-*n*-hexylsilane

3.3.2.1 Isolation of an orange powder from addition of one equivalent of di-n-hexylsilane to $RhCl(PPh_3)_3$, 1

As mentioned in Section 3.3.1.1, a number of reactions were done aimed at isolating pure Rh-containing compounds resulting from silane additions. Addition of one equivalent of di-*n*-hexylsilane, in toluene, to $RhCl(PPh_3)_3$, **1**, causes a dark orange solution to form. A light orange powder was precipitated from this solution upon addition of hexanes, which was then analyzed spectroscopically independent of the reaction solution mixture.

At room temperature a very broad singlet ($\omega_{1/2}$ = 640 Hz) is observed in the $^{31}P\{^1H\}$ NMR spectrum (not shown here) at 42.5 ppm. A single rhodium hydride resonance, a broad doublet with an intensity of one, is observed in the ^1H NMR spectrum of the orange powder in Figure 3.26. This complex does not seem to have any silane (starting material or a derivative of di-*n*-hexylsilane) associated with it according to the ^1H NMR spectrum, as no signals in the aliphatic CH region were observed. It is interesting to note that the $^{31}P\{^1H\}$ and ^1H NMR spectra observed for the orange powder are not consistent with that of compound A/complex **5** (see Figure 3.10). No catalysis reactions with the orange powder were attempted due to time constraints. It is not yet known if the orange powder is catalytically competent as was observed for complex **5**.

References p111

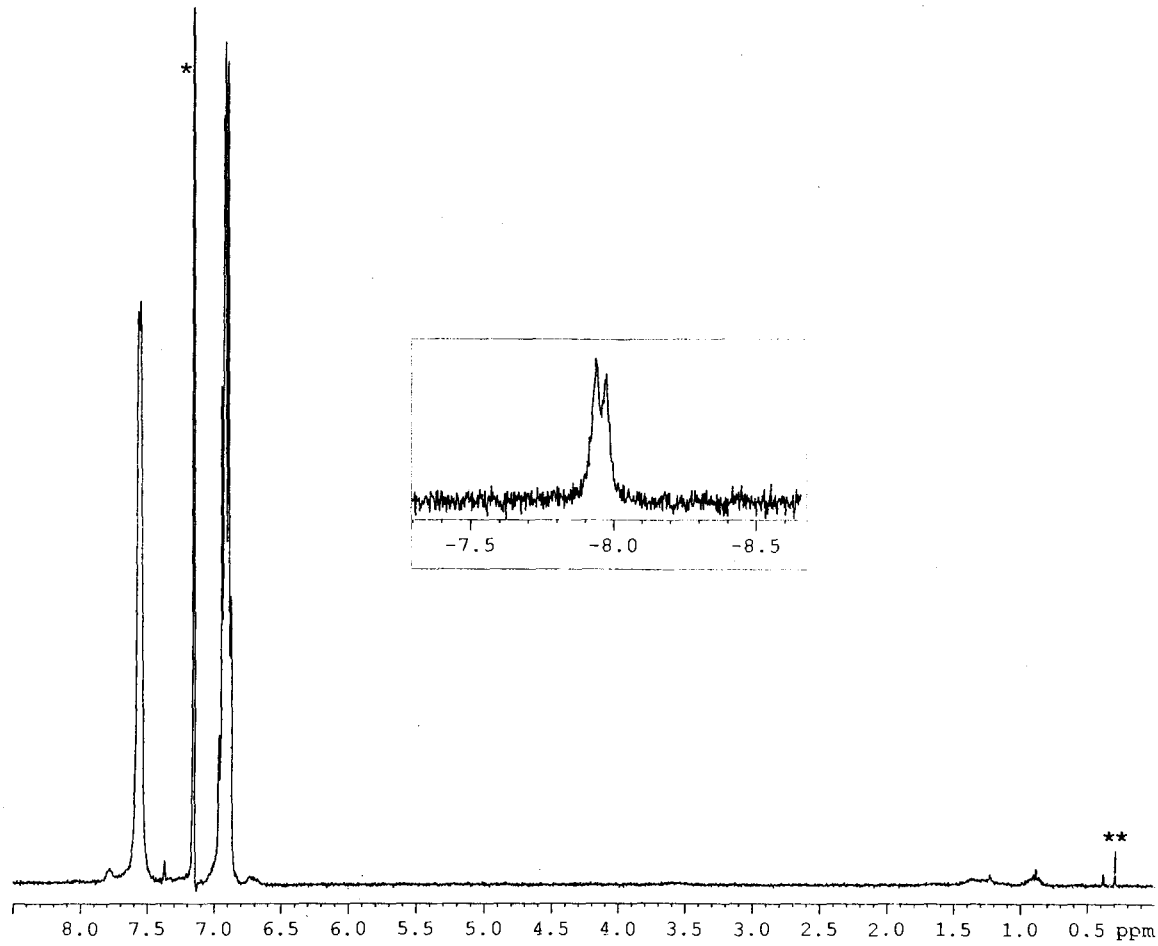

Figure 3.26: 360 MHz ^{1}H NMR spectrum of orange powder isolated from addition of one equivalent of di-*n*-hexylsilane to $RhCl(PPh_3)_3$, **1** in C_6D_5H (*).The "**" marks an impurity, silicone grease

The broadness of the signal observed in the $^{31}P\{^{1}H\}$ NMR spectra suggests that this complex may be fluxional in solution. Variable temperature $^{31}P\{^{1}H\}$ and ^{1}H NMR spectroscopic studies were carried out on the orange powder to analyze the sample further. The low temperature $^{31}P\{^{1}H\}$ and ^{1}H (hydride region) NMR spectra of the orange powder are shown in Figure 3.27 and Figure 3.28, respectively.

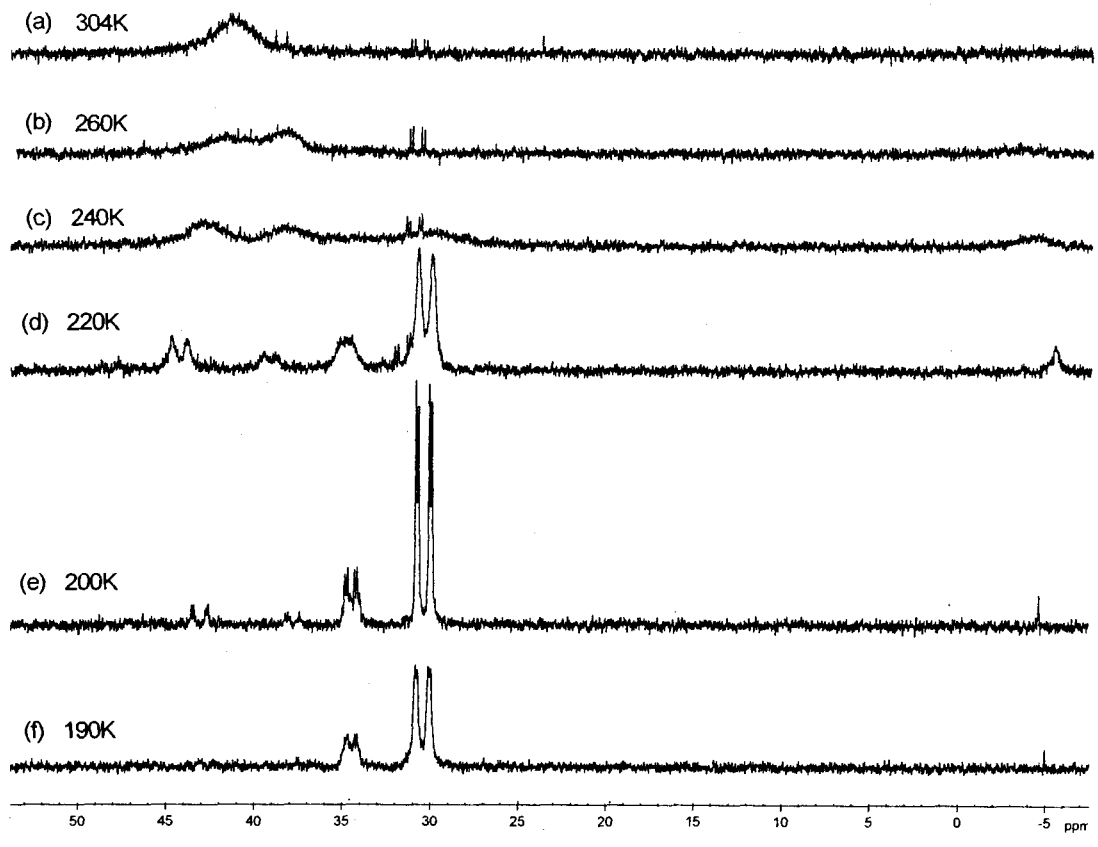

Figure 3.27: Low temperature 202 MHz $^{31}P\{^{1}H\}$ NMR spectra of the orange powder isolated from addition of one equivalent of di-*n*-hexylsilane to $RhCl(PPh_3)_3$, **1** in C_7D_8

In Figure 3.27 (a) to (d), the very broad signal at 42.0 ppm decoalesces to give two slightly sharper signals at 43.0 and 38.0 ppm, and then disappears into the baseline at the low temperature limit (Figure 3.27 (f)). A sharp doublet of doublets pattern at 30.5 ppm ($^{1}J_{P\text{-}Rh}$ = 160 Hz and $^{2}J_{P\text{-}P}$ = 30 Hz) along with a second signal, a doublet of multiplets, at approximately 34.0 ppm ($^{1}J_{P\text{-}Rh}$ = 140 Hz) were observed to grow in (Figure 3.27 (b) to (f)). A small amount of PPh_3 is also observed to resolve out of the baseline in Figure 3.27 (e) indicating that one of these compounds may be undergoing reversible dissociation of PPh_3.

References p111

The corresponding low temperature ^{1}H NMR spectra for the orange powder shows a coalescence of the signal at –7.9 ppm in Figure 3.28 (c). At even lower temperatures this sharp signal then decoalesces slightly to give a broad signal in Figure 3.28 (d) to (f). A second signal is observed to grow in at –13.1 ppm (Figure 3.28 (d) to (f)), giving a broad doublet with fine splitting. The complete ^{1}H NMR spectrum (not shown here) has a broad singlet around 5.0 ppm and another around 3.5 ppm. These signals are attributed to Si-H containing by-products, possibly some chloroorganosilanes and/or the Si-H bond of Rh-Si complexes (i.e. Rh-SiHR$_2$). No unreacted di-*n*-hexylsilane (at 3.9 ppm) was observed.

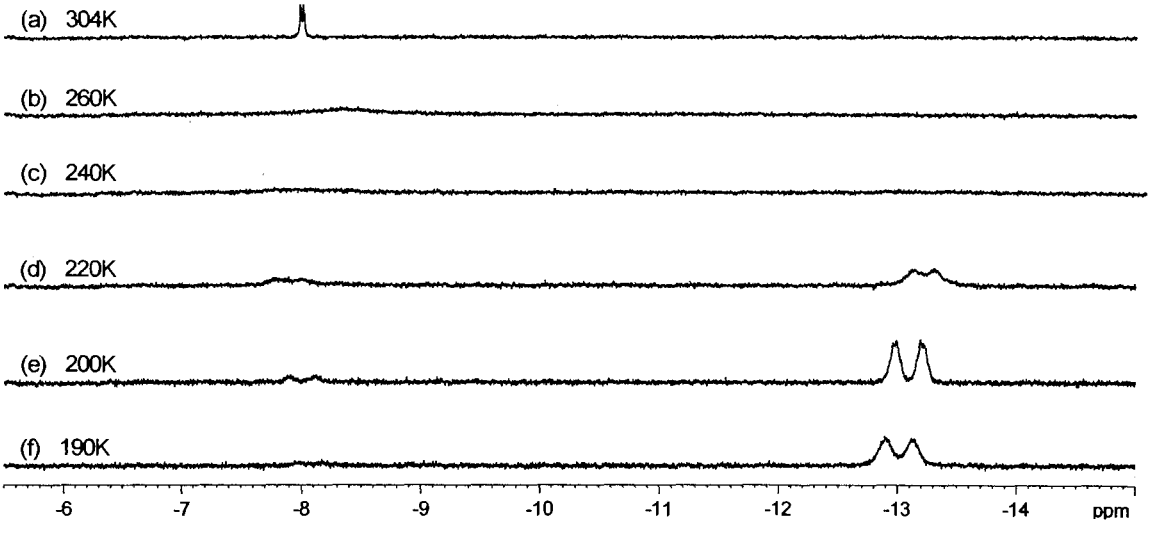

Figure 3.28: Low temperature 500 MHz ^{1}H NMR spectra of the orange powder isolated from addition of one equivalent of di-*n*-hexylsilane to RhCl(PPh$_3$)$_3$, **1** in C_7D_8

Coupling constants for the signals at 29.5 and 34.0 ppm, in the low temperature ^{31}P{^{1}H} NMR spectra Figure 3.27, seem to indicate the presence of a Rh(I) complex with possibly three phosphorus ligands (two being non-equivalent). This Rh-P containing

complex also has one or more hydride-type ligands associated with it, based on the signals found in the low temperature ^{1}H NMR spectra (Figure 3.28).

3.3.2.2 Monitoring the reaction of $RhCl(PPh_3)_3$, 1, with one equivalent of n-hex_2SiH_2

Upon addition of one equivalent of di-*n*-hexylsilane to a pale burgundy suspension of $RhCl(PPh_3)_3$, **1**, in d_6-benzene, the mixture immediately became light orange and bubbled vigorously, similar to the reaction of $[(PPh_3)_2Rh(\mu\text{-}Cl)]_2$, **2** with one equivalent of silane. This evolution of H_2(g) slowed after 5-10 minutes. Approximately 15 minutes after the silane was added to the Rh complex **1** a darker red-orange colour was observed. When the solution was left at room temperature for several hours it eventually changed to a burgundy-orange colour. Compared to the colour progression for $[(PPh_3)_2Rh(\mu\text{-}Cl)]_2$, **2** with one equivalent of silane per Rh centre, this reaction mixture took less time to turn a red-orange colour and did not become a red-purple colour; instead becoming burgundy-orange.

Room temperature $^{31}P\{^1H\}$ and ^{1}H NMR show that the mononuclear rhodium complex $RhCl(PPh_3)_3$, **1**, reacted with one equivalent of di-*n*-hexylsilane to afford initially up to four major products labelled A, G, H and I in Figure 3.29 (a) and 3.30 (a). A small amount of free PPh_3 was also observed in these reactions, indicated by a broad signal at –5 ppm, suggesting that one of these compounds may be undergoing reversible dissociation of PPh_3. Compound 'G' appears to be an isomer of compound 'A'. Similar patterns are observed for signals in $^{31}P\{^1H\}$ and ^{1}H NMR spectra, along with comparable P-Rh coupling constants (A: d, $^1J_{P\text{-}Rh}$ = 124 Hz; G: d, $^1J_{P\text{-}Rh}$ = 123 Hz).

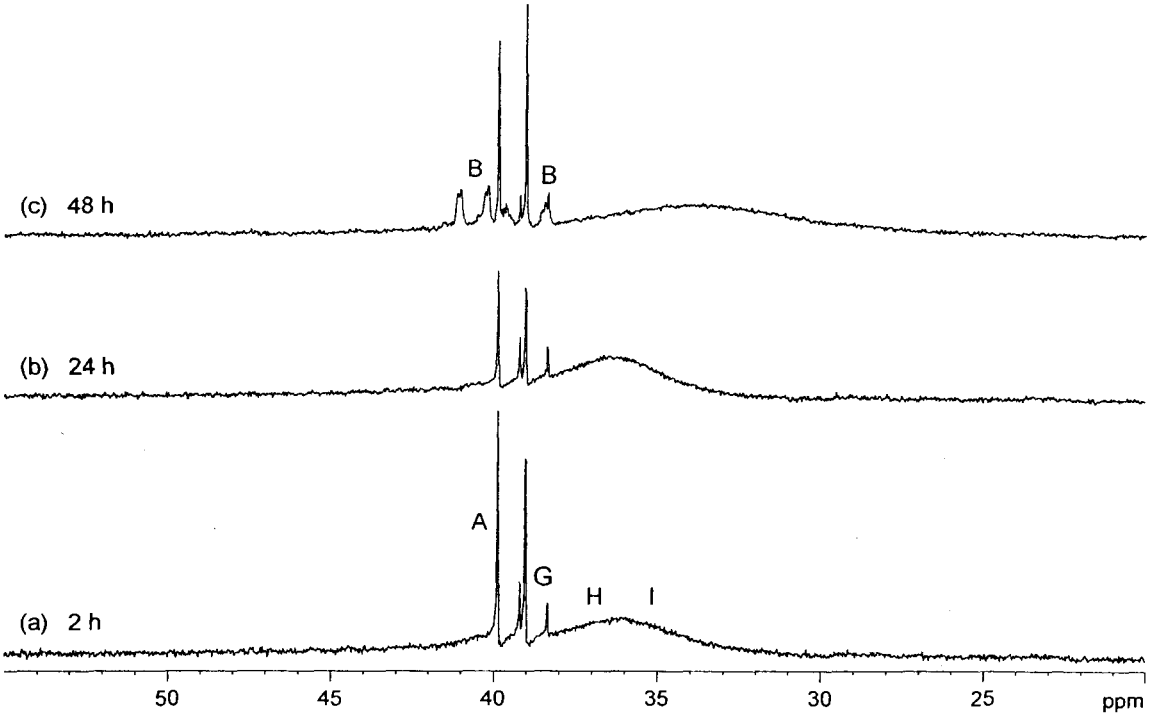

Figure 3.29: Room temperature 145.8 MHz $^{31}P\{^{1}H\}$ NMR spectra of $RhCl(PPh_3)_3$, **1** with one equivalent of di-*n*-hexylsilane in C_6D_6. Note: relative integrations of H and I appear different in other $^{31}P\{^{1}H\}$ NMR spectra.

After 48 h in solution a total of five products were observed by room temperature $^{31}P\{^{1}H\}$ and ^{1}H (hydride region) NMR spectroscopy, including signals due to compound B (Figures 3.29 (c) and 3.30 (c)).

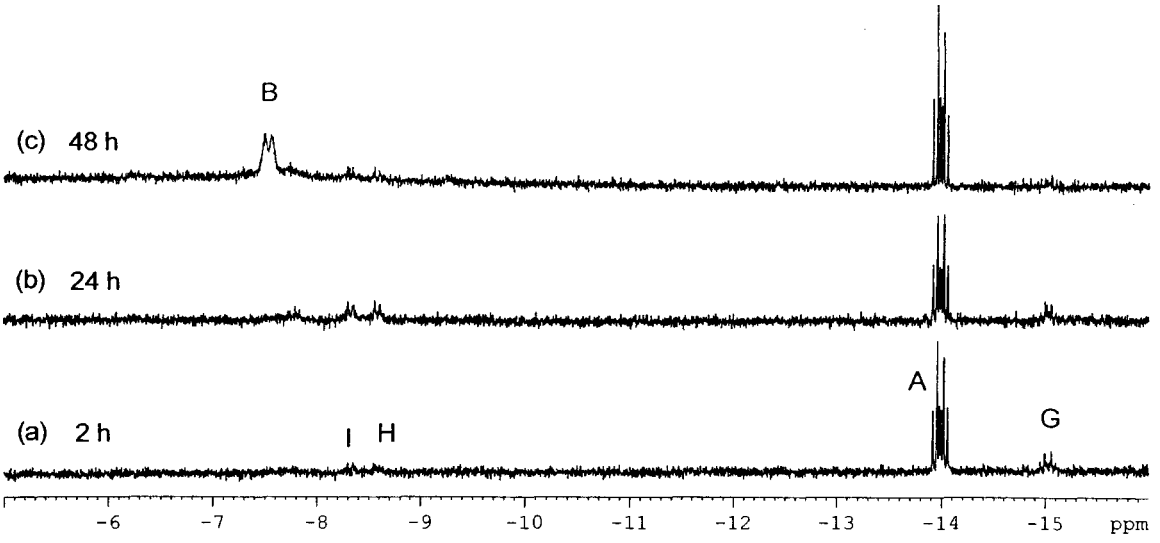

Figure 3.30: Room temperature 360 MHz ^{1}H NMR spectra of $RhCl(PPh_3)_3$, **1** with one equivalent of di-*n*-hexylsilane in C_6D_6

Some of the species observed by $^{31}P\{^1H\}$ and ^1H NMR, such as compounds A and B, are the same as those observed in the stoichiometric reactions with $[(PPh_3)_2Rh(\mu\text{-}Cl)]_2$, **2**. This is not surprising because $RhCl(PPh_3)_3$, **1**, not only contains the dimer, **2**, as an impurity in the starting complex mixture, but also typically exists in equilibrium with **2** in solution (Equation 3.4).[15] These two rhodium (I) complexes are also believed to act similarly in catalysis in terms of their active catalyst fragments (See Chapter 2, Section 2.2).

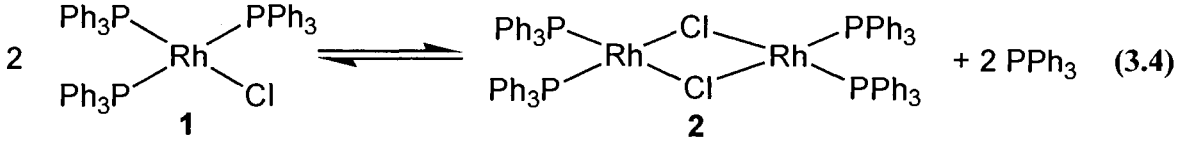

(3.4)

3.3.2.3 Monitoring the reaction of $RhCl(PPh_3)_3$, 1, with five equivalents of n-hex_2SiH_2

Upon addition of five equivalents of di-*n*-hexylsilane to a pale burgundy suspension of $RhCl(PPh_3)_3$, **1**, in d_6-benzene, the mixture immediately became yellow

and then red-orange and gave even more bubbles than complex **1** with one equivalent of silane. This evolution of H_2(g) slowed after 10-15 minutes. The solution turned a medium orange colour after 15-20 minutes. When the solution was left at room temperature for several hours or more it eventually changed to a dark red-orange colour, similar to the reaction of $[(PPh_3)_2Rh(\mu\text{-}Cl)]_2$, **2**, with one equivalent (per Rh centre) of di-*n*-hexylsilane after 24 h .

After two hours, NMR monitoring of this room temperature reaction of the mononuclear rhodium complex $RhCl(PPh_3)_3$, **1**, with five equivalents of di-*n*-hexylsilane indicated only a broad lump around 37.5 ppm was present in the $^{31}P\{^1H\}$ NMR spectrum (Figure 3.31 (a)) . This is similar to the broad signal around 42.5 ppm in the $^{31}P\{^1H\}$ NMR spectrum of the orange powder (isolated from addition of one equivalent of di-*n*-hexylsilane to $RhCl(PPh_3)_3$, **1**). The formation of two major products, labelled G and I was observed after 24 h (Figure 3.31 (b)). These signals are both also observed for $[(PPh_3)_2Rh(\mu\text{-}Cl)]_2$, **2**, with five equivalents (2.5 equivalents per Rh centre) of di-*n*-hexylsilane) in Figure 3.18 (b). After 48 h in solution a number of broad signals were observed by room temperature $^{31}P\{^1H\}$ and ^1H NMR spectroscopy (Figure 3.31 (c) and 3.32 (c)), indicating the presence of two or more products. No signal was observed for free PPh_3 at –5 ppm.

References p111

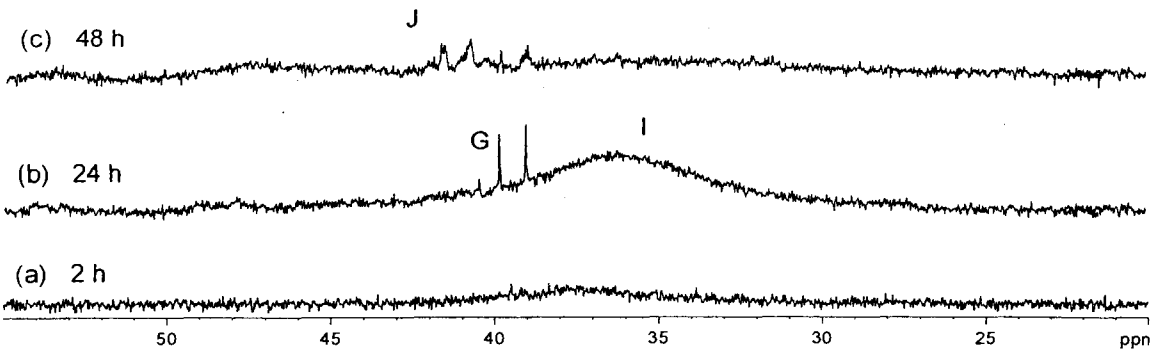

Figure 3.31: Room temperature 145.8 MHz $^{31}P\{^{1}H\}$ NMR spectra of $RhCl(PPh_3)_3$, **1** with five equivalents of di-*n*-hexylsilane in C_6D_6

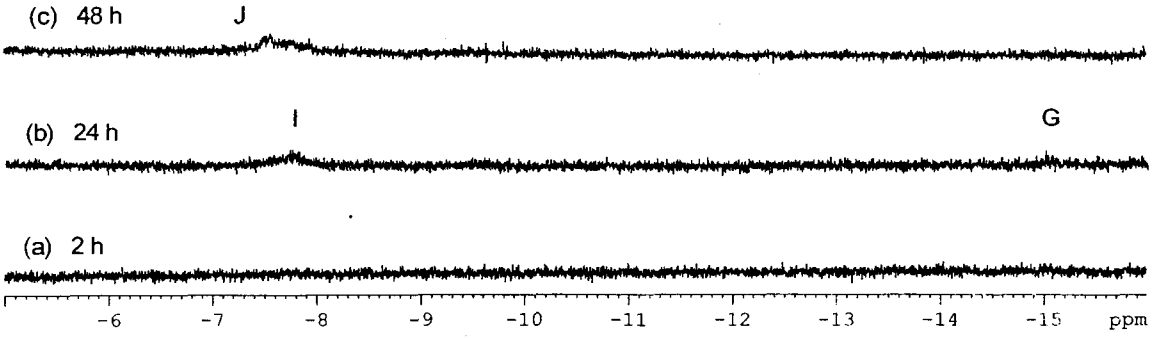

Figure 3.32: Room temperature 360 MHz ^{1}H NMR spectra of $RhCl(PPh_3)_3$, **1** with five equivalents of di-*n*-hexylsilane in C_6D_6. (Note that signals labeled I and G were assigned based on previously observed ^{1}H NMR spectra)

The major product observed in the room temperature ^{1}H NMR after 48 h shows a hydride signal (broad singlet) at –7.5 ppm labelled J in Figure 3.32 (c). The complete ^{1}H NMR spectrum (not shown here) has broad singlets at 5.0, 4.0 and 3.7 ppm and multiple signals in the hexyl region. These signals are attributed to Si-H containing by-products, possibly some chloroorganosilanes and/or the Si-H bond of Rh-Si complexes (i.e. Rh-$SiHR_2$). The signal at 4.0 ppm could indicate the di-, and/or trisilane product. No unreacted di-*n*-hexylsilane (at 3.9 ppm) was observed.

Two of the three major products from the reaction of $RhCl(PPh_3)_3$, **1** with five equivalents of di-*n*-hexylsilane matched those observed for $[(PPh_3)_2Rh(\mu\text{-}Cl)]_2$, **2** with five equivalents (2.5 equivalents per Rh centre) of di-*n*-hexylsilane. The breadth of the signal at 36.0 ppm ($\omega_{1/2}$ = 1010 Hz) observed in the $^{31}P\{^1H\}$ NMR spectra in Figure 3.31 (b) and (c) suggests that this complex may be fluxional or involved in some exchange equilibrium in solution. Variable temperature $^{31}P\{^1H\}$ and ^1H NMR spectroscopic studies were not carried out, but will be necessary in order to study this mixture further.

The signals observed in the $^{31}P\{^1H\}$ and ^1H NMR spectra for the reactions of $RhCl(PPh_3)_3$, **1** with one and/or five equivalents of di-*n*-hexylsilane per rhodium centre, that have not yet been assigned to specific structures, could be similar to the ones suggested in Halpern's olefin hydrogenation mechanism (Figure 3.2; Section 3.1). Halpern's work confirmed the presence of both mono- and dinuclear Rh-P containing complexes and some modified structures of those intermediates are shown in Figure 3.33.

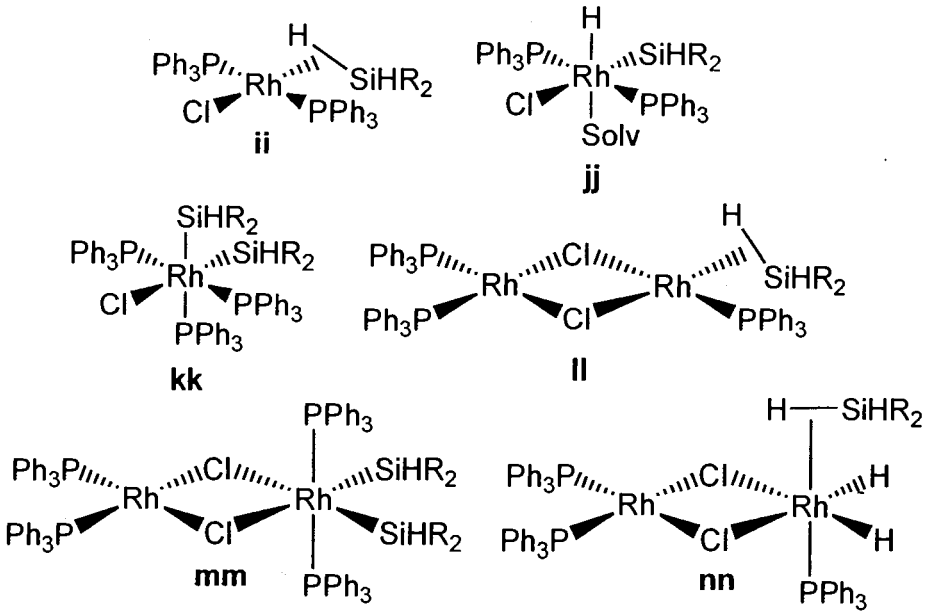

Figure 3.33: Possible Rh-P structures based on known intermediates from Halpern's olefin hydrogenation mechanism (see Figure 3.2, Section 3.1)

3.3.3 Stoichiometric reactions of Dppe dimer (3) with di-*n*-hexylsilane

3.3.3.1 Monitoring the reaction of [Rh(dppe)μ-Cl]$_2$, 3, with two equivalents of n-hex$_2$SiH$_2$

Upon addition of two equivalents (one equivalent per Rh centre) of di-*n*-hexylsilane to an orange suspension of [Rh(dppe)μ-Cl]$_2$, **3**, in d_6-benzene, the mixture immediately became yellow and then medium orange. Bubbles of gas were evolved, but much less than with the analogous reactions of silane with RhCl(PPh$_3$)$_3$, **1**, and [(PPh$_3$)$_2$Rh(μ-Cl)]$_2$, **2**. This evolution of H_2(g) slowed after 5 minutes, which was a much shorter time period compared to reactions of **1** or **2**. The solution turned a medium orange colour after 15-20 minutes. When the solution was left at room temperature for several hours it eventually changed to an orange-brown colour.

Room temperature $^{31}P\{^1H\}$ and ^1H NMR spectra of the dinuclear rhodium complex [Rh(dppe)μ-Cl]$_2$, **3**, with one equivalent per Rh centre of di-*n*-hexylsilane indicated the formation of one major product. A mixture of the starting dppe dimer **3** and a dinuclear species with a bridging hydride was present in solution. A single rhodium hydride resonance, a sharp multiplet, is observed in the ^1H NMR spectrum (Figure 3.34). The ^1H NMR spectrum (Figure 3.34) has signals at 5.2-4.9 ppm and more than one set of signals in the hexyl region. These signals are attributed to Si-H containing by-products, possibly some chloroorganosilanes ((R$_2$Si(H)(Cl)) and oligosilane derivatives. No unreacted di-*n*-hexylsilane (at 3.9 ppm) was observed.

References p111

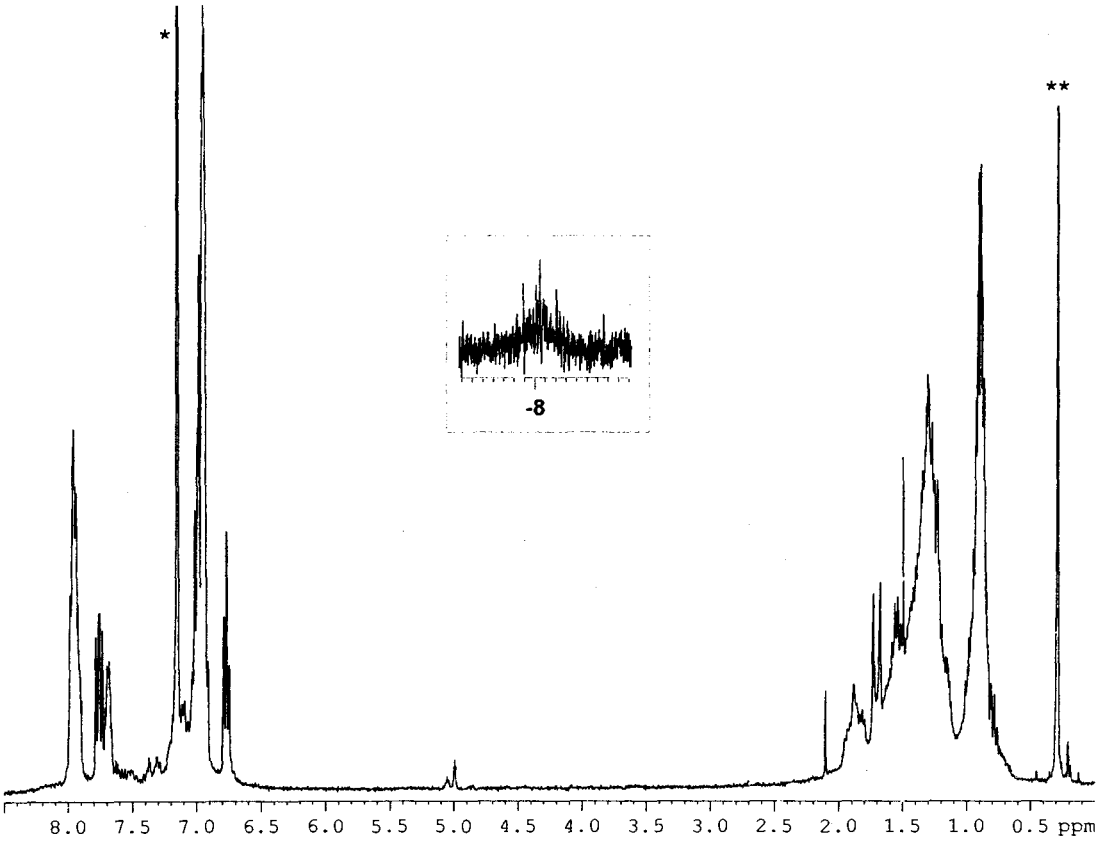

Figure 3.34: Room temperature 360 MHz ^{1}H NMR spectrum of $[Rh(dppe)\mu\text{-}Cl]_2$, **3** with one equivalent of di-*n*-hexylsilane in C_6D_5H (*). The "**" represents an impurity, silicone grease

Symmetric, doublet of multiplets patterns at 78.6 ppm ($^{1}J_{P\text{-}Rh}$ = 201 Hz) and 66.0 ppm ($^{1}J_{P\text{-}Rh}$ = 175 Hz) are observed in the room temperature $^{31}P\{^{1}H\}$ NMR spectrum in Figure 3.35.

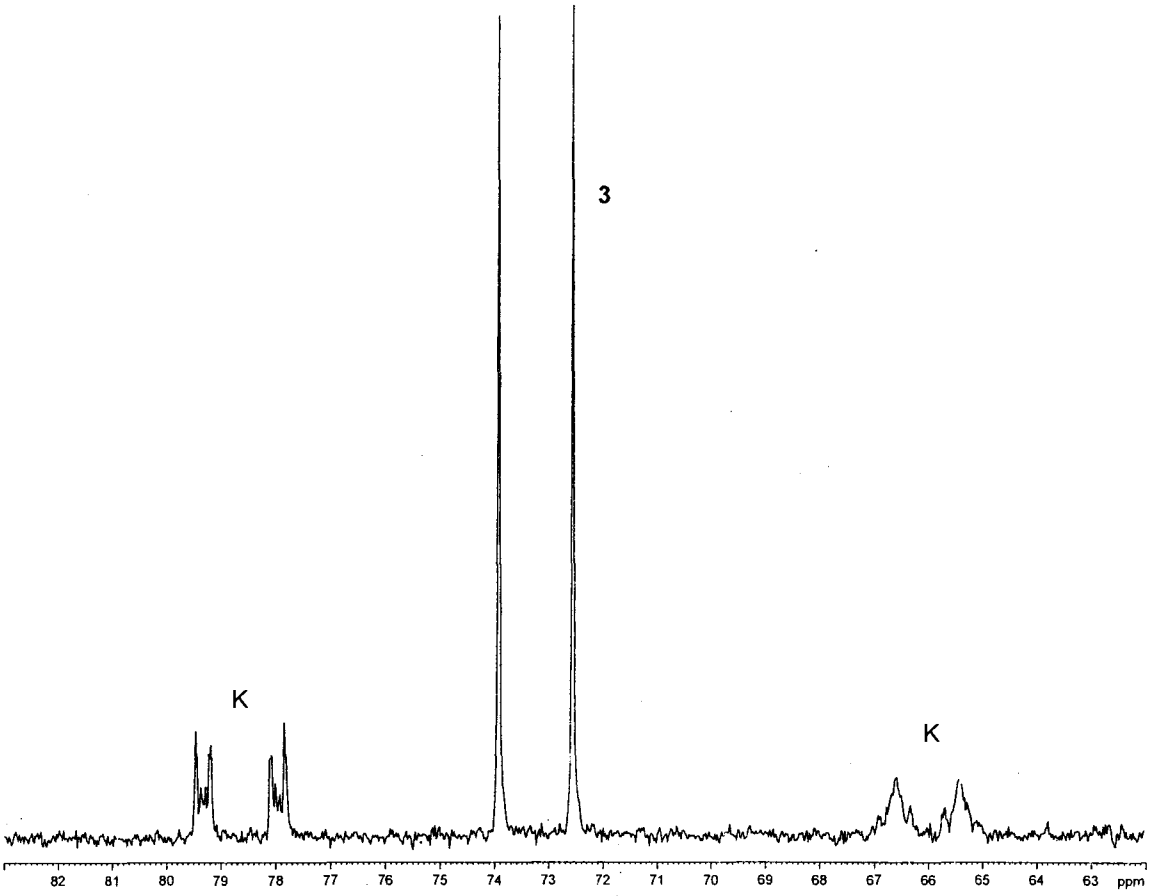

Figure 3.35: Room temperature 145.8 MHz $^{31}P\{^{1}H\}$ NMR spectrum of $[Rh(dppe)\mu\text{-}Cl]_2$, **3** with one equivalent of di-*n*-hexylsilane per rhodium centre in C_6D_6

These observations are consistent with the structure shown in Figure 3.36, a known bridged hydride species of formulation $[\{Rh(dppe)\}_2(\mu\text{-}H)(\mu\text{-}Cl)]$ (**7**)[6], introduced in Section 3.2.2. This complex has one bridging rhodium hydride and one bridging chloride ligand and a spin system of an AA'BB'XX' pattern where A, B = P and X = Rh.

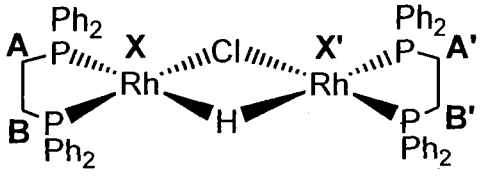

Figure 3.36: Possible structure in solution of complex **7**

Using a ^{31}P-^{31}P COSY NMR experiment, it was shown that the two sets of phosphorus signals, K, were correlated to each other, indicating the presence of one compound. If allowed to sit at room temperature, the solution mixture slowly reverts to the starting complex, **3** over approximately one week and complex **7** disappears.

3.3.3.2 Monitoring the reaction of [Rh(dppe)μ-Cl]$_2$, 3, with five equivalents of n-hex$_2$SiH$_2$

Upon addition of five equivalents (2.5 equivalents per Rh centre) of di-*n*-hexylsilane to the light orange suspension of [Rh(dppe)μ-Cl]$_2$, **3**, in d_6-benzene, the mixture immediately became yellow and gave a large amount of bubbles. This evolution of H_2(g) slowed after 5-10 minutes. The solution turned a medium orange colour after 15-20 minutes. When the solution was left at room temperature for several hours or more it eventually changed to a yellow-orange colour.

Room temperature $^{31}P\{^1H\}$ and ^1H NMR spectra of the above reaction mixture indicated a number of products after 20 minutes (Figure 3.37 and 3.38).

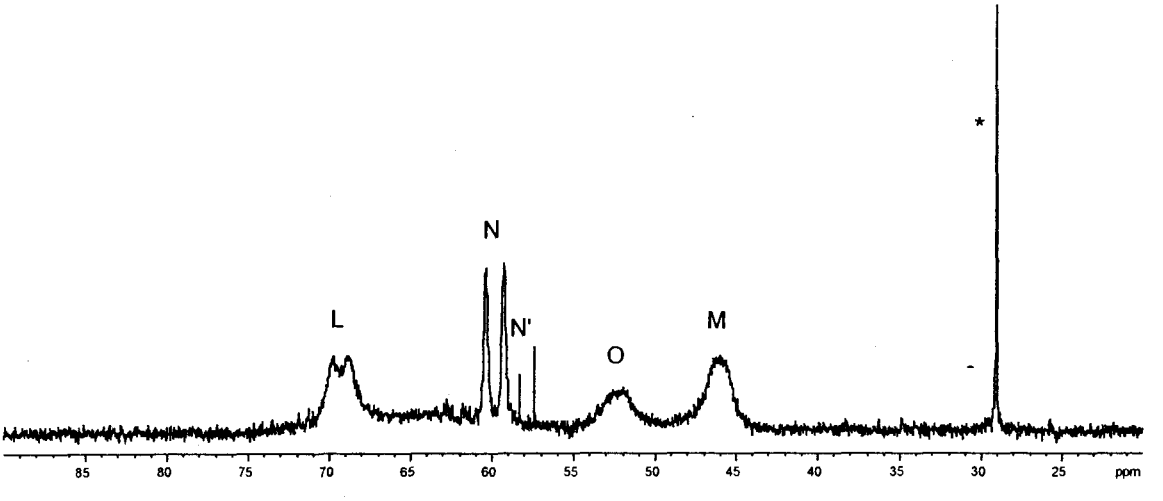

Figure 3.37: Room temperature 145.8 MHz $^{31}P\{^1H\}$ NMR spectrum of [Rh(dppe)μ-Cl]$_2$, **3** with 2.5 equivalents of di-*n*-hexylsilane per rhodium centre in C_6D_6 after 20 min. The "*" marks an impurity, bis(diphenylphosphino)ethane oxide

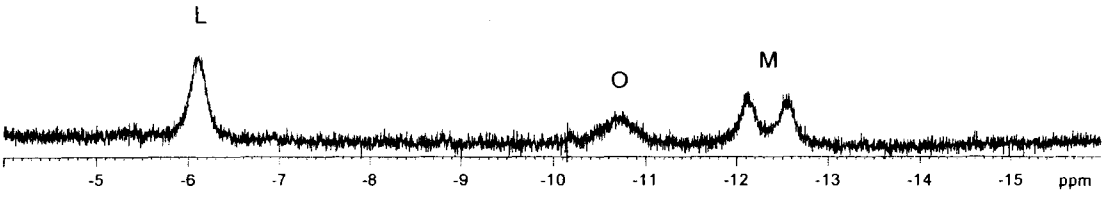

Figure 3.38: Room temperature 360 MHz ^{1}H NMR (hydride region) spectrum of $[Rh(dppe)\mu\text{-}Cl]_2$, **3** with 2.5 equivalents of di-*n*-hexylsilane per rhodium centre in C_6D_6 after 20 min

The breadth of the signals observed in the $^{31}P\{^{1}H\}$ NMR spectra in Figure 3.37 suggests that these complexes may be fluxional in solution. Variable temperature $^{31}P\{^{1}H\}$ and ^{1}H NMR spectroscopic studies were carried out to look at the reaction mixture further. The low temperature $^{31}P\{^{1}H\}$ and ^{1}H (hydride region) NMR spectra of **3** with five equivalents (2.5 equivalents per Rh centre) of di-*n*-hexylsilane are shown in Figure 3.39 and Figure 3.40, respectively.

Two major species, labelled L and M, were observed at low temperature in the $^{31}P\{^{1}H\}$ NMR spectrum in Figure 3.39 (f). Decoalescence of the broad signals at 69.7 and 46.3 ppm to give better resolved signals, with some fine splitting, was observed in Figure 3.39 (a) to (f). Spin-spin couplings for the peaks at 69.7 ppm and 46.3 ppm were measured to give approximate values of $^{1}J_{P\text{-}Rh}$ = 109 Hz and $^{1}J_{P\text{-}Rh}$ = 99 Hz, respectively. These low J values seem to indicate the presence of Rh(III)-containing complexes. The broad signal, labelled O, at 53.0 ppm in Figure 3.39 (a) appears to disappear (or coalesce), while the signals from approximately 65.0 to 57.5 ppm broaden slightly at lower temperatures.

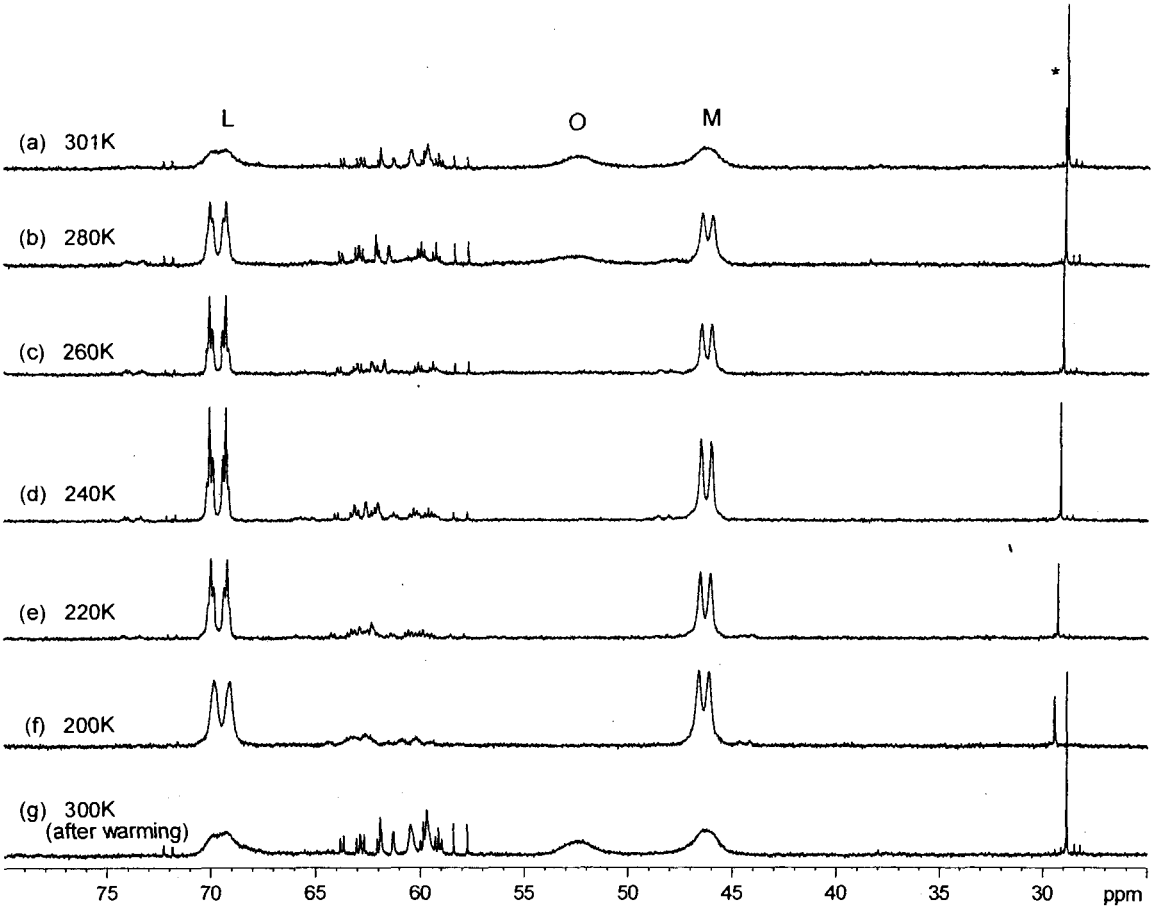

Figure 3.39: Low temperature 202 MHz $^{31}P\{^{1}H\}$ NMR spectra of $[Rh(dppe)\mu\text{-}Cl]_2$, **3** with 2.5 equivalents of di-*n*-hexylsilane per rhodium centre in C_7D_8. The "*" marks an impurity, bis(diphenylphosphino)ethane oxide

The products from this reaction of $[Rh(dppe)\mu\text{-}Cl]_2$, **3**, with five equivalents (2.5 equivalents per Rh centre) of di-*n*-hexylsilane do not match those seen for the reaction of $[Rh(dppe)\mu\text{-}Cl]_2$, **3**, with one equivalent (per Rh centre) of di-*n*-hexylsilane in Figures 3.32 and 3.33. The hydride region of the low temperature ^{1}H NMR spectra in Figure 3.40 (a) to (d) shows two very broad signals, labelled L and M, become better resolved to give a doublet at –12.2 ppm and what appears to be a sharp singlet with finer splitting at –6.3

ppm, indicating one or more hydride ligands for these species. The complete ^{1}H NMR spectrum (not shown here) has signals around 5.3-4.8 ppm and more than one set of signal in the hexyl region. These signals are attributed to Si-H containing by-products, possibly some chloroorganosilanes and/or the Si-H bond of Rh-Si complexes (i.e. Rh-$SiHR_2$). Some unreacted di-*n*-hexylsilane was observed at 3.9 ppm.

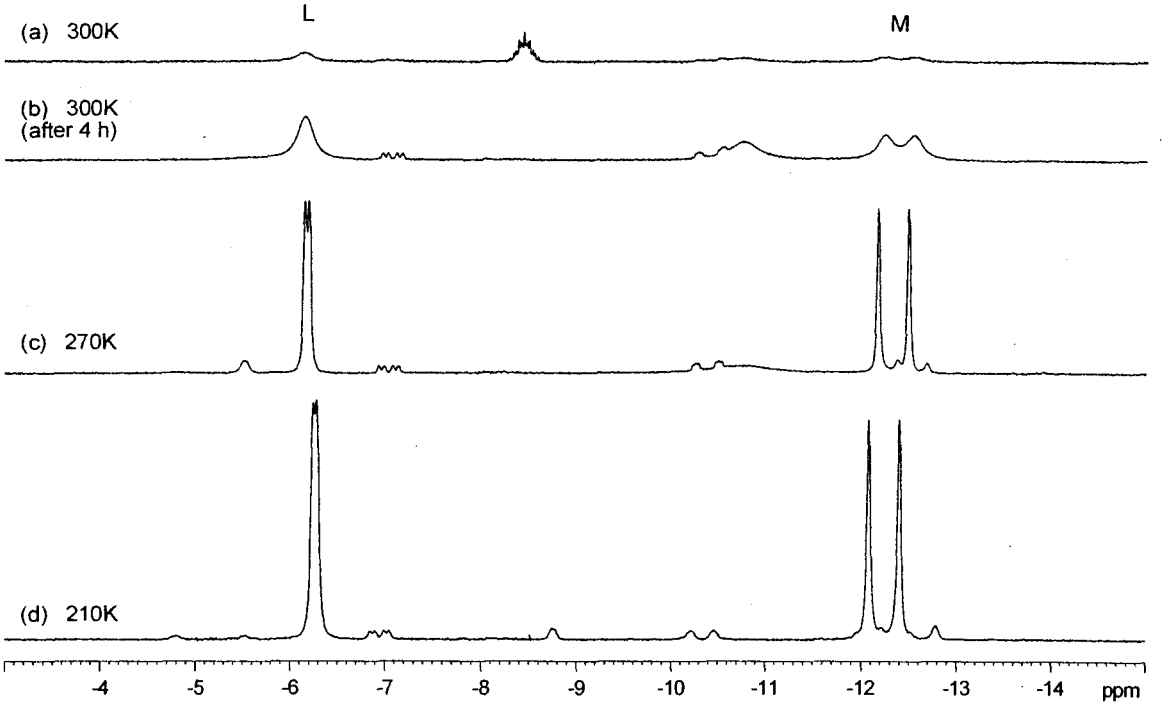

Figure 3.40: Low temperature 500 MHz ^{1}H NMR (hydride region) spectra of $[Rh(dppe)\mu\text{-}Cl]_2$, **3** with 2.5 equivalents of di-*n*-hexylsilane per rhodium centre in C_7D_8

The complexity observed for some of the signals in the low temperature $^{31}P\{^1H\}$ NMR spectra, usually indicative of dinuclear compounds, suggests that possible Rh-P containing products for the reaction of $[Rh(dppe)\mu\text{-}Cl]_2$, **3**, with 2.5 equivalents of di-*n*-hexylsilane per rhodium centre may include those presented in Figure 3.41. Mononuclear

complexes are also possible (similar to those in Figure 3.33, Section 3.3.2.3), but are expected to give less complicated signals.

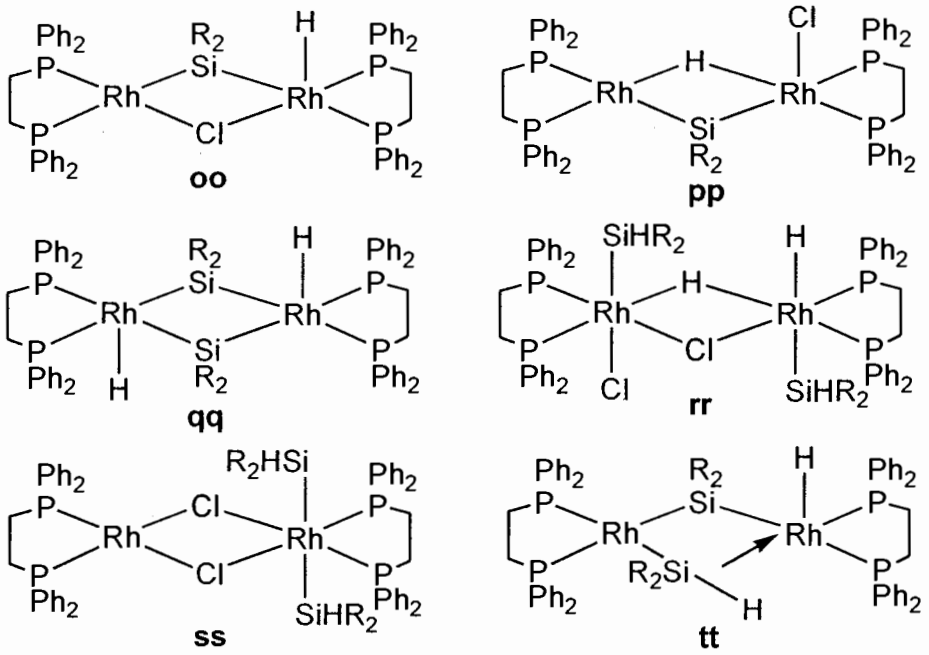

Figure 3.41: Possible dinuclear structures, in solution, of [Rh(dppe)μ-Cl]$_2$, **3** with 2.5 equivalents of di-*n*-hexylsilane per rhodium centre

3.3.4 Stoichiometric reactions of a cationic rhodium complex (4) with di-*n*-hexylsilane

3.3.4.1 Monitoring the reaction of [Rh(COD)(PPh$_3$)$_2$]$^+$PF$_6^-$, 4, with one equivalent of n-hex$_2$SiH$_2$

Upon addition of one equivalent of di-*n*-hexylsilane to a yellow-orange solution of [Rh(COD)(PPh$_3$)$_2$]$^+$PF$_6^-$, **4**, in methylene chloride, the mixture immediately became medium orange-red and gave a small number of bubbles. This evolution of H_2(g) slowed after 5-10 minutes. The solution turned a dark orange-red colour after 15-20 minutes. When the solution was left at room temperature for one hour or more it eventually changed to a red-purple colour.

Work has been done with cationic complexes of the type $[Rh(diene)(PR_3)_2]PF_6^-$ by B. R. James, as well as other groups, and they have noted that solvation of these complexes can give the species $[Rh(PR_3)_2(solv)_2]PF_6^-$.[16] Room temperature $^{31}P\{^1H\}$ and ^1H NMR spectra of the mononuclear rhodium complex $[Rh(COD)(PPh_3)_2]^+PF_6^-$, **4**, with one equivalent of di-*n*-hexylsilane in deuterated benzene indicated the formation of three products after 20 minutes. A sharp doublet was observed in the $^{31}P\{^1H\}$ NMR spectrum at 43.7 ppm ($^1J_{P\text{-}Rh}$ = 206 Hz), labelled P, along with a broad doublet, at 28.5 ppm ($^1J_{P\text{-}Rh}$ ≈ 150 Hz), labelled Q, in Figure 3.42. The starting catalyst, **4**, is still present after several hours, indicating that this reaction is fairly slow.

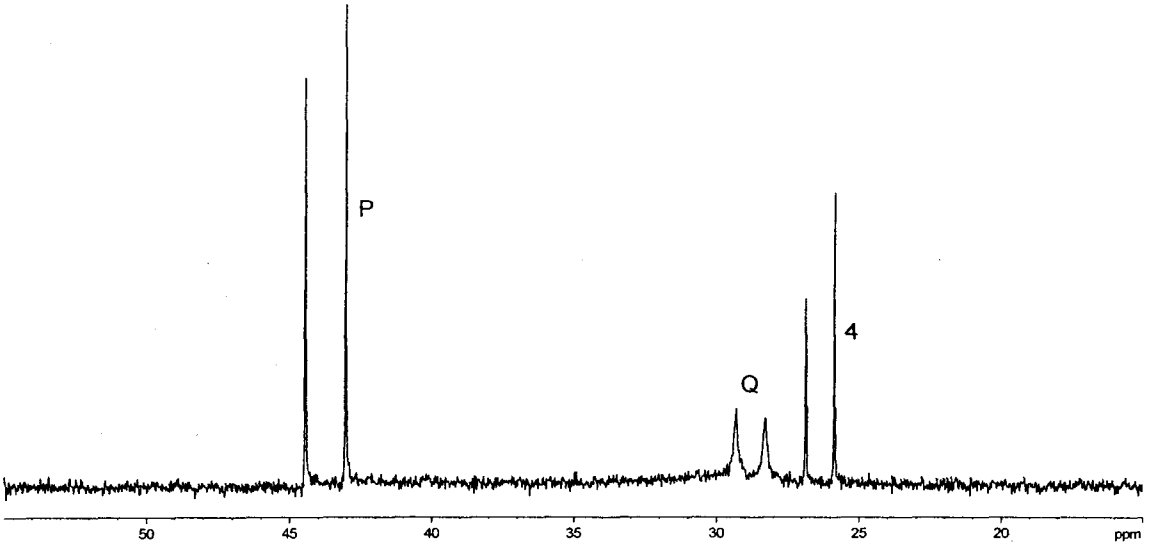

Figure 3.42: Room temperature 145.8 MHz $^{31}P\{^1H\}$ NMR spectrum of $[Rh(COD)(PPh_3)_2]^+PF_6^-$, **4**, with one equivalent of di-*n*-hexylsilane per rhodium centre in C_6D_6

References p111

Based on literature precedent, this result is consistent with the structure shown in Figure 3.43, with solvent coordination at the rhodium center (S = solvent). The spin system for complex **8** follows an A_2X pattern where A = P and X = Rh.

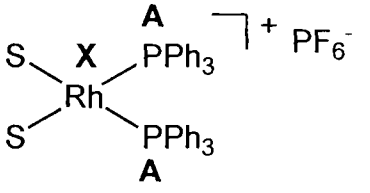

Figure 3.43: Possible structure in solution of complex **8**

The complete ^{1}H NMR spectrum (not shown here) has two sets of signals in the alkyl region (hexyl groups) and two broad singlets at 5.5 and 3.2 ppm. These signals are attributed to Si-H containing products and could indicate the presence of Rh-$SiHR_2$ type complexes, since the signals do not correspond to any of the signals (identified as free organosilanes) observed in earlier experiments with complexes **1**, **2** and/or **3**. Also, no unreacted di-*n*-hexylsilane (at 3.9 ppm) was observed.

3.3.4.2 Monitoring the reaction of $[Rh(COD)(PPh_3)_2]^+PF_6^-$, 4, with five equivalents of n-hex_2SiH_2

Upon addition of five equivalents of di-*n*-hexylsilane to a yellow-orange solution of $[Rh(COD)(PPh_3)_2]^+PF_6^-$, **4**, in methylene chloride, the mixture immediately became dark red-orange-purple and gave much more bubbling than complex **4** with one equivalent of silane. This evolution of H_2(g) slowed after 10-15 minutes. When the solution was left at room temperature for one hour or more it eventually changed to a dark red-purple-brown colour. The colour progression is very similar to that observed for complex **4** with one equivalent of silane, but occurs faster.

The mononuclear rhodium complex $[Rh(COD)(PPh_3)_2]^+PF_6^-$, **4**, reacted with five equivalents of di-*n*-hexylsilane to afford two products after 20 minutes in solution as observed by room temperature $^{31}P\{^1H\}$ NMR spectroscopy. The same signals seen above for $[Rh(COD)(PPh_3)_2]^+PF_6^-$, **4** with one equivalent of di-*n*-hexylsilane (43.7 and 28.5 ppm and the starting catalyst, **4**) are also observed for the reaction with five equivalents of silane, indicating that the same type of species are present in either stoichiometric solution. Similar to the reaction above, a broad signal around 3.3 ppm is observed in the Si-H region of the complete room temperature ^1H NMR spectrum (not shown here). Multiple (although fairly weak) signals are also observed in the hexyl region, indicating the presence of SiR_2 containing products. Unlike the reaction of complex **4** with one equivalent of silane, a small amount of unreacted di-*n*-hexylsilane is observed at 3.9 ppm.

3.4 Conclusions

In this chapter, multiple stoichiometric reactions were carried out (and monitored by NMR spectroscopy) with catalyst precursors, $RhCl(PPh_3)_3$, **1**, $[(PPh_3)_2Rh(\mu\text{-}Cl)]_2$, **2**, $[Rh(dppe)\mu\text{-}Cl]_2$, **3**, and $[Rh(COD)(PPh_3)_2]^+PF_6^-$, **4**. Hydrogenation intermediates from Halpern's work on catalytic hydrogenation of alkenes by Wilkinson's catalyst and early silane addition chemistry, reported by Osakada and Haszeldine were found to be useful guides for the analysis of these stoichiometric reactions and the resulting $^{31}P\{^1H\}$ and ^1H NMR spectra.

Although no NMR spectroscopic evidence for intermediates containing a metal silylene ("M=Si") was observed for these stoichiometric reactions, with any of the catalyst precursors used (**1-4**), it should be noted that there is great difficulty presented in

References p111

"seeing" these types of ligands by ^{1}H NMR spectroscopy, if they have no Si-H bond. Silyl-type ligands resulting from oxidative addition of a Si-H bond to a metal centre were observed by ^{1}H NMR spectroscopy. Signals due to Rh-H bonds were observed in the hydride region along with signals in the Si-H region of the ^{1}H NMR, which were attributed to coordinated $-SiHR_2-$ at the Rh centre. $^{31}P\{^{1}H\}$ NMR was also useful in helping to identify these metal-silyl complexes.

Complex **5**, $[(PPh_3)_2Rh(H)(Cl)(SiHR_2)]$, a product of oxidative addition of a Si-H bond to a Rh centre, was isolated from the reaction of $[(PPh_3)_2Rh(\mu\text{-}Cl)]_2$, **2**, with one equivalent of di-*n*-hexylsilane per rhodium centre, and was found to be catalytically competent. The formation of this complex is proposed to be the first step in the catalytic cycle.

Complexes **5** and **6** have been conclusively identified in the reaction mixtures of **1** and **2**, while complexes **7** and **8** have been conclusively identified in the reaction mixtures of **3** and **4**, respectively. Other signals observed in the $^{31}P\{^{1}H\}$ and ^{1}H NMR spectra, for all reactions of catalyst precursors (**1-4**) with di-*n*-hexylsilane, have not yet been assigned to specific structures. Patterns in the $^{31}P\{^{1}H\}$ NMR spectra suggest the presence of both mono- and dinuclear Rh-P containing complexes, while the spin-spin coupling values ($^{1}J_{P\text{-}Rh}$), suggest that both Rh(I) and/or Rh(III) containing complexes are present as intermediates for these stoichiometric dehydrocoupling silane reactions.

The signals observed in the $^{31}P\{^{1}H\}$ and ^{1}H NMR spectra for catalyst precursors **1** and **2**, with varying amounts of di-*n*-hexylsilane, were very dissimilar compared to the signals observed for **3** and **4**, possibly indicating the presence of different intermediate structures. Although a great deal of information has been compiled on complexes likely

References p111

to be involved in these dehydrocoupling of silane reactions, more work is necessary toward elucidating specific structures and mechanisms.

3.5 Experimental

3.5.1 General conditions, reagents and instruments

General conditions are the same as mentioned in the experimental section for Chapter 2 (Section 2.6, page 38).

3.5.2 Stoichiometric reactions – general procedure

Stoichiometric studies were carried out for each of the four Rh(I) complexes of interest: $RhCl(PPh_3)_3$, **1**, $[Rh(PPh_3)_2\mu\text{-}Cl]_2$, **2**, $[Rh(dppe)\mu\text{-}Cl]_2$, **3**, and $[Rh(COD)(PPh_3)_2]^+PF_6^-$, **4**. Each catalyst was reacted with one, two and five equivalents of neat di-*n*-hexylsilane (per rhodium catalyst center). These stoichiometric reactions were screened first using regular NMR tubes (caps sealed with parafilm to slow O_2 diffusion into the sample) to observe the initial results. The NMR experiments that gave promising product distributions were then carried out with sealable NMR tubes.

All sealed NMR samples were made up in the glove box under nitrogen. They were then attached to a Schlenk line and flame sealed under partial vacuum. The NMR sample tube and contents were kept frozen in liquid nitrogen during the flame-sealing process. All of these stoichiometric reactions were carried out at room temperature and monitored by $^{31}P\{^1H\}$ and ^1H NMR spectroscopy. When the reactions had appeared to reach a steady state mixture, they were also monitored by variable temperature NMR and further 2D NMR experiments.

References p111

Table 3.1: ^{1}H NMR chemical shift values, multiplicity and coupling constants. δ in ppm (multiplicity, RI, assignment), J (or $\omega_{1/2}$) in Hz. Unless otherwise noted all ^{1}H NMR experiments were carried out at 360 MHz in C_6D_6

Cmpd	Aromatic region	Si-H region	Alkyl region	Hydride region
A [c] (5)	7.01-7.15 (m, 12H, H_o) 7.98-8.03 (m, 18H,$H_{m/p}$)	≈ 3.60 (br s), $\omega_{1/2}$ ≈ 40	0.90 (t, 3H,CH_3) 0.87-0.96 (m, 2H,CH_2) 1.13-1.32(m) 1.43-1.54(m)	-13.98 (d of t, 1H, Rh-*H*) $^1J_{H\text{-}Rh}$ = 22, $^2J_{H\text{-}P}$ = 14
B	7.14-7.16 (m) 7.44-7.53 (br m) 7.78-7.82 (m)	4.57-4.54 (m) 4.86- (br m) 5.01-4.98 (br m) 5.07-5.04 (br m)	0.88-1.55 [a]	-7.54 (br d), $^1J_{H\text{-}Rh}$ ≈ 25
C (6)	6.92-6.47 (ov m) 7.25-7.26 (m) 7.58-7.61 (m)	No signals	0.88-1.55 [a]	-8.37 to –8.41 (br m), $^1J_{H\text{-}Rh}$ ≈ 19
D	7.01-6.69(ov m)[a] 7.83-7.91 (m)	2.50-6.50 [b]	0.88-1.55 [a]	-14.48 to –14.53 (br m)
E	7.68-6.72 [a]	2.50-6.50 [b]	0.88-1.55 [a]	-6.80 to –4.30 (br d of m)
F	7.04-7.08 (m) 7.19-7.17 (m) 7.89-7.77 (br m)	≈3.80 (br s), $\omega_{1/2}$ ≈ 130 ≈4.80 (br s), $\omega_{1/2}$ ≈ 105	0.88-1.55 [a]	-7.76 (br s), $\omega_{1/2}$ ≈ 70
G	7.03-7.06 (m) 7.99-8.04 (br m)	≈ 3.60 (br s), $\omega_{1/2}$ ≈ 35	0.92 (t, 3H, CH_3) 0.89-0.98 (m, 2H,CH_2) 1.14-1.32(m) 1.45-1.56(m)	-14.98 to –15.03 (br m)
H	8.00-6.50 [b]	2.50-6.50 [b]	0.88-1.55 [b]	-8.30 to –8.56 (br d of m)
I	8.00-6.50 [b]	2.50-6.50 [b]	0.88-1.55 [b]	-7.79 (br s, $\omega_{1/2}$ ≈ 35)
J	8.00-6.50 [a]	≈ 4.08 (br s), $\omega_{1/2}$ ≈ 40 ≈ 3.06 (br s) $\omega_{1/2}$ ≈ 45	0.88-1.55 [a]	-7.52 (br s, $\omega_{1/2}$ ≈ 90)
K (7)	7.77-7.75 (m) 6.97-6.94 (m)	3.90 (m, *n*-hex$_2$SiH) 4.51 (br s), $\omega_{1/2}$ ≈ 10 4.89-4.88 (br m) 5.04-5.01 (br m) 5.15-5.12 (br m)	0.88-1.55 [a]	-7.95 to –8.10 (br m)

References p111

Cmpd	Aromatic region	Si-H region	Alkyl region	Hydride region
L	8.00-6.50 [a]	3.90 (m, *n*-hex$_2$SiH) 4.89-4.88 (br m) 5.04-5.01 (br m)	0.88-1.55 [a]	-6.11 (br s, $\omega_{1/2} \approx 75$)
M	8.00-6.50 [a]	3.90 (m, *n*-hex$_2$SiH) 4.89-4.88 (br m) 5.04-5.01 (br m)	0.88-1.55 [a]	-12.33 (br d), $^1J_{H\text{-}Rh} = 145$ [e]
N	8.00-6.50 [a]	2.50-6.50 [b]	0.88-1.55 [a]	-10.5 (br s, $\omega_{1/2} \approx 126$)
Orange powder [d]	7.51-7.59 (br m)	No signals	No signals	-8.01 (d), $^1J_{H\text{-}Rh} = 13$

a Large region of overlapping, unassignable signals
b Weak, unassignable signals
c ^{1}H-NMR (500 MHz, C_6D_6)
d Isolated from addition of one equivalent of di-*n*-hexylsilane to $RhCl(PPh_3)_3$, **1**
e Large coupling value possibly be due to presence of two hydrides

Table 3.2: ^{31}P NMR chemical shift values, multiplicity and coupling constants. Unless otherwise noted all ^{31}P NMR experiments were carried out at 360 MHz in C_6D_6

Cmpd	δ (ppm) $^{31}P\{^1H\}$	Multiplicity	Coupling constants J (or $\omega_{1/2}$) in Hz
A [a] **(5)**	39.9	d	$^1J_{P\text{-}Rh} = 123$
B	39.0 40.6	br d of m d of br d	$^1J_{P\text{-}Rh} \approx 166$ $^1J_{P\text{-}Rh} \approx 121$
C [a] **(6)**	34.6 45.0	br d of dd br d of m	$^1J_{P\text{-}Rh} = 161$; $^2J_{P\text{-}P} = 28$ $^1J_{P\text{-}Rh} = 194$
D	47.6-46.8	br m	
E	42.2-40.4	br d of m	$^1J_{P\text{-}Rh} \approx 205$
F	48.8-47.5 44.3-42.2	br dd br dd	$^1J_{P\text{-}Rh} = 153$; $^2J_{P\text{-}P} = 48$ $^1J_{P\text{-}Rh} = 201$; $^2J_{P\text{-}P} = 45$
G	38.7	d	$^1J_{P\text{-}Rh} = 124$
H	36.9	br s	$\omega_{1/2} \approx 540$
I	34.8	br s	$\omega_{1/2} \approx 580$
J	60.0-20.0	complex br ov m	

Cmpd	δ (ppm) $^{31}P\{^1H\}$	Multiplicity	Coupling constants J (or $\omega_{1/2}$) in Hz
K (7)	78.6 66.0	d of m d of m	$^1J_{P\text{-}Rh} \approx 175$ $^1J_{P\text{-}Rh} \approx 201$
L	69.7-68.9	br d of m	$^1J_{P\text{-}Rh} \approx 116$
M	46.3	br s	$\omega_{1/2} = 292$
N	59.8	br d	$^1J_{P\text{-}Rh} = 162$
N'	57.8	d	$^1J_{P\text{-}Rh} = 133$, $[Rh(dppe)_2]Cl$
O	51.9	br s	$\omega_{1/2} = 364$
P (8)	43.7	d	$^1J_{P\text{-}Rh} = 206$
Q	28.7	br d	$^1J_{P\text{-}Rh} \approx 150$
R	46.3	d	$^1J_{P\text{-}Rh} = 176$
S	40.2	dd	$^1J_{P\text{-}Rh} = 125$; $^2J_{P\text{-}P} = 32$
Orange powder *b*	38.9	br s	$\omega_{1/2} \approx 640$

a $^{31}P\{^1H\}$-NMR (202 MHz, C_6D_6)
b Isolated from addition of one equivalent of di-*n*-hexylsilane to $RhCl(PPh_3)_3$, **1**

Isolation of complex 5, $[(PPh_3)_2Rh(H)(Cl)(SiHR_2)]$, from addition of two equivalents of di-n-hexylsilane to $[(PPh_3)_2Rh(\mu\text{-}Cl)]_2$, 2

Addition of two equivalents (one equivalent per Rh centre) of di-*n*-hexylsilane (6.0 mg, 0.030 mmol) in toluene to $[(PPh_3)_2Rh(\mu\text{-}Cl)]_2$, **2**, (20 mg, 0.015 mmol) caused an orange solution to form. Addition of a non-polar solvent (e.g. pentane or hexanes) at -5°C caused precipitation of a yellow powder, **5**, $[(PPh_3)_2Rh(H)(Cl)(SiHR_2)]$. Not enough product (complex **5**) available to weigh (no yield obtained).

Isolation of an orange powder from addition of one equivalent of di-n-hexylsilane to $RhCl(PPh_3)_3$, 1

Addition of one equivalent of di-*n*-hexylsilane (4.3 mg, 0.022 mmol), in toluene, to $RhCl(PPh_3)_3$, **1**, (20 mg, 0.022 mmol) causes a dark orange solution to form. A light orange powder was precipitated from this solution with the addition of hexanes.

Stoichiometric reactions of Wilkinson's dimer (2) with di-*n*-hexylsilane

Reaction of [(PPh$_3$)$_2$Rh(μ-Cl)]$_2$, 2, with two equivalents of n-hex$_2$SiH$_2$

The reaction was performed as per Section 3.5.2 using the following reagents and amounts:

Di-*n*-hexylsilane	$[(PPh_3)_2Rh(\mu\text{-}Cl)]_2$, **2**
6.0 mg, 0.030 mmol	20 mg, 0.015 mmol in d_6-benzene (0.6 mL)

The progress of reaction was described in Section 3.3.1.2. The products observed over time are as follows:

Time elapsed after sealing NMR tube	**Solution colour**	**Species observed by $^{31}P\{^1H\}$, ^1H NMR**
2 h	Orange	A, B
48 h	Red-orange	A, B, C, D, E

Reaction of [Rh(PPh$_3$)$_2$μ-Cl]$_2$, 2, with five equivalents of n-hex$_2$SiH$_2$

The reaction was performed as per Section 3.5.2 using the following reagents and amounts:

Di-*n*-hexylsilane	$[(PPh_3)_2Rh(\mu\text{-}Cl)]_2$, **2**
15.1 mg, 0.075 mmol	20 mg, 0.015 mmol in d_6-benzene (0.6 mL)

The progress of reaction was described in Section 3.3.1.2. The products observed over time are as follows:

Time elapsed after sealing NMR tube	**Solution colour**	**Species observed by $^{31}P\{^1H\}$, ^1H NMR**
2 h	Light orange	B, F
48 h	Dark orange	B, E, F

References p111

Stoichiometric reactions of Wilkinson's catalyst (1) with di-*n*-hexylsilane

Reaction of $RhCl(PPh_3)_3$, 1, with one equivalent of n-hex_2SiH_2

The reaction was performed as per Section 3.5.2 using the following reagents and amounts:

Di-*n*-hexylsilane	$RhCl(PPh_3)_3$, **1**
4.3 mg, 0.022 mmol	20 mg, 0.022 mmol in d_6-benzene (0.6 mL)

The progress of reaction was described in Section 3.3.1.2. The products observed over time are as follows:

Time elapsed after sealing NMR tube	**Solution colour**	**Species observed by $^{31}P\{^1H\}$, ^1H NMR**
2 h	Red-orange	A, G, H, I
48 h	Burgundy-orange	A, B, G, H, I

Reaction of $RhCl(PPh_3)_3$, 1, with five equivalents of n-hex_2SiH_2

The reaction was performed as per Section 3.5.2 using the following reagents and amounts:

Di-*n*-hexylsilane	$RhCl(PPh_3)_3$, **1**
21.7 mg, 0.11 mmol	20 mg, 0.022 mmol in d_6-benzene (0.6 mL)

The progress of reaction was described in Section 3.3.1.2. The products observed over time are as follows:

Time elapsed after sealing NMR tube	**Solution colour**	**Species observed by $^{31}P\{^1H\}$, ^1H NMR**
24 h	Medium orange	G, I
48 h	Dark red-orange	J

References p111

Stoichiometric reactions of dppe dimer (3) with di-*n*-hexylsilane

Reaction of [Rh(dppe)μ-Cl]$_2$, 3, with two equivalents of n-hex$_2$SiH$_2$

The reaction was performed as per Section 3.5.2 using the following reagents and amounts:

Di-*n*-hexylsilane	[Rh(dppe)μ-Cl]$_2$, **3**
7.6 mg, 0.038 mmol	20 mg, 0.019 mmol in d_6-benzene (0.6 mL)

The progress of reaction was described in Section 3.3.1.2. The products observed over time are as follows:

Time elapsed after sealing NMR tube	**Solution colour**	**Species observed by $^{31}P\{^1H\}$, ^1H NMR**
2 h	Medium orange	K, **3**

Reaction of [Rh(dppe)μ-Cl]$_2$, 3, with five equivalents of n-hex$_2$SiH$_2$

The reaction was performed as per Section 3.5.2 using the following reagents and amounts:

Di-*n*-hexylsilane	[Rh(dppe)μ-Cl]$_2$, **3**
18.7 mg, 0.093 mmol	20 mg, 0.019 mmol in d_6-benzene (0.6 mL)

The progress of reaction was described in Section 3.3.1.2. The products observed over time are as follows:

Time elapsed after sealing NMR tube	**Solution colour**	**Species observed by $^{31}P\{^1H\}$, ^1H NMR**
20 min	Medium orange	L, M, N, N',O

References p111

Stoichiometric reactions of a cationic rhodium complex (4) with di-*n*-hexylsilane

Reaction of [Rh(COD)(PPh$_3$)$_2$]$^+$PF$_6^-$, 4, with one equivalent of n-hex$_2$SiH$_2$

The reaction was performed as per Section 3.5.2 using the following reagents and amounts:

Di-*n*-hexylsilane 4.6 mg, 0.023 mmol	$[Rh(COD)(PPh_3)_2]^+PF_6^-$, **4** 20 mg, 0.023 mmol in CH_2Cl_2 and d_6-benzene (0.2 mL)

The progress of reaction was described in Section 3.3.1.2. The products observed over time are as follows:

Time elapsed after sealing NMR tube	**Solution colour**	**Species observed by $^{31}P\{^1H\}$, ^1H NMR**
20 min	Dark orange-red	P, Q, **4**
48 h	Red-purple	P, Q, R, S, **4**

Reaction of [Rh(COD)(PPh$_3$)$_2$]$^+$PF$_6^-$ 4 with five equivalents of n-hex$_2$SiH$_2$

The reaction was performed as per Section 3.5.2 using the following reagents and amounts:

Di-*n*-hexylsilane 23 mg, 0.11 mmol	$[Rh(COD)(PPh_3)_2]^+PF_6^-$, **4** 20 mg, 0.023 mmol in CH_2Cl_2 and d_6-benzene (0.2 mL)

The progress of reaction was described in Section 3.3.1.2. The products observed over time are as follows:

Time elapsed after sealing NMR tube	**Solution colour**	**Species observed by $^{31}P\{^1H\}$, ^1H NMR**
20 min	Red-purple-brown	P, Q, **4**

References p111

3.6 References

(1) (a) Tilley, T.D. *Comments Inorg. Chem.* **1990**, *10*, 37; (b) Corey, J.Y., in *Dehydrogenative Coupling Reactions of Hydrosilanes;* G.L. Larson, Ed. JAI Press Inc., 1991. Vol. 1, p. 327; (c) Gauvin, F., Harrod, J.F., Woo, H.G. *Adv. Organomet. Chem.* **1998**, *42*, 363; (d) Reichl, J.A., Berry, D.H. *Adv. Organomet. Chem.* **1999**, *43*, 197; (e) Original paper postulates an Rh=Si intermediate, but with no evidence given: Ojima I., Inaba, S-I., Kogure, T. *J. Organomet. Chem.* **1973**, *55*, C7.

(2) Spessard, G.O., Meissler, G.L. *Organometallic Chemistry;* Prentice Hall: USA, 1996, p. 279.

(3) Halpern, J., Okamoto, T., Zakhariev, A. *J. Mol. Cat.* **1976**, *2*, 65.

(4) Collman, J. P., Hegedus, L. S., Norton, J. R., Finke, R. G. *Principles and Applications of Organotransition Metal Chemistry*; University Science Books, USA, 1987, p. 533.

(5) Akitt, J.W. *NMR and Chemistry Second Edition: An Introduction to the Fourier Transform-Multinuclear Era*; J.W. Arrowsmith Ltd.: Great Britain, 1983, p. 45.

(6) Ball, G.E., Cullen, W.R., Fryzuk, M.D., Henderson, W.J., James, B.R., MacFarlene, K.S. *Inorg. Chem.* **1994**, *33*, 1464.

(7) (a) Aizenberg, M., Ott, J., Elsevier, C.J., Milstein, D. *J. Organomet. Chem.* **1998**, 551, 81; (b) Mann, B.E., Guzman, M.H. *Inorg. Chem. Acta.* **2002**, *330*, 143.

(8) Glaser, P.B., Tilley, T.D. *Organometallics* **2004**, *23*, 5799.

(9) Gansle, P.B., Gruber, B.C., Jarvis, J.T., Slaitas, A., De Jesus, S., De Jesus, K. *Microchemical Journal* **1997**, *55*, 222.

(10) Haszeldine, R.N., Parish, R.V., Parry, D.J. *J. Chem. Soc. (A)* **1969**, 683.

(11) Powell, P. *Principles of Organometallic Chemistry: 2nd Edition*; Chapman and Hall Ltd.: New York, 1988, p. 104.

(12) Günther, H. *NMR Spectroscopy: Second Edition: Basic Principles, Concepts, and Applications in Chemistry*; John Wiley & Sons: New York. 1992, p. 341.

(13) Ibid, p. 363

(14) Corey, J and Braddock-Wilking, J., *Chem. Rev.* **1999**, *99*, 175.

(15) Cotton, F.A., Wilkinson, G., Murillo, C. A., Bochmann, M. *Advanced Inorganic Chemistry: 6th Edition*; John Wiley & Sons: USA, 1999, p. 1245.

(16) Marcazzan, P., Patrick, B.O., James, B.R. *Organometallics* **2003**, *22*, 1177.

References p111

CHAPTER 4

Prospects for Future Studies

4.1 Prospects for future studies

In this thesis, the reactions of di-*n*-hexylsilane with four late transition metal Rh(I) catalyst precursors: $RhCl(PPh_3)_3$, **1**, $[(PPh_3)_2Rh(\mu\text{-}Cl)]_2$, **2**, $[Rh(dppe)\mu\text{-}Cl]_2$, **3**, $[Rh(COD)(PPh_3)_2]^+PF_6^-$, **4** were examined for their potential utility, on a synthetically useful scale, in the production of Si-H functionalized oligosilane reagents. Attempts were made to identify the best catalyst precursor for the production of dialkyl-substituted di- and trisilanes, to understand the importance of key catalyst structural features in a putative catalytic cycle, and to identify species present in the catalytic mixtures.

The ability of Rh(I) phosphine catalyst precursors (**1-4**) to couple di-*n*-hexylsilane and give oligosilane products has been shown in this thesis. Future work to further optimize reaction conditions (ie. method of hydrogen gas removal, reaction time, catalyst/substrate ratio), to obtain higher amounts of oligosilane products from the dehydrocoupling reactions is of interest. Exploring new and/or improve existing methods for separation of resulting oligosilane mixtures, to allow the opportunity to use the di- and trisilane products as substrates in other reactions, should also be possible for these systems.

Although the reaction work-up required for dehydrocoupling di-*n*-hexylsilane with $[Rh(dppe)\mu\text{-}Cl]_2$, **3**, was very easy compared to $RhCl(PPh_3)_3$, **1** and $[(PPh_3)_2Rh(\mu\text{-}Cl)]_2$, **2**, the activities observed for complex **3** were very low. As discussed in Chapter 2, this low activity could have been due to solubility issues of the catalyst precursor in neat

silane. Another reason that complex **3** gave low activities for the dehydrocoupling of silanes is related to the structure of the catalyst precursor. It seems likely that the first step toward forming Si-Si bonds via 'P_2Rh' catalysts is through an oxidative addition complex, $[(PPh_3)_2Rh(H)(Cl)(SiHR_2)]$, **5**, where the phosphorus ligands are in the trans position. If this type of trans configuration is required, then perhaps the bite angle between the two phosphorus ligands, for complex **3**, is too small to accommodate the formation of such a structure. To examine this hypothesis, it would be advantageous to study the complex $[Rh(dppb)\mu\text{-}Cl]_2$, **11**, (dppb = diphenylphosphinobutane) in the dehydrocoupling of di-*n*-hexylsilane. Instead of the ethane backbone found in complex **3**, there are four carbons in the butane backbone of complex **11** that increases the size of the chelate ring (Equation 4.1).

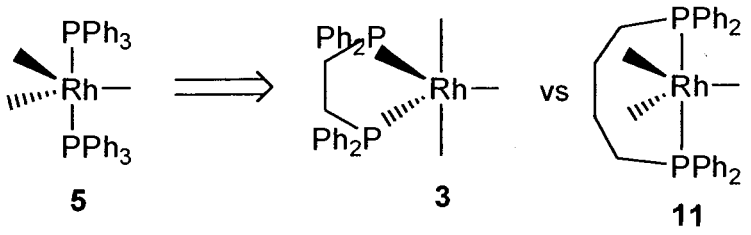

(4.1)

Probing the dehydrocoupling reactions of di-*n*-hexylsilane with complex **11**, and comparing corresponding activities with complex **3** will help answer this question of structure criteria of the catalyst precursor.

Future studies of the dehydrocoupling reactions of di-*n*-hexylsilane, described in this thesis, might involve the investigation of other Rh(I) phosphine complexes for the production of Si-H functionalized oligosilane reagents. Complexes of interest include a cationic rhodium complex, $[Rh(dppb)(COD)]^+PF_6^-$ and a neutral zwitterionic rhodium complex, $[Rh(PPh_2BPh_2)(COD)]$, are given below in Figure 4.1. The boron–containing ligand, in the second example, may help increase the solubility of this complex in the

substrate silane, perhaps aiding in the ease of carrying out dehydrocoupling reactions and increasing catalytic activities.

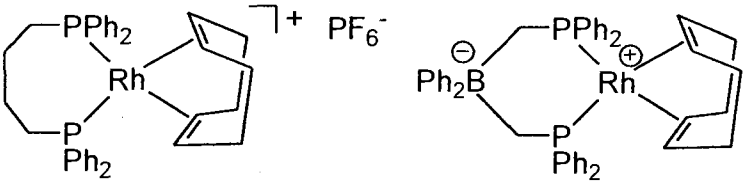

Figure 4.1: Possible Rh(I) phosphine complexes for use in further dehydrocoupling of silane studies

Should the dppb derivative, [Rh(dppb)μ-Cl]$_2$, **11**, exhibit high activity for the dehydrocoupling of di-*n*-hexylsilane, it would be attractive to look at using a chiral ligand on a Rh centre to influence the stereochemistry of the resulting disilane product. One possible example of this dehydrocoupling reaction using a chiral phosphine ligand, (-) – 1,2 – Bis ((2R, 5R) – 2,5 – dimethyl – phosphalano) benzene, also referred to as (R, R)–Me-DUPHOS, **12**, is shown in Equation 4.2. The disilane product obtained is a mixture of diastereomers. It should be noted that the starting silane substrate must be unsymmetrically-substituted for the formation of these diastereomers occur.

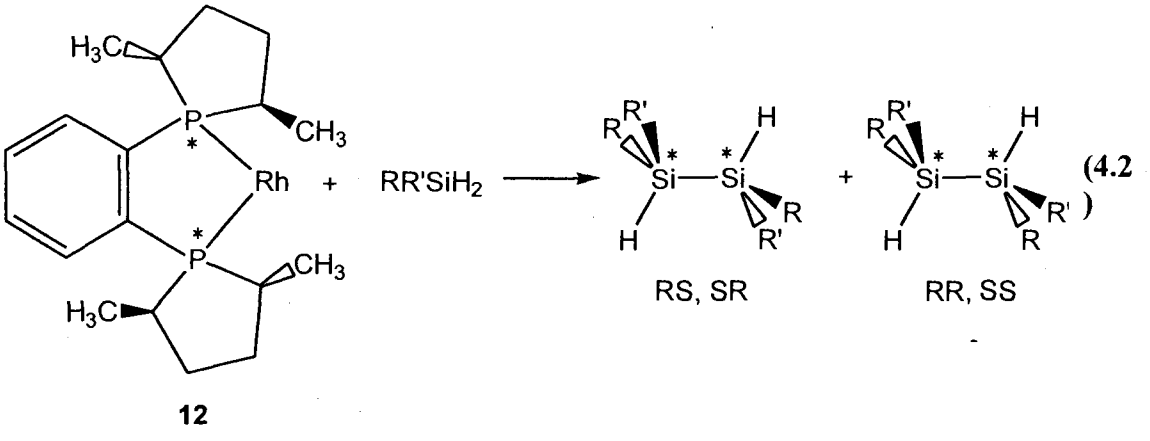

Information compiled by the stoichiometric dehydrocoupling of di-*n*-hexylsilane reactions presented in Chapter 3 should help in identifying key intermediates in the

catalytic cycle. Future work to aid in the elucidation of other intermediate structures would include variable temperature NMR spectroscopy studies for $RhCl(PPh_3)_3$, **1**, with one and five equivalents of di-*n*-hexylsilane, dehydrocoupling reactions with the orange powder isolated from the addition of $RhCl(PPh_3)_3$, **1**, with one equivalent of di-*n*-hexylsilane to see if it exhibits catalytic competency, and further stoichiometric reactions of $[Rh(COD)(PPh_3)_2]^+PF_6^-$, **4**. Additional experiments to help compile more information for these systems could include using bulky R groups on silicon to help determine if a metal-silylene ($M=SiR_2$) intermediate is occurring, selective ^{31}P-decoupling NMR experiments, FT-IR spectroscopy (diagnostic Si-H and Rh=Si stretches, etc.), Mass spectrometry (mass peaks of the 'parent' compounds) and UV-vis spectroscopy (quantify the observed colours from reactions).

Appendix

A.1 Conversions/consumption calculated from ^{1}H NMR:

1 Si R_2SiH_2 RI = 2H so, RI/2 = 1 Si

2 Si 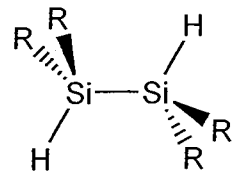 RI = 2H so, RI = 2 Si

3 Si 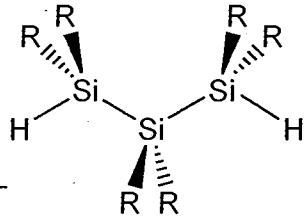 RI = 2H so, RI x 3/2 = 3 Si

Si_{Total} = 1/2 (RI monosilane) + RI disilane + 3/2 (RI trisilane)